NAVAL POSTGRADUATE SCHOOL
MONTEREY, CALIFORNIA

THESIS

ANALYSIS OF TARGET CONTRAST IMPROVEMENT USING POLARIZATION FILTERING IN THE INFRARED REGION

by

David Gavin Moretz

December, 1994

Thesis Advisor: Alfred W. Cooper

Approved for public release; distribution is unlimited.

REPORT DOCUMENTATION PAGE

Form Approved OMB No. 0704-0188

1. AGENCY USE ONLY *(Leave blank)*	2. REPORT DATE December 1994	3. REPORT TYPE AND DATES COVERED Master's Thesis

4. TITLE AND SUBTITLE
ANALYSIS OF TARGET CONTRAST IMPROVEMENT USING POLARIZATION FILTERING IN THE INFRARED REGION

5. FUNDING NUMBERS

6. AUTHOR(S) David G. Moretz

7. PERFORMING ORGANIZATION NAME(S) AND ADDRESS(ES)
Naval Postgraduate School
Monterey CA 93943-5000

8. PERFORMING ORGANIZATION REPORT NUMBER

9. SPONSORING/MONITORING AGENCY NAME(S) AND ADDRESS(ES)

10. SPONSORING/MONITORING AGENCY REPORT NUMBER

11. SUPPLEMENTARY NOTES The views expressed in this thesis are those of the author and do not reflect the official policy or position of the Department of Defense or the U.S. Government.

12a. DISTRIBUTION/AVAILABILITY STATEMENT
Approved for public release; distribution is unlimited.

12b. DISTRIBUTION CODE

13. ABSTRACT *(maximum 200 words)*

Computer analysis with IDL was performed on polarized infrared image data obtained during the MAPTIP coastal experiment. Analysis of contrast enhancement of the oceanographic ship Hr. Ms. Tydeman and a Lynx helicopter using polarization filters is presented. Contrast of vertical and horizontal polarized images was determined by two methods. Unpolarized image contrast was developed from polarization data and used to calculate contrast improvement factors for vertical and horizontal polarizations. Background effects upon contrast were explored. Dependence of projected ship area on contrast improvement was analyzed. Vertical and horizontal polarized images were compared to verifiy preliminary observations of negligible predominant polarization of man-made targets.

Results of this analysis confirm that vertically polarized sea background radiance can be reduced by polarization filtering to enhance ship-to-backround contrast. Man-made targets appear to present negligible polarization. Sky background immediately above the horizon also appears unpolarized. Combining radiance from both sky backround above the horizon and sea background to form an average background reference radiance reduces overall contrast improvement. Ship-to-background contrast should be calculated with respect to the horizon location.

14. SUBJECT TERMS
Infrared targets, MAPTIP, Infrared polarization, Infrared images, AGA 780, Contrast, Contrast improvement, Thermal radiation

15. NUMBER OF PAGES 123

16. PRICE CODE

17. SECURITY CLASSIFICATION OF REPORT	18. SECURITY CLASSIFICATION OF THIS PAGE	19. SECURITY CLASSIFICATION OF ABSTRACT	20. LIMITATION OF ABSTRACT
Unclassified	Unclassified	Unclassified	UL

NSN 7540-01-280-5500

Standard Form 298 (Rev. 2-89)
Prescribed by ANSI Std. 239-18 298-102

Approved for public release; distribution is unlimited.

ANALYSIS OF TARGET CONTRAST IMPROVEMENT USING POLARIZATION FILTERING IN THE INFRARED REGION

by

David G. Moretz
Lieutenant, United States Navy
B.S., North Carolina State University, 1987

Submitted in partial fulfillment
of the requirements for the degree of

MASTER OF SCIENCE IN PHYSICS

from the

NAVAL POSTGRADUATE SCHOOL
December 1994

Author: _____
David G. Moretz

Approved by: _____
Alfred W. Cooper, Thesis Advisor

_____
Scott Davis, Second Reader

_____ For
William B. Colson, Chairman
Department of Physics

ABSTRACT

Computer analysis with IDL was performed on polarized infrared image data obtained during the MAPTIP coastal experiment. Analysis of contrast enhancement of the oceanographic ship Hr. Ms. Tydeman and a Lynx helicopter using polarization filters is presented. Contrast of vertical and horizontal polarized images was determined by two methods. Unpolarized image contrast was developed from polarization data and used to calculate contrast improvement factors for vertical and horizontal polarizations. Background effects upon contrast were explored. Dependence of projected ship area on contrast improvement was analyzed. Vertical and horizontal polarized images were compared to verifiy preliminary observations of negligible predominant polarization of man-made targets.

Results of this analysis confirm that vertically polarized sea background radiance can be reduced by polarization filtering to enhance ship-to-backround contrast. Man-made targets appear to present negligible polarization. Sky background immediately above the horizon also appears unpolarized. Combining radiance from both sky backround above the horizon and sea background to form an average background reference radiance reduces overall contrast improvement. Ship-to-background contrast should be calculated with respect to the horizon location.

TABLE OF CONTENTS

ACKNOWLEDGEMENTS

This research effort was supported by NCCOSC-RDT&E Code 54.

Two individuals contributed greatly to the completion of this work. I wish to thank Mr. Jerry Lentz for his valuable support and assistance in IDL programming. His patience with my sluggish grasp of programming was appreciated. I also would like to thank Professor Alfred W. Cooper for his guidance and consultation in the course of this thesis. I will forever be thankful for the knowledge gained from my association with him.

Lastly, I would most like to thank my wife Gina for her endless patience and support throughout my course of study, and my daughter Brittany for greeting me each night with her bright eyes and a smile.

I. INTRODUCTION

As the U. S. Navy moves to increase weapons systems capability in the littoral environment, the ability to detect craft with low or negligible radar cross-section such as fiberglass hulled gunboats demands increased consideration. Infrared detection and tracking systems enhance the combat capability of both ships and aircraft in this environment. However, infrared signatures of interest often exist in substantially cluttered backgrounds. Design of infrared systems capable of satisfactory operation despite clutter requires improvement of target to background contrast to meet the system detection threshold limit. Successful clutter resistant infrared systems could fill the gap between longer range radar detection and short range daytime visibility detection.

Current infrared detection and tracking systems use a variety of filtering methods for target detection and recognition. Various spatial and spectral filtering techniques achieve some improvement in target to background contrast. However, polarization filtering could provide significant improvement in target to background contrast.

Polarization filters reduce polarized apparent sea radiance clutter in the target scene and improve target to background contrast. Specifically, the electric vector of sea radiance clutter appears perpendicularly (horizontally) polarized within sun glint regions and parallel (vertically) polarized otherwise (Cooper, Crittenden, Milne, Moss, Gregoris, 1992). Man-made targets appear much less polarized than sea backgrounds. Polarization filters aligned horizontally while viewing target scenes outside of sun glint indicate a greater reduction of sea background radiance clutter compared to vertically aligned filters viewing the same target scene (Cooper, Lentz, Walker, Chan, April 94). For infrared system applications, the target scene contrast achieved with polarizers should exceed that of an unpolarized scene in order to reduce the system detection threshold value. This in turn would increase minimum detection and recognition ranges.

This thesis analyzes marine environment polarization images taken during the MAPTIP experiment of 18-31 October 1993 off the coast of the Netherlands. These images provide the apparent radiance from target scenes involving ships and aircraft as viewed through vertical and horizontal filters. Computer code was generated to

perform the analysis, providing the apparent average ship and background radiance in vertical polarization, horizontal polarization, and unpolarized representation. Also provided are vertical, horizontal, and unpolarized target to background scene contrasts. As a result, contrast improvement attained through vertical and horizontal polarizations compared with unpolarized scenes is produced.

Chapter II provides a discussion of essential infrared radiation fundamental concepts and equations necessary for more involved development of infrared radiation theory. Chapter III describes the concepts involved in light polarization and the theory of infrared polarization in the marine environment. Chapter IV describes the image data utilized and also the specifics of the analysis procedure. Chapter V provides a discussion of the results, conclusions and recommendations. Appendix A contains the three computer programs used and Appendix B provides the results of the analysis.

II. INFRARED RADIATION FUNDAMENTALS

A. THEORY OF INFRARED RADIATION

Infrared radiation is a part of the total electro-magnetic spectrum. The infrared region spans wavelengths from 0.72 μm to 1000 μm as shown in the diagram of the electro-magnetic spectrum in Fig. 2.1 (Grum and Becherer, 1979). The red end of visible light borders the infrared region's lower limit and the microwave end of radio waves borders the upper limit. The infrared region subdivides further into near (0.72-1.5 μm), middle (1.5-5.6 μm), and far (5.6-1000 μm) infrared regions (Hackforth, 1960). Any material at a temperature above absolute zero emits radiation. A body above absolute zero contains a finite value of internal energy associated with the excitation of atoms and molecules. Excitation comprises the storage of energy in electronic, vibrational, and/or rotational states. The levels of excitation in vibrational states occur in multiples of some discrete value of energy. When the atom or molecule returns to the lower energy state, it releases radiation in the form of a photon at a frequency proportional to the change in energy between states,

$$\Delta E = h\nu \qquad \textbf{2.1}$$

where, ΔE = change in energy between states (J or eV)

h = Plank's constant (6.6256×10^{-34} J-s)

ν = frequency of released radiation (Hz)

The change in energy associated with electronic states typically ranges from one to ten electron volts (1.24-0.124 μm), whereas vibrational and rotational state changes in energy are typically 0.1 eV (12.4 μm) and 10^{-4} eV (12,424 μm), respectively. Therefore, molecular infrared radiation primarily involves vibrational changes of state with rotational changes superimposed. Fig. 2.2 shows the absorption spectrum of diatomic molecules of HCL gas. The actual emission spectrum contains rotational changes of state superimposed upon the vibrational changes. (Cooper 4253 notes, 1994)

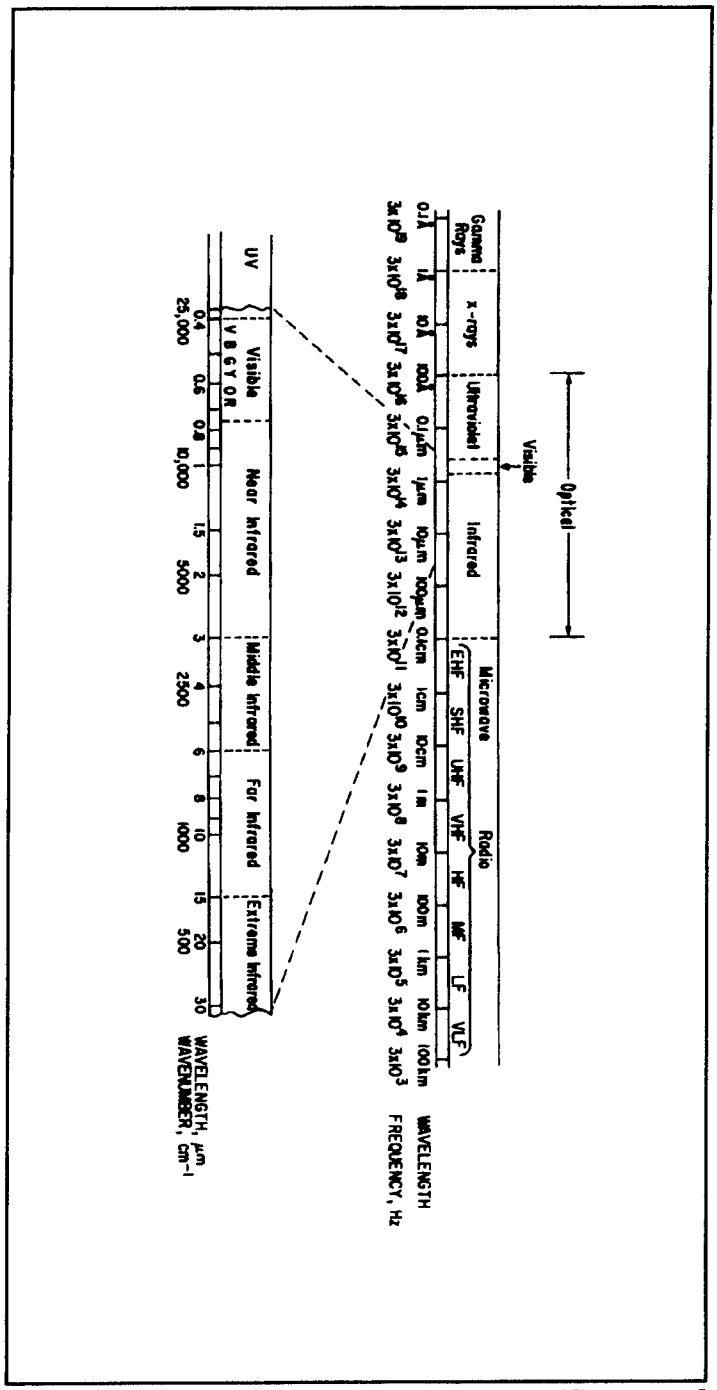

Figure 2.1 Electro-magnetic spectrum (Grum and Becherer, 1979).

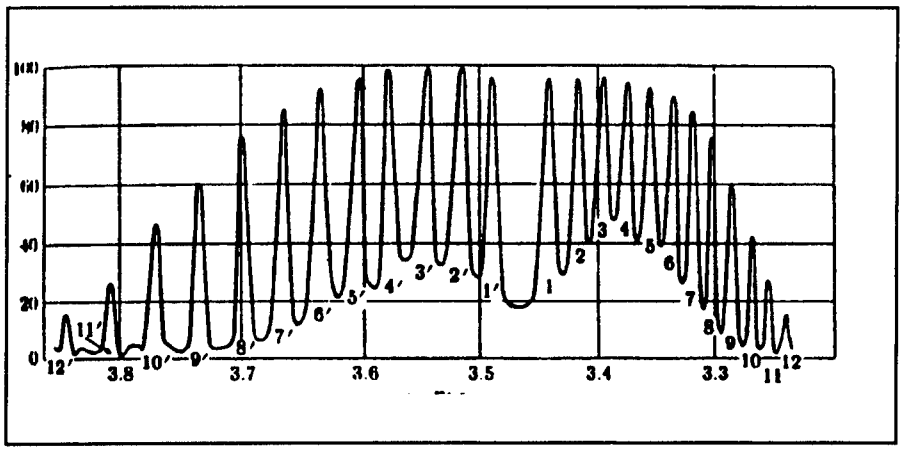

Figure 2.2 Vibration-rotation spectrum of HCL (Cooper 4253 notes, 1994).

1. Infrared Definitions and Units

Several definitions and units require introduction for an understanding of infrared science. Table 2.1 shows fundamental radiometric quantities associated with infrared radiation. Radiant exitance (emittance) or flux density, M, is the radiant flux exiting an infinitesimal area divided by that infinitesimal area. Irradiance or radiant flux surface density, E, is the radiant power incident upon a unit area of surface. Radiant intensity, I, is the radiant power exiting a point source along a given direction within a unit solid angle. Radiance or radiant intensity surface density in a given direction, L, is the radiant power per unit solid angle exiting from or incident on an area projected perpendicular to the direction of radiant energy flow. (Grum and Becherer, 1979, Cooper Class Notes, 1994; Wolfe and Zissis, 1978, Bramson, 1968, Smith, 1993)

2. Blackbody Radiation

The blackbody is fundamental to the study of infrared radiation. Figure 2.3 shows typical blackbody radiant emittance curves for several temperatures. The total radiant emittance or area under the curve and the peak value of emittance depend upon the blackbody temperature, the peak value shifting to the left at greater temperatures. The radiation emitted at a given temperature is a maximum for a blackbody. As the standard for radiation theory, blackbody emission and absorption efficiency, designated as the emissivity factor, equals one.(Hackforth, 1960)

Quantity(Symbol)	Defining Equation	Units
Radiant energy (Q)		J (joule)
Radiant energy density (w)	$\omega wdQ/dV$	J/m^3
Radiant power or flux (Φ)	$\Phi=dQ/dt$	W (watt)
Radiant exitance (M)	$M=d\Phi/dA$	W/m^2
Irradiance (E)	$E=d\Phi/dA$	W/m^2
Radiant intensity (I)	$I=d\Phi/d\omega$	W/Sr
Radiance (L or N)	$L=d^2\Phi/d\omega(dA\cos\theta)$ $=dI/(dA\cos\theta)$	W/m^2Sr
Emissivity (ε)	$\varepsilon=M/M_{bb}$	___

Table 2.1 Radiometric quantities (Grum and Becherer, 1979).

a. Planck's Law

During the late 19th century many scientists grappled with deriving the equation fitting the experimentally obtained radiant emittance curves similar to those in Figure 2.3. Max Planck successfully established this equation and simultaneously ushered in the era of quantum theory. Planck theorized that oscillating modes of frequency ω excite higher oscillation energy levels in discrete increments or quanta. This theory led to Planck's law which follows,

$$M_\lambda(T)=\frac{2\pi c^2 h}{\lambda^5(e^{\frac{hc}{k\lambda T}}-1)}[Wcm^{-2}cm^{-1}] \qquad 2.2$$

where $M_\lambda(T)$ = spectral radiation emitted into a hemisphere per unit area per unit wavelength interval ($Wcm^{-2}cm^{-1}$)

T = absolute temperature of the body (°K)

λ = wavelength (cm)

h = Plank's constant (6.6256×10^{-34} J-s)

c = speed of light in a vacuum (2.998×10^{10} cm/s)

k = Boltzmann's constant (1.38054×10^{-23} $J-K^{-1}$).

As seen from this equation and Figure 2.3, as the temperature increases the radiant emittance increases significantly. In fact, the total radiant exitance increases with the fourth power of absolute temperature as shown by the Stefan-Boltzmann law described below.(Hudson, 1969, Hackforth, 1960)

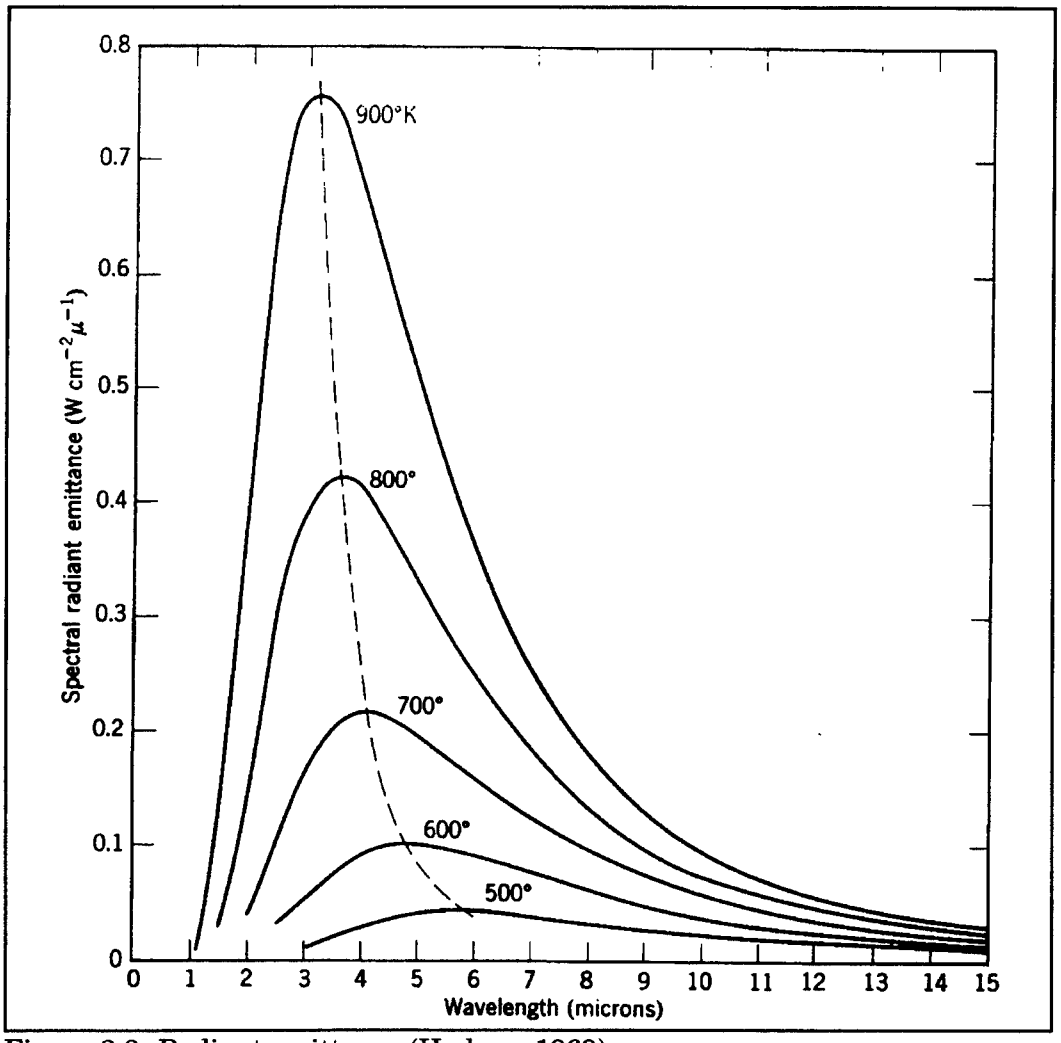

Figure 2.3 Radiant emittance (Hudson, 1969).

b. Emissivity

No real bodies emit and absorb radiation ideally as the blackbody. Emissivity depends on the body constituents, temperature, incident radiation quantity and wavelength, and surface finish. The ratio of a body's total radiant emittance, M,

to that of a blackbody, M_{BB}, defines the body's emissivity,

$$\epsilon = \frac{M}{M_{BB}} \qquad 2.3$$

Again, blackbody emissivity equals one. Some materials approximate blackbody behavior. Many others, called gray bodies, display emissivity factors less than one, but are independent of wavelength as is a blackbody. Still other materials, called selective emitters, emit and absorb radiation variably dependent upon wavelength. The following equation accounts for the possible spectral dependence of emissivity, $\varepsilon(\lambda)$,

$$\epsilon = \frac{\int_0^\infty \epsilon(\lambda) M_\lambda d\lambda}{\int_0^\infty M_\lambda d\lambda} \qquad 2.4$$

Figure 2.4 displays radiant emittance curves for a gray body and selective emitter compared with a blackbody curve.(Hudson, 1969)

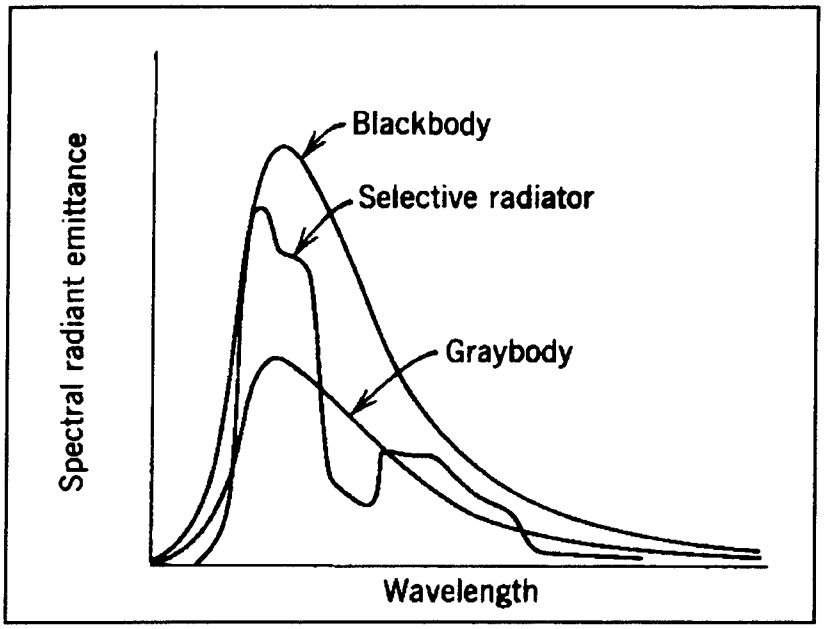

Figure 2.4 Radiant emittance for selective, graybody, and blackbody emission spectra (Hudson, 1969).

c. Stefan-Boltzmann Law

The integration of Planck's Law over all wavelengths produces the total radiant exitance emitted from a blackbody as a function of temperature as shown below,

$$M(T)=\int_0^\infty M_\lambda(T)d\lambda=\sigma T^4[W/cm^2] \qquad 2.5$$

where, M(T) = total radiant emittance at temperature T (Wcm^{-2})

σ = Stefan-Boltzmann constant (5.670×10^{-12} $Wcm^{-2}K^{-4}$).

For a graybody, this function becomes,

$$M(T)=\epsilon\sigma T^4. \qquad 2.6$$

Quite often, spectral filters used with infrared systems permit only a specified wavelength interval of irradiance to reach the detector. Therefore, effective radiant emittance then results from integrating M(T) over only the desired wavelength interval.(Hudson, 1969, Hackforth, 1960)

d. Wien's Displacement Law

Differentiating the radiant emittance M_λ of Equation 2.2 and setting the result equal to zero yields the wavelength of maximum emittance. This is known as Wien's displacement law,

$$\lambda_m T=K \qquad 2.7$$

where, λ_m = wavelength of maximum emittance (cm or μm)

T = absolute temperature (°K)

K = constant = 0.2897 cmK for λ_m in cm = 2897 μmK for λ_m in μm.

Since the wavelength of maximum emittance times the absolute temperature equals a constant, then λ_m displaces to shorter wavelengths as temperature increases as shown in Figure 2.3 by the dashed line.(Hudson, 1969, Hackforth, 1960)

e. Kirchoff's Law

A blackbody absorbs all incident radiation and emits an equal amount of radiation. Applying conservation of energy to a non-blackbody yields,

where U_i = incident radiant energy

$$U_i = U_\rho + U_\alpha + U_\tau \qquad 2.8$$

U_ρ = reflected radiant energy

U_α = absorbed radiant energy

U_τ = transmitted radiant energy.

Normalizing with respect to U_i produces

$$1 = \rho + \alpha + \tau \qquad 2.9$$

where, $\rho = U_\rho/U_i$ = reflectivity

$\alpha = U_\alpha/U_i$ = absorptivity

$\tau = U_\tau/U_i$ = transmissivity.

Kirchoff showed that the ratio of radiant emittance, M, to absorptivity for a body at a specified temperature equals a constant value of the radiant emittance of a blackbody, M_{BB}, at the same temperature or

$$M_{BB} = \frac{M}{\alpha.} \qquad 2.10$$

Substituting in the Stefan-Boltzmann equation produces

$$\sigma T^4 = \frac{\epsilon \sigma T^4}{\alpha} \qquad 2.11$$

$$\alpha = \epsilon. \qquad 2.12$$

So, the emissivity of a body equals its absorptivity. For opaque bodies, $\tau = 0$, thus

$$\epsilon = 1 - \rho \qquad 2.13$$

which means good emitters reflect poorly.(Hudson, 1969)

f. Lambert's Law

Since a blackbody is a diffuse radiator, it has the same radiance in all directions. However, the radiant intensity of an element of the blackbody surface varies with the angle from the normal to the surface. Lambert's Law states this effect as,

$$dI = LdA\cos\theta \qquad (2.14)$$

where, dI = element of radiant intensity

L = radiance

dA = surface area element of body

θ = angle from normal to observation direction.

Figure 2.5 shows the geometry involved in Lambert's Law.(Jamieson, Plass, McFee, Grube, and Richards, 1963, Hackforth, 1960). The π steradians in Figure 2.5 denotes the quadrant of space to the left of the source area and above the horizontal line that passes through the center of the source.

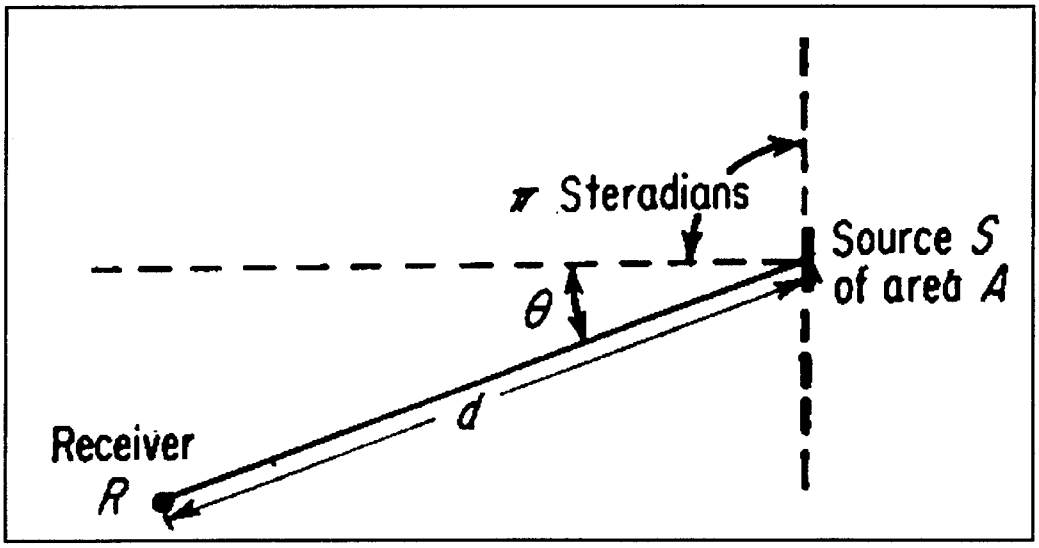

Figure 2.5 Lambert's law of cosines (Hackforth, 1960).

B. INFRARED RADIATION SOURCES

As stated before, any body above absolute zero emits radiation. Types of infrared radiation sources include artificial, natural, and background. Figure 2.6 depicts the many types of infrared radiation sources. Artificial sources consist of primarily man-made materials such as lamps, filaments, and laboratory blackbody sources. Trees, water, mud, vehicles, and people makeup terrestrial natural sources. Atmospheric gas molecules, dust, and water droplets are also terrestrial sources. Terrestrial sources emit, reflect, absorb and reradiate radiation characteristic to each particular material. Celestial natural sources include the sun, moon, planets, and

stars. Terrestrial and celestial sources serve as background source radiation if superimposed on the primary source radiation.(Hackforth, 1960)

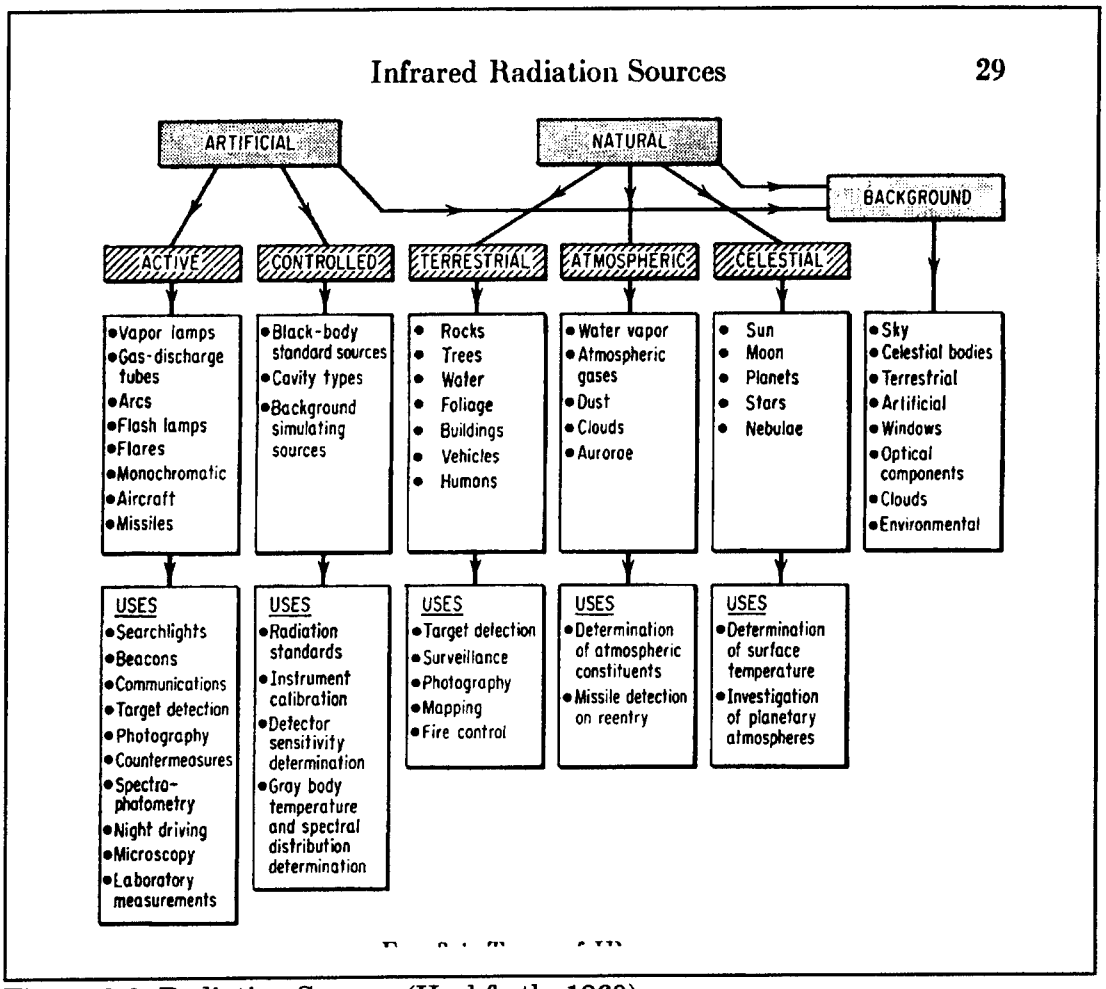

Figure 2.6 Radiation Sources (Hackforth, 1960).

Background radiation also differs with respect to day or night. Figure 2.7 depicts the relative radiant energy of clear day and night skies. During the day, reflection and scattering of sunlight by atmospheric particles, water droplets, dust particles, and clouds as well as emission from atmospheric constituents at ambient temperatures contribute to background radiation. Daytime background radiation increases in the direction of the sun and horizon and remains higher than nighttime levels in all directions. The angle of elevation and atmospheric temperature affect both

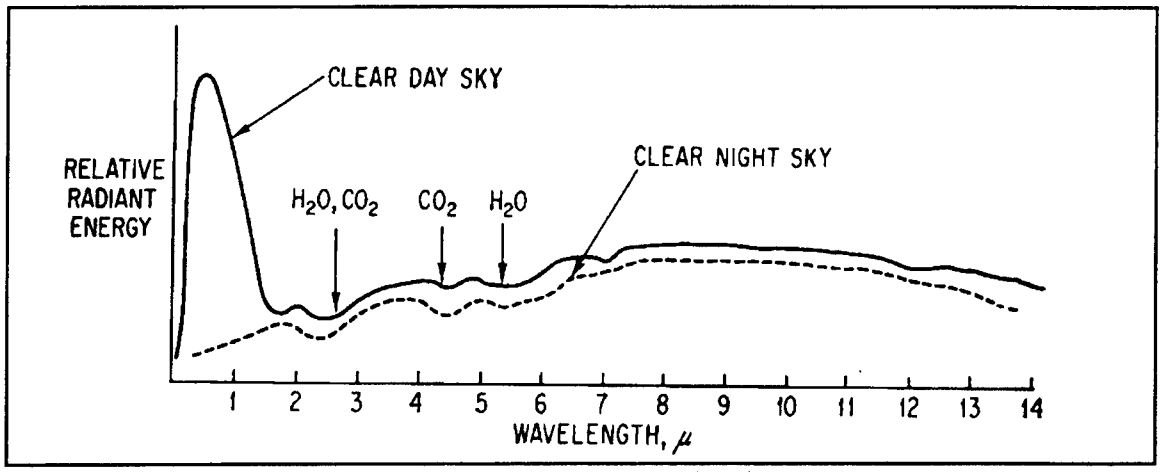

Figure 2.7 Spectral energy distribution of background radiation from clear day and night skies (Hackforth, 1960).

daytime and nighttime radiation intensity. At night, the high frequency radiation scattered by small particles and molecules vanishes. Background radiation at night is emitted from atmospheric molecules and particles with the moon and stars providing additional low-level radiation. (Hackforth, 1960)

Discrimination of a primary source against its background requires a finite primary source temperature different from its background, or a difference in source and background emissivities. The magnitude of the required temperature difference depends upon both the detection system capabilities and the ambient photon noise environment. The background signal generates noise for the detector. Systems use various methods such as spatial, spectral, or electronic filtering to reduce the background signal to enhance primary source or target detection. (Hackforth, 1960)

C. ATMOSPHERIC PROPAGATION OF INFRARED RADIATION

Whatever the source, the detectable radiation received at a detector differs from that radiation emitted at the source. The atmosphere or some other intermediate medium through which the radiation passes attenuates the radiation through scattering and absorption. These effects occur independently from the source, but vary according to the wavelength of radiation. Current meteorological conditions play an important role in radiation propagation. As the atmosphere changes so does its propagation characteristics. Cloud type, base, and ceiling, fog, suspended particles, and molecular constituents of the atmosphere all impact absorption and scattering

effects of the atmosphere on infrared radiation. Beer's Law quantifies the total attenuation by the atmosphere as

$$I(z)=I(0)e^{-\mu z} \qquad \textbf{2.15}$$

where, I(0) = initial intensity of radiation

I(z) = intensity of radiation after propagation distance z in the atmosphere

μ = extinction coefficient of atmosphere

z = propagation distance.

Therefore, the transmittance, τ results from,

$$\tau=\frac{I(z)}{I(o)}=e^{-\mu z}. \qquad \textbf{2.16}$$

The atmospheric absorption (μ_a) and scattering (μ_s) coefficients sum to produce the total atmospheric extinction coefficient (μ)

$$\mu=\mu_a+\mu_s \qquad \textbf{2.17}$$

where,

$$\mu_a=\kappa_m+\kappa_a \qquad \textbf{2.18}$$

$$\mu_s=\sigma_m+\sigma_a \qquad \textbf{2.19}$$

and κ_m = molecular absorption coefficient

κ_a = aerosol absorption coefficient

σ_m = molecular scattering coefficient

σ_a = aerosol scattering coefficient.

The magnitudes of each coefficient depend upon the atmospheric composition and constituent density and distribution. Aerosol scattering dominates infrared radiation extinction below 1.2 μm. Above 1.2 μm, molecular absorption dominates. In addition, atmospheric transmittance depends significantly on wavelength.(Cooper class notes, 1994) Figure 2.8 shows transmittance as affected by infrared absorption by the predominant atmospheric molecules over a horizontal path of 6000 meters at sea level with 17 mm of precipitable water (Hudson, 1960).

1. Absorption Effects

Absorption occurs when infrared radiation interferes with a free molecule, atom or a liquid or solid at about the frequency corresponding to an energy level separation, and the electric field of infrared radiation excites that material to the higher energy level. The radiation disapears as a result (Hackforth, 1960). Lorentzian curves depict the frequency lineshape of absorption which follows the classical resonance phenomenon. Inhomogeneous broadening results in frequency lineshape that are Gaussian. Also, collisional, Doppler, or pressure broadening increases the possible range of frequencies for absorption (Cooper class notes, 1994). Carbon dioxide and water dominate infrared molecular absorption in the atmosphere (Hudson, 1969).

To a much lesser extent, absorption and scattering by aerosols affects infrared propagation. Particles suspended in the atmosphere such as dust and volcanic ash generate aerosols. Their distributions and number densities vary considerably from one environment to another. Several aerosol models available predict aerosol composition of the atmosphere and effects on propagation.(Cooper class notes, 1994)

2. Scattering Effects

Scattering results from the absorbing molecule, atoms, or aerosol subsequently reradiating but over a 4π solid angle, thus reducing the directivity of the original radiation. Where the incident radiation wavelength greatly exceeds the size of the molecule or aerosol particle, the following reradiation approximates isotopic radiation. As particle size increases compared to the incident radiation wavelength, the radiation increasingly tends to be scattered into the forward hemishpere. Rayleigh scattering theory effectively describes small particle scattering, while Mie theory covers the entire range of particle sizes.(Cooper class notes, 1994)

a. Rayleigh Scattering

Rayleigh scattering theory describes scattering for small particles of radius r, typically molecules, where $2\pi r/\lambda \ll 1$. Other assumptions for Rayleigh scattering include nonionized isotropic particles, index of refraction approximately one, and incident radiation whose frequency is different from particle resonant frequencies. Since diatomic nitrogen and oxygen constitute most of the atmosphere, the isotropic assumption requires a molecular anisotropy correction factor. The equation governing

Rayleigh scattering follows,

$$\frac{I}{I'}=K^4\frac{V^2}{\lambda^4 r^2}(1+\cos^2\theta) \qquad 2.20$$

where, I = intensity of scattered radiation

I' = intensity of incident radiation

K = characteristic of medium

V = particle volume

r = distance to particle from observation point

λ = wavelength of radiation

θ = scattering angle.

Synchronously induced dipole moments from the incident radiation produce Rayleigh scattering. (Smith, 1993) The scattered radiation frequency equals the incident radiation frequency. Thus Rayleigh scattering is elastic (Coulson, 1988).

b. Mie Scattering

Mie scattering applies to both large and small particles compared to incident wavelength. This theory assumes isolated spherical particles as the scattering medium. Although most particles are non-spherical, large numbers of randomly orientated non-spherical particles approximate spherical particle distributions except for determining properties of backscatter and polarization. (Smith, 1993) As with Rayleigh scattering, Mie scattering describes the excitation of particles by incident radiation and the reradiation of that energy into a 4π steradian solid angle (Coulson, 1988). The Mie scattering cross section per unit volume follows,

$$\beta_{sca}=\int_0^\infty C_{sca}(r)n(r)dr \qquad 2.21$$

where, β_{sca} = scattering cross section per unit volume

$C_{sca}(r)$ = scattering cross section

n(r) = particle size distribution function (# particles/unit volume between r and r+dr (Smith, 1993)

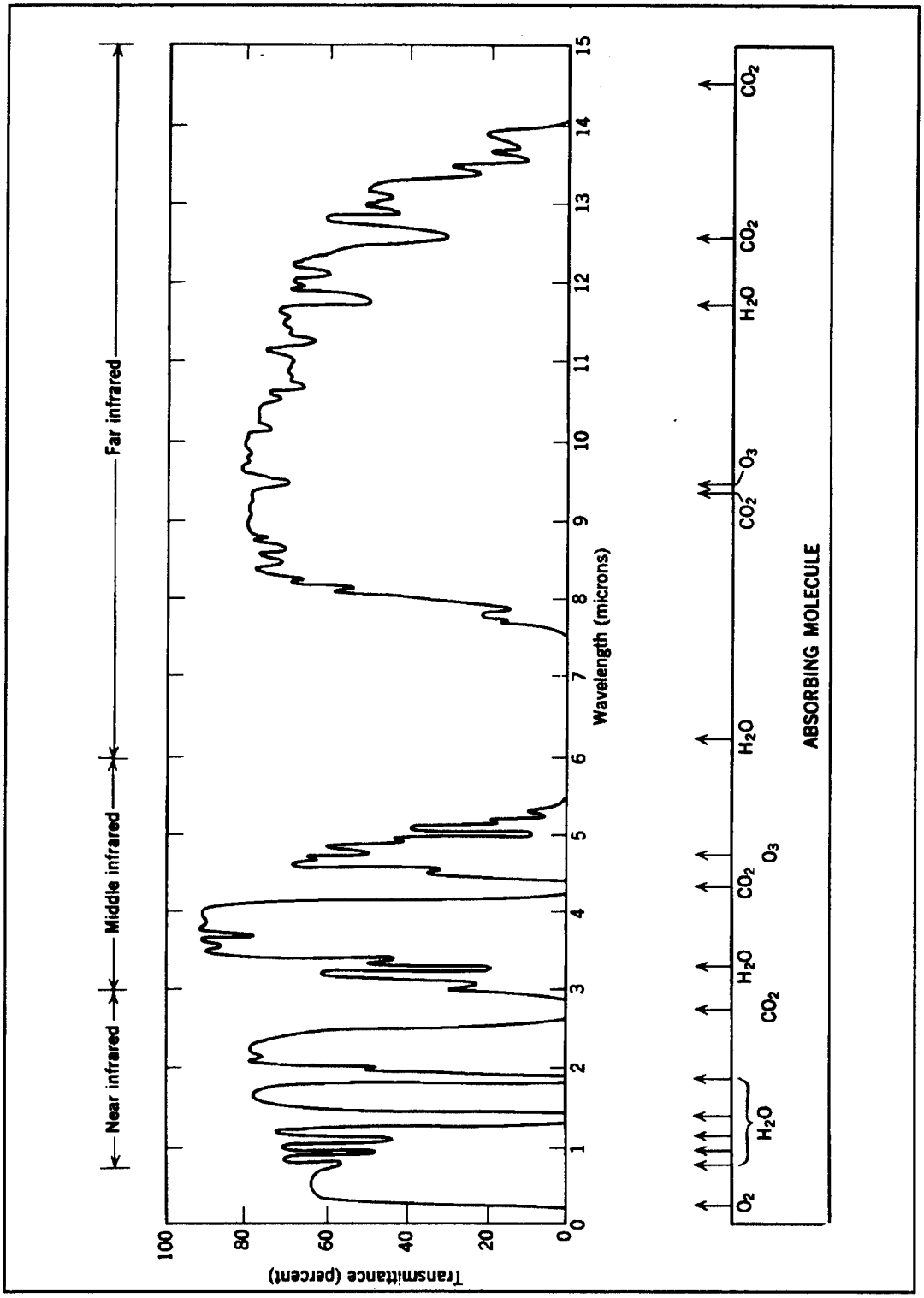

Figure 2.8 Atmospheric transmittance over a horizontal path of 6000 meters at sea level with 17 mm of precipitable water (Hudson, p.115).

III. INFRARED POLARIZATION IN THE MARINE ENVIRONMENT

A. POLARIZATION OF LIGHT

Much experimentation by Fresnel and Arago led to the conclusion that a light wave consists of two components perpendicular to the direction of propagation. The components for a wave propagating in the z-direction may be represented by

$$E_x(z,t)=E_{0x}\cos(\omega t+\delta_x) \qquad 3.1$$

$$E_y(z,t)=E_{0y}\cos(\omega t+\delta_y) \qquad 3.2$$

where E_{ox} and E_{oy} denote the component electric field amplitudes, δ_x and δ_y are the respective phases, ω is frequency, and t is time. $E_x(z,t)$ and $E_y(z,t)$ produce a vector in the plane perpendicular to propagation that generates a curve in that plane known as the polarization ellipse described by

$$\frac{E_x^2}{E_{0x}^2}+\frac{E_y^2}{E_{0y}^2}-2\frac{E_x}{E_{0x}}\frac{E_y}{E_{0y}}\cos\delta=\sin^2\delta \qquad 3.3$$

where $\delta = \delta_y + \delta_x$. This ellipse is shown in Fig. 3.1. Degenerate forms of the polarization ellipse include circular and linear polarizations.(Collett, 1993)

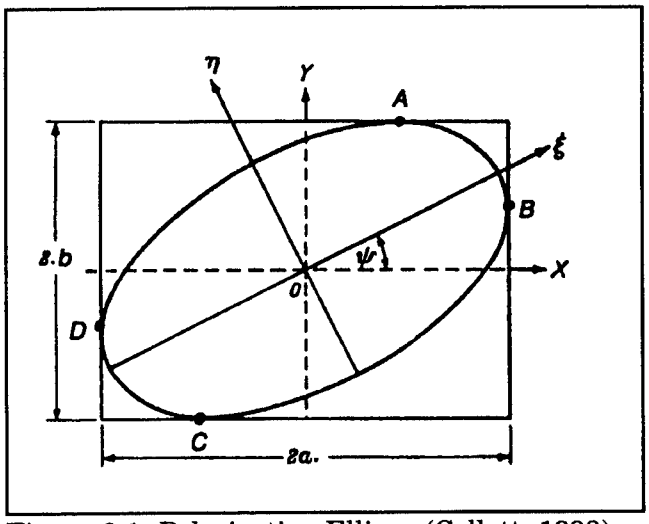

Figure 3.1 Polarization Ellipse (Collett, 1993).

The polarization ellipse is applicable to completely polarized light only, and not useful for describing partially or unpolarized light. Sir George Gabriel Stokes resolved this problem by describing light with observable intensities. He determined that light of any polarization can by described by the four Stokes parameters given by

$$S_0^2 \geq S_1^2 + S_2^2 + S_3^2 \qquad 3.4$$

$$S_1 = E_{0x}^2 - E_{0y}^2 \qquad 3.5$$

$$S_2 = 2E_{0x}E_{0y}\cos\delta \qquad 3.6$$

$$S_3 = 2E_{0x}E_{0y}\sin\delta \qquad 3.7$$

where

$$S_0 = E_{0x}^2 + E_{0y}^2. \qquad 3.8$$

(Collett, 1993) Then the beam intensity is given in terms of Stokes parameters as,

$$I(\theta,\phi) = \frac{1}{2}[S_0 + S_1\cos(2\theta) + S_2\cos(\phi)\sin(2\theta) + S_3\sin(\phi)\sin(2\theta)] \qquad 3.9$$

where ϕ is an induced phase angle (Collett, 1993).

Stokes parameters of two independent light beams may be added to obtain Stokes parameters for the resultant beam. Thus partially polarized light may be represented by the summation of unpolarized light with completely polarized light. Both unpolarized light and partially polarized light may be represented by summing two oppositely polarized beams. For unpolarized light, the intensities of the two beams must be equal. Thus a partially polarized target scene in a marine environment may be represented by two beams of vertical and horizontal polarization.(Collett, 1993)

B. REFLECTION AND REFRACTION

Reflection and refraction of light is described by the Fresnel equations and Snell's law. The incident, reflected, and transmitted waves are shown in Figure 3.2.

Serving as a starting point are Maxwell's equations of electro-magnetism in a source-free medium,

$$\nabla x\vec{E}=-\mu^*\frac{\partial\vec{H}}{\partial t} \qquad \textbf{3.10}$$

$$\nabla x\vec{H}=\epsilon^*\frac{\partial\vec{E}}{\partial t} \qquad \textbf{3.11}$$

$$\nabla\bullet\vec{E}=0 \qquad \textbf{3.12}$$

$$\nabla\bullet\vec{H}=0 \qquad \textbf{3.13}$$

where **E** and **H** are the electric and magnetic field intensities, respectively. The complex permitivity and complex permeability are denoted by ε^* and μ^*, respectively. For plane waves of the form,

$$E_x=E_{0x}e^{j\omega t-\gamma_x} \qquad \textbf{3.14}$$

$$H_y=E_{0y}e^{j\omega t-\gamma_y} \qquad \textbf{3.15}$$

$$\gamma=j\omega(\mu*\epsilon*)^{1/2}=\alpha+j\beta \qquad \textbf{3.16}$$

incident at a boundary between two media of different complex refractive indices n_1^* and n_2^* the angle of reflection equals the angle of incidence. The angle of transmission θ_t as a function of incident angle θ_i is given by Snell's law

$$n_1^*\sin(\theta_i)=n_2^*\sin(\theta_t). \qquad \textbf{3.17}$$

For nonmagnetic media the Fresnel equations can be written

$$r_{\perp} = -\frac{\sin(\theta_i - \theta_t)}{\sin(\theta_i + \theta_t)} \qquad \textbf{3.18}$$

$$r_{\parallel} = -\frac{\tan(\theta_i - \theta_t)}{\tan(\theta_i + \theta_t)} \qquad \textbf{3.19}$$

$$t_{\perp} = \frac{2\sin(\theta_t)\cos(\theta_i)}{\sin(\theta_i + \theta_2)} \qquad \textbf{3.20}$$

$$t_{\parallel} = \frac{2\sin(\theta_t)\cos(\theta_i)}{\sin(\theta_i + \theta_t)\cos(\theta_i - \theta_t).} \qquad \textbf{3.21}$$

The Brewster or polarizing angle occurs where

$$\frac{n_2}{n_1} \geq 0 \qquad \textbf{3.22}$$

and

$$\theta_i + \theta_t = 90. \qquad \textbf{3.23}$$

The reflection coefficients then become

$$r_{\parallel} = 0 \qquad \textbf{3.24}$$

$$r_{\perp} \neq 0. \qquad \textbf{3.25}$$

Thus the reflected light is completely polarized normal to the plane of incidence.(Sandus, 1965)

C. SEA SURFACE INFRARED POLARIZATION

Background infrared radiation from the sea surface is composed of reflected radiation from the sky, sun, moon, stars, etc. Another contribution to background radiation comes from thermally emitted radiation from the water, and molecular and particle volume scattering (Sidran, 1981). Sea surface reflection is governed by the Fresnel equations with polarization of reflected radiation greater near the Brewster angle. Polarization of emitted radiation is somewhat more involved.

1. Sea Surface Reflectance and Emissivity

Polarized light emanating from a surface may be due to emitted radiation as well as reflected radiation. Arago showed that light from an incandescent solid or liquid is partially polarized even for non-polished surfaces. Arago's work was qualitative. Millikan later described Arago's work in quantitative terms.(Sandus, 1965)

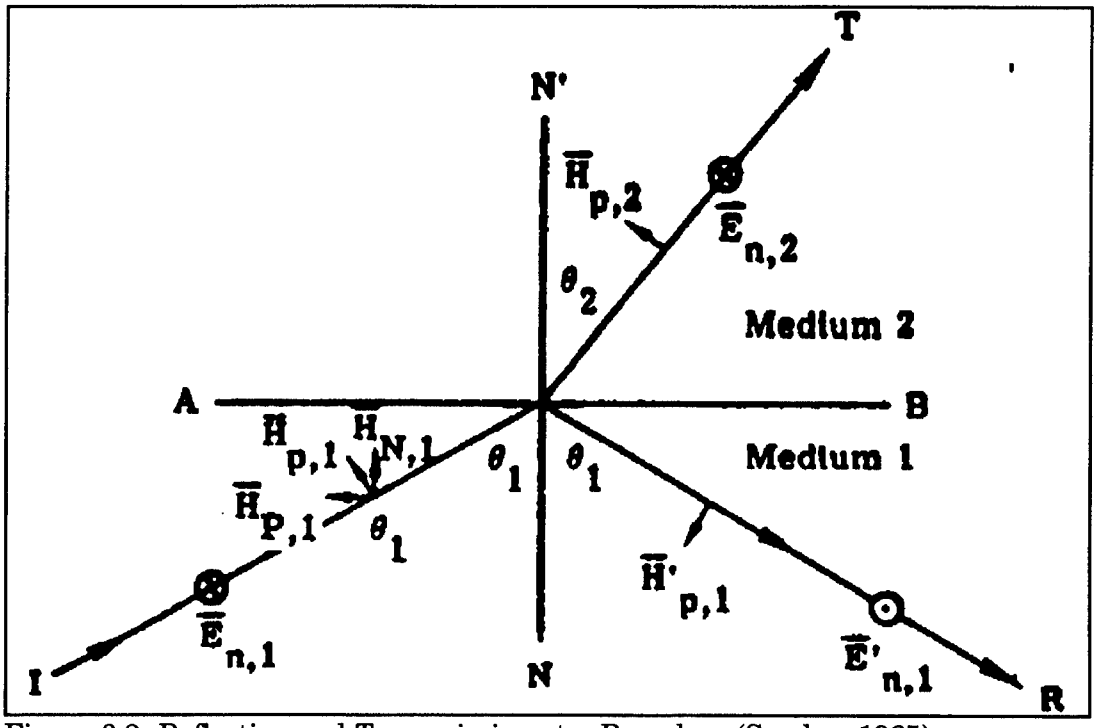

Figure 3.2 Reflection and Transmission at a Boundary (Sandus, 1965).

Millikan studied the polarization characteristics of uranium glass fluorescence. He observed that uranium glass fluorescence emission reached a maximum polarization at near grazing angles. Furthermore, the emitted light was polarized parallel to the plane of emission. As described above, at least partial polarization should be observed for reflected light. However, this light would be polarized normal to the plane of incidence. Therefore, the polarized light Millikan observed from the fluorescence of uranium glass could only have come from emitted light undergoing refraction.(Sandus 1965)

Extending the understanding of emission polarization, Basener and McCoyd developed a model to predict the percent polarization of emitted infrared radiation from the sea surface as a function of wind speed and viewing angle. This model is based upon a sea surface of tiny plane facets of varying orientations. The facet orientation is statistically distributed depending on wind speed.(Basener and McCoyd, 1967)

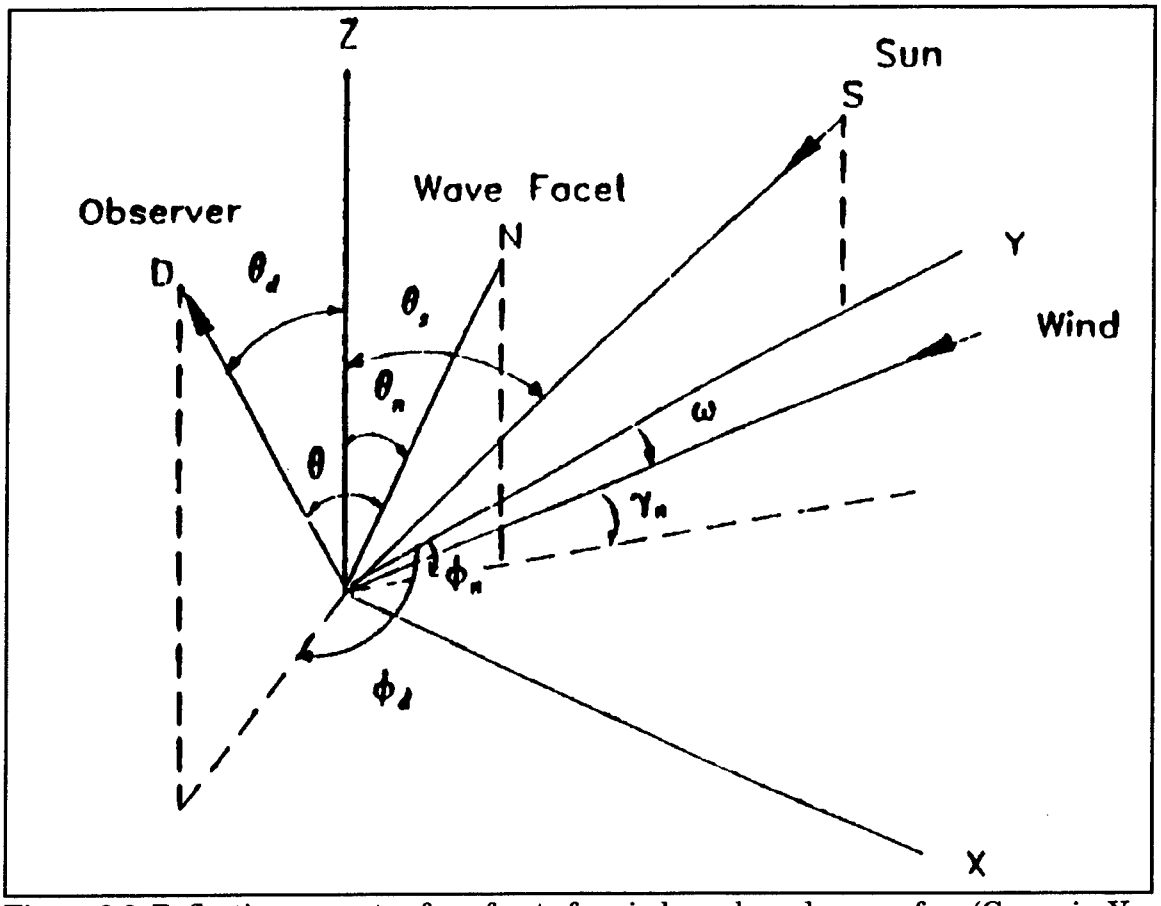

Figure 3.3 Reflection geometry for a facet of a wind roughened sea surface (Gregoris, Yu, Cooper, Milne, 1992).

Given that the sea surface emits polarized radiation, Basener and McCoyd investigated the affects on emissivity of the variable nature of the sea surface. Figure 3.3 shows the reflection geometry for a facet of a wind roughened sea surface. Each facet is assumed flat. For a flat blackbody surface z=f(x,y) the directional emissivity $\varepsilon_r(\theta,\phi)$ is related to the directional reflectance $R(\theta,\phi)$ through

$$\epsilon_r(\theta,\phi)=1-R_r(\theta,\phi) \qquad \textbf{3.26}$$

where r is polarization mode. Thus, the radiant flux emitted per unit solid angle per unit area per unit wavelength interval is

$$F_r(\theta,\phi)=\frac{1}{2}\epsilon_r(\theta,\phi)\cos(\theta)B(\lambda,T) \qquad \textbf{3.27}$$

where $B(\lambda,T)$ is the Planck blackbody function. The reflectance is found from the Fresnel equations above. For complex indices of refraction, the emissivity is given by

$$\epsilon_r=\frac{2}{(1+z_r)} \qquad \textbf{3.28}$$

where z_r is a complex index of refraction.(Basener and McCoyd, 1967)

The above equation is for a flat surface and the sea surface is not flat. However, the sea surface can be approximated by many facets with distributed orientations. For the facets to be considered flat then they must be large compared to the wavelength of light. Sea surface waves easily meet this constraint. Referring again to Fig 3.3, the vector **O** points in the direction of the observer, **S** is the sun direction, and the vector **N** is the facet normal. Therefore, the emissivity depends on the angle between **S** and **N**. The radiant flux emitted per unit solid angle per unit wavelength interval from a unit horizontal area is given by

$$F_r(\theta,\phi)=\frac{1}{2}B(\lambda,T)\int\epsilon_r'(\beta,\gamma)\sec(\beta)f(\beta,\gamma)\cos(\psi)d\omega \qquad \textbf{3.29}$$

where $\varepsilon'(\beta,\gamma)$ is the emissivity referenced to the main plane of vision defined by **S** and k, where k is the unit vector in the z-direction, β is the zenith angle of the facet normal, and γ is the azimuth of the facet normal. The facet distribution function is denoted by $f(\beta,\gamma)$ and ψ is the angle between **S** and **N**. Cox and Munk (Basener and

McCoyd, 1967) have determined experimentally that the distribution of slopes given by $f(\beta,\gamma)$ as a function of wind speed is given by

$$f(\beta,\gamma)d\omega = p(z_x(\beta,\gamma),z_y(\beta,\gamma))\frac{1}{\cos^3(\beta)}d\omega \qquad 3.30$$

where

$$z_x = -\tan(\beta)\sin(\gamma) \qquad 3.31$$

$$z_y = -\tan(\beta)\cos(\gamma) \qquad 3.32$$

and denote the surface slope where y points upwind and p(z,y) gives the fraction of a horizontal unit area of surface whose slopes are within $z_x \pm 1/2\ \delta z_x$ and $z_y \pm 1/2\delta z_y$ (Basener and McCoyd, 1967). The facet slope distribution for crosswind and upwind-downwind situations are shown in Figures 3.4 and 3.5, respectively. The horizontal axis shows the value of beta, the surface normal angle from the vertical direction (Sidran, 1981).

The above formulation ignores affects due to shadowing. Correction factor equations were developed by Wagner and also by Saunders (Sidran, 1981 and Gregoris, Yu, Cooper, and Milne, 1992). Omitting spectral dependencies and including Saunders' correction factor $S(\theta)$, the average apparent radiance from the sea is

$$N_{s,p}(\theta_d,\phi_d,\theta_s) = \frac{s(\theta_d)\tau(\theta_d)}{2\cos(\theta_d)} \qquad 3.33$$

$$\left[\int_{-\pi}^{\pi}\int_{0}^{\frac{\pi}{2}}\left[(\epsilon_{eff}^{s,p}(\theta_n,\gamma_n,\theta_d,\phi_d)N_{sea} + (1-\epsilon_{eff}^{s,p}(\theta_n,\gamma_n,\theta_d,\phi_d)N_{sky})\frac{\tan(\theta_n)\cos(\theta_n,\gamma_n,\theta_d,\phi_d)f(\theta_n,\gamma_n)}{\cos^3(\theta_n)}\right]d\theta_n d\gamma_n\right]$$
$$+(1-\epsilon_{eff}^{s,p}(\theta_d,\phi_d,\theta_s))N_{solar}f(\theta_d,\phi_d,\theta_s)].$$

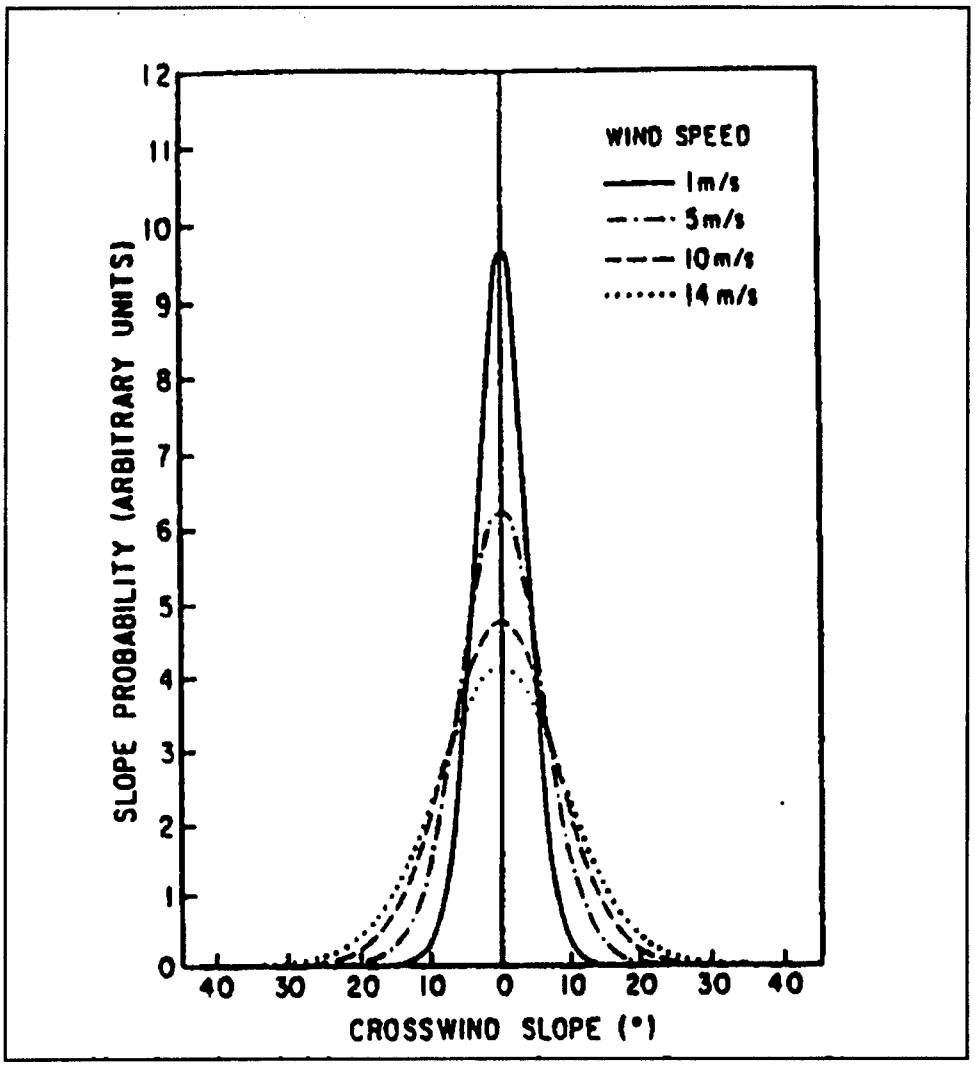

Figure 3.4 Facet slope distribution - crosswind case (Sidran, 1981).

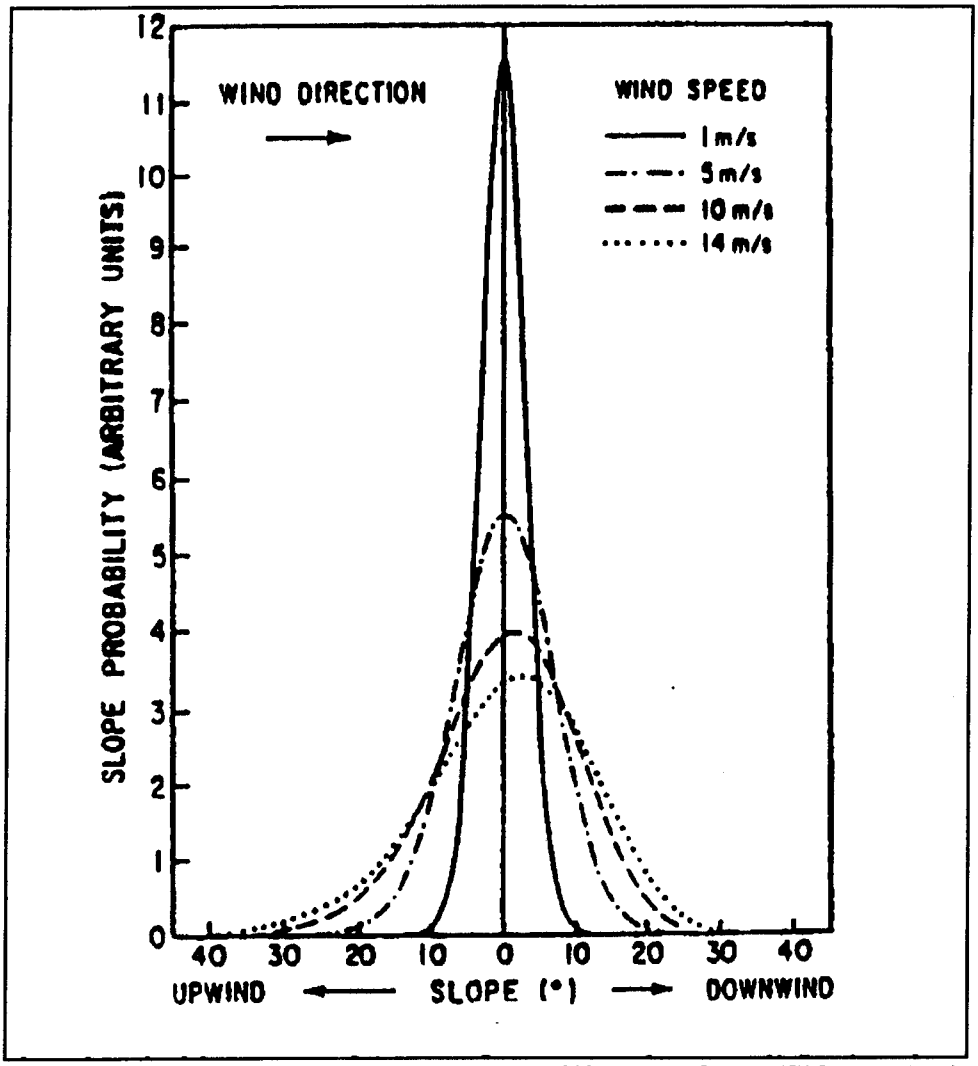

Figure 3.5 Facet slope distribution - upwind/downwind case (Sidran, 1981).

Then the effective polarization is represented by

$$P_{eff}=\frac{N_s-N_p}{N_{path}+N_s+N_p} \qquad 3.34$$

where N_{path} is the unpolarized path radiance which can be obtained with LOWTRAN atmospheric modeling. Fig 3.6 shows the theoretical values of polarization for MWIR(4-5.5μm) and LWIR(8-11.5μm) in and near sun glint regions. Note the negative values of polarization outside of the sun glint regions. Here the sea emission is greater than the reflected sky contribution. The negative values indicate parallel or vertical polarization. The effect is greater in the LWIR since the solar radiance is predominantly in the MWIR. (Gregoris, Yu, Cooper, Milne, 1992)

Also, if Q represents the percent polarization of sea surface emitted radiation, then

$$Q=100\frac{\epsilon_{\parallel}-\epsilon_{\perp}}{\epsilon_{\parallel}+\epsilon_{\perp}}. \qquad 3.35$$

Figure 3.7 shows emissivities and percent polarization as a function of viewing angle θ. Polarization is independent of surface roughness for theta less than approximately 25 degrees. Beyond this value of theta, the polarization increases with viewing angle, but is partially reduced with increasing roughness. In this case an increase in polarization again indicates parallel polarization. Figure 3.8 shows observed data by Hale and Querry for emissivities and percent polarization for both reflected and emitted radiation for all wavelengths below 10 microns. The observed and theoretical results are comparable.(Sidran, 1981)

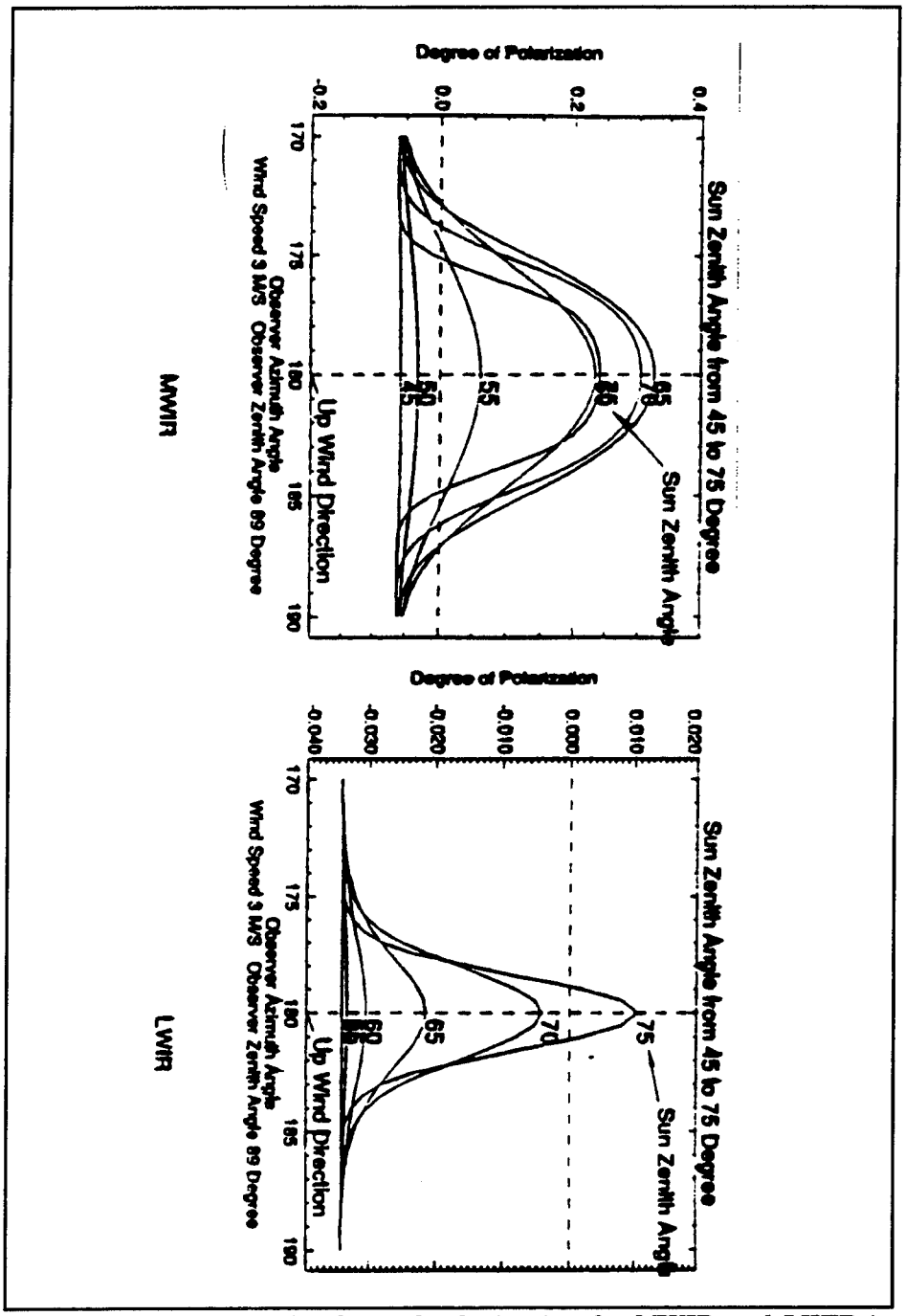

Figure 3.6 Theoretical values of polarization for MWIR and LWIR in and near sun glint regions (Gregoris, Yu, Cooper, Milne, 1992).

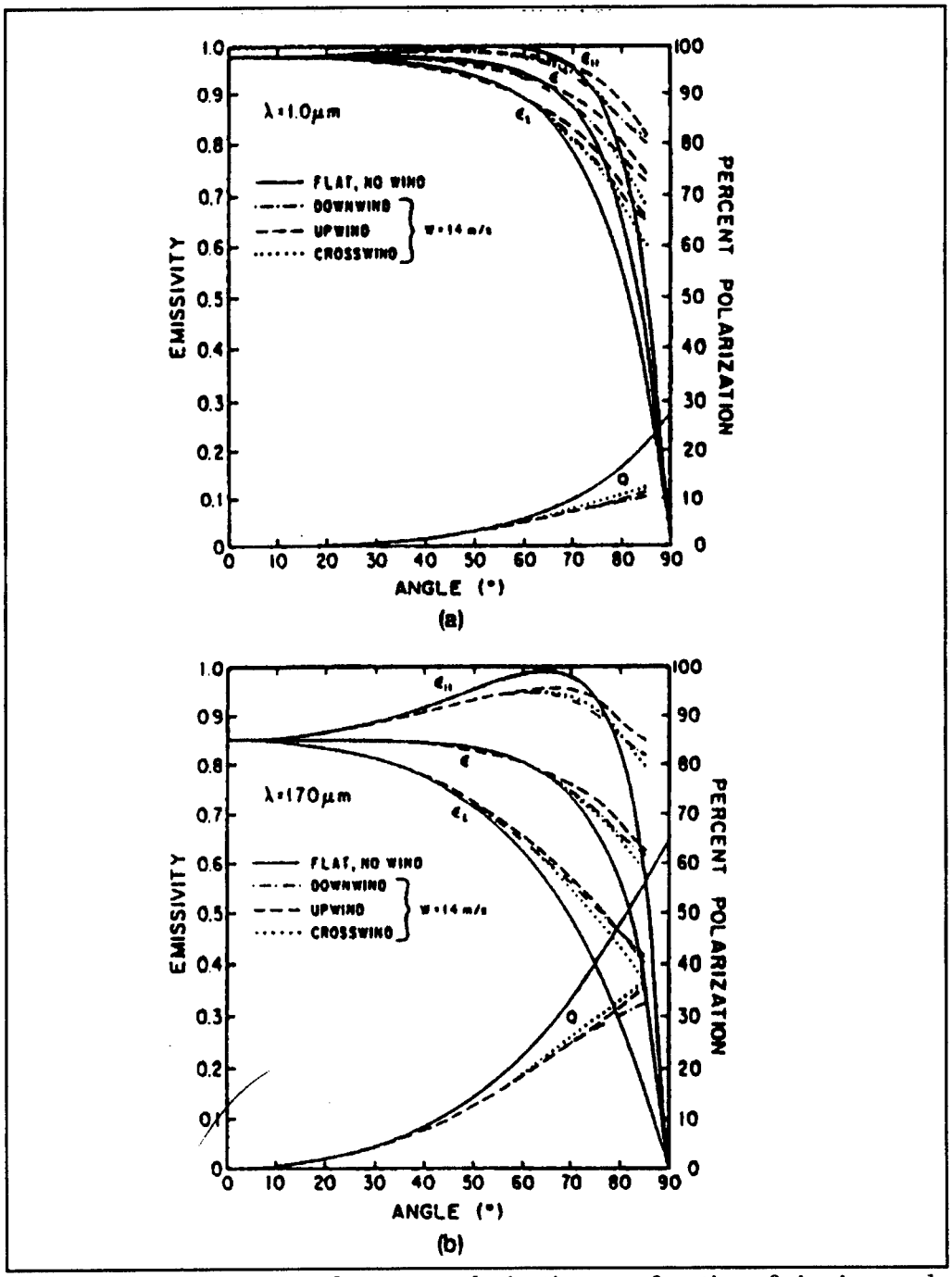

Figure 3.7 Emissivities and percent polarization as a function of viewing angle (Sidran, 1991).

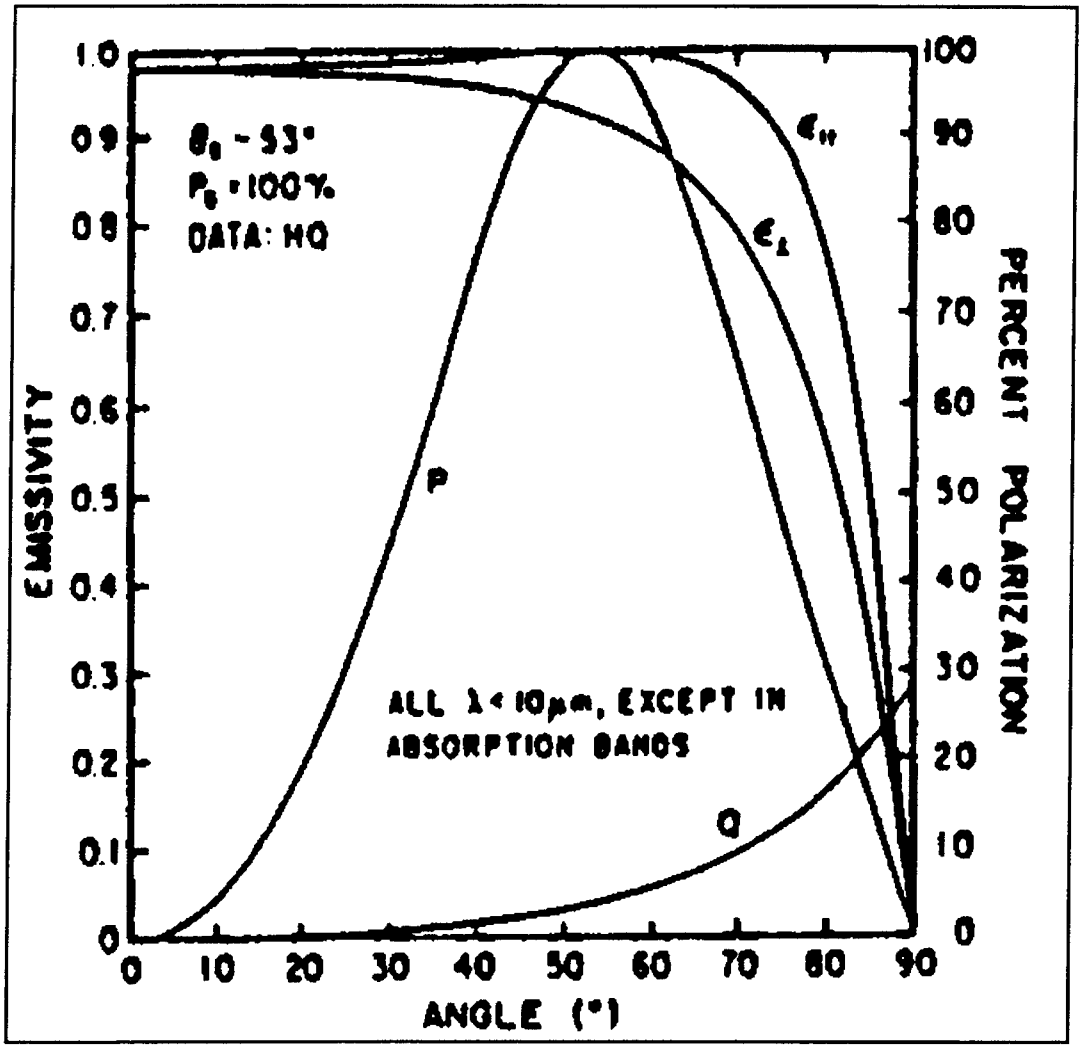

Figure 3.8 Emissivities and percent polarization for reflected and emitted radiation for all wavelengths below 10 microns (Sidran, 1991).

2. Infrared Polarization of Ship Signatures and Background Contrast

As stated before, the infrared radiance from the sea surface is composed of two components. These are the thermally emitted and reflected radiation given by

$$N_{tot}=(N_{sky})'+(N_{sea})' \tag{3.36}$$

$$N_{tot}=\rho(\theta)N_{sky}+\rho(\theta)N_{sea} \tag{3.37}$$

where each component depends on the reflectivity and emissivity of the sea surface averaged over the distribution of wave facet orientations. The emissivities for parallel and perpendicular polarizations are

$$\epsilon_{eff}^{h}=\epsilon_{h}\cos^2(\alpha)+\epsilon_{v}\sin^2(\alpha) \tag{3.38}$$

$$\epsilon_{eff}^{v}=\epsilon_{h}\sin^2(\alpha)+\epsilon_{v}\cos^2(\alpha). \tag{3.39}$$

In terms of average apparent radiance the degree of polarization is given by

$$POL=\frac{<N_v>-<N_h>}{<N_v>+<N_h>} \tag{3.40}$$

and the radiance difference (absolute contrast) for any polarization can be written as

$$\Delta N=<N_{target}>-<N_{bkgd}>. \tag{3.41}$$

Thus, the polarization improvement factor for contrast for horizontal filters over vertical filters is

$$F=\frac{\Delta N_v-\Delta N_h}{\Delta N_v+\Delta N_h} \tag{3.42}$$

(Cooper, Lentz, Walker, Chan, 1994).

Contrast relative to the background is most commonly defined as the difference between target radiance and background radiance divided by the background radiance,

$$C=\frac{N_{tgt}-N_{bkgd}}{N_{bkgd}} \qquad \textbf{3.43}$$

Contrast improvement then is defined as the ratio between polarized contrast and unpolarized contrast,

$$(C_{imp})_{pol}=\frac{C_{pol}}{C_{up}} \qquad \textbf{3.44}$$

Contrast between an unpolarized target against a sea background outside of sun glint regions should be improved with the use of polarization filters. Man-made targets do not indicate any predominant polarization (Cooper, Lentz, Walker, Chan, 1994). Therefore, horizontal polarization filters would reduce the predominantly vertically polarized sea background radiance. Although each filter will reduce the unpolarized target radiance by a factor of approximately two, the reduction in sea background radiance should be greater. This will increase the numerator of Equation 3.43 for horizontal polarization while reducing the denominator. Thus, an overall improvement in contrast would be realized.

IV. DATA ANALYSIS

A. MAPTIP EXPERIMENT

The polarization image data utilized in this thesis was obtained during the Marine Aerosol Properties and Thermal Imager Performance Trial (MAPTIP) held October 11 through November 5, 1993. The purpose of the experiment was to obtain atmospheric propagation data below 10 meters elevation in the 3-5μm and 8-12μm bands. Accurate atmospheric prediction codes are necessary for properly analyzing the performance of electro-optical detection and tracking systems. Currently the Navy Atmospheric Model (NAM) used in LOWTRAN7 effectively predicts infrared propagation in the marine boundary layer above 10 meters. The Navy Oceanic Vertical Atmospheric Model (NOVAM) predicts dynamic marine aerosol composition for specific marine environments within the marine boundary layer. MAPTIP is expected to provide coastal atmospheric propagation information to extend NOVAM to the littoral environment (Jensen and de Leeuw, 1993). Image data used in this thesis was obtained during the experiment and is of the Hr. Ms. Tydemann (TDM), an oceanographic ship, and of a Lynx helicopter.

B. DATA COLLECTION EQUIPMENT

Image data was acquired during MAPTIP using the NPS AGA 780 Thermovision Thermal Imaging system. Images were stored using AGEMA CATS data acquisition program.

1. AGA 780 Thermovision Thermal Imaging System

The version of the AGA 780 Thermovision Thermal Imaging System used during MAPTIP is a dual band serial scanning infrared imager. The AGA 780 operates two scanning systems side-by-side. One system covers the 3-5.6 μm and the other covers 8-14 μm wavelength bands. Each utilizes a 7°x7° field of view lens that focuses incoming infrared radiation through a dual rotating prism system onto their respective detectors. The short wave lens is silicon, and its detector is an indium antimonide (InSb) photovoltaic detector. The long wave lens is germanium and its detector is a mercury-cadmium-telluride (HgCdTe) photovoltaic detector. The detectors are cooled to 77K by dewars filled with liquid nitrogen. The radiation passes through a vertically mounted prism rotating at 180 rpm followed by a horizontally mounted

prism rotating at 18000 rpm. The rotating prisms are synchronized electronically to the monitor's vertical and horizontal scans. This synchronization of the prisms serves to generate four fields of 100 horizontal scan lines each. Only 70 lines in each field are used for producing an image; the four fields are interlaced to produce an image of 280 lines. The scanner operates at 25 fields per second. Thus, 6.25 images per second are generated. The detectors produce a current signal called "thermal value" proportional to the intensity of radiation received. This signal is amplified and converted into a video signal for monitor display.(AGA Operating Manual, 1980)

2. Thermal Imager Calibration Technique

The Stefan-Boltzmann law predicts a bolometric intensity proportional to the fourth power of temperature. Although the intensity of radiation received at the detector is presumed to be proportional to the system's "thermal values," this signal is a non-linear function of temperature. The AGA 780 requires calibration with a laboratory blackbody source. The system output of "thermal value" is recorded against the blackbody temperature through a range of temperatures. The calibration curve is generated through a least squares fit method and is of the form

$$I=\frac{A}{Ce^{\frac{B}{T}}-1}-OC \qquad 4.1$$

where A, B, C are constants specific to the combination of scanner, lens, and filters used during the calibration.(AGA Operating Manual, 1980) The OC is for an offset correction. This correction was applied during MAPTIP to adjust for detector response drift (Chan, 1993).

3. Polarizers

The polarizers utilized during MAPTIP were Cambridge Physical Sciences Model IGP-228-71 with a diameter of 71 mm. The polarizing material is a 0.12 μm aluminum grid of 0.25 μm pitch on a substrate of barium fluoride. They have 85% transmissivity and 98% polarization at 3.9 μm. The polarizers were placed externally on the scanner lens systems and rotated manually to achieve vertical and horizontal polarizations.(Chan, 1993) The filters placed externally reduce the system sensitivity due to the added attenuation effects of the filters. Any change in system setup, such as including filters requires recalibration on the AGA 780 (AGA OP MANUAL, 1980).

4. AGEMA CATS Program

The AGEMA CATS software allows for processing images immediately or for storing images to be analyzed in the future. The program is used by two PC's, each connected to one of the scanner channels and obtains every other field produced by the AGA 780. Thus CATS generates a 140x140 array for each image recorded.

C. IMAGE PROCESSING AND ANALYSIS

Although processing capability is available with AGEMA CATS, this thesis utilizes the Interactive Data Language for all image processing and analysis.

1. Interactive Data Language (IDL)

The Interactive Data Language (IDL) program was used to conduct the analysis in this thesis. This software is an array-based system with extensive capabilities in image processing. Numerous analysis methods and graphical representations are available for both programming and interactive manipulation. All images and most plots displayed in this thesis were produced with IDL and converted to TIFF files. The files were then printed with Pagemaker4. Three IDL programs were produced in the course of this thesis and are presented in Appendix A. Also, numerous routines were generated to help with the analysis of images and subsequently to assist in the formulation of the three analysis techniques contained in the programs of Appendix A.

2. Image Format

As stated earlier, all images were recorded by AGEMA CATS for processing by IDL. Each image is stored as a 140x140 byte file. The first 846 bytes of the file contain various image information tags, such as filename, date, time, offset correction applied, etc. An example of this "header" information is shown below.

Thu Nov 17 17:42:44 1994 Date of ANALYSIS
e:\holland\oct19\lw

filename	level	range	offset	over	under	date	time
OCT19100.IMG	48.80	2.00	-32.00	19600	0	10/19/93	13: 4:54
OCT19101.IMG	44.20	2.00	-32.00	1226	13379	10/19/93	13:13:11
OCT19102.IMG	44.20	2.00	-32.00	1175	16313	10/19/93	13:13:19
OCT19103.IMG	44.40	5.00	-32.00	226	5716	10/19/93	13:13:29

The image file is read into a 140x140 array in IDL. The array values are the scanner generated thermal values scaled from 0 to 255. Zero represents the coldest value in the image and 255 represents the hottest value viewed (AGA Manual, 1980).

3. Narcissus Effect

All the MAPTIP images show a dark spot in the center of the image similar to that shown in Figure 4.1. This is known as a Narcissus spot. The Narcissus spot is created by retro-reflection of radiation from the detector plane by the external filters. Radiation from the cold detector mounting at approximately 77K reflects back toward the detector. The geometry of the internal optics are such that the cold detector radiation focuses on the detector as a small circular region near the center of the image. The effect of the Narcissus spot in addition to the scene obstruction encountered is to reduce the effective dynamic range. The extremely low values of irradiance from the Narcissus relative to the average scene value compresses the range of scene values in the upper end of the dynamic range, resulting in a loss of scene resolution.(Lloyd, 1975)

The Narcissus in the system used occurs because the filters are mounted normal to the radiation from the detector plane collimated by the lens system. The reflected radiation is then focused back on the detector plane. Without the filters installed, the Narcissus is not present.

Images were taken with regard to the Narcissus spot. Target images were placed away from the central Narcissus spot during data collection to reduce its affect. Although the Narcissus could in principle be removed by image processing (Chan, 1993), it would be difficult if not impossible to replace the lost information accurately with other than an average or a randomly modulated average background radiance value. In many images, a substantial depression in background is realized that is difficult to ascertain from a strict viewing of the image alone. This affect can be seen in Figure 4.11 as not only the hole from the Narcissus, but also the depressed trough spanning the length of the image.

4. Ship Location Techniques

Calculating ship-to-background contrast requires a distinction between ship data and background data. The ship or other target of interest must be located within the image array in order to process the target data separately from the background

data. This requires a contrast between the ship and background as given by Equation 3.41. Three primary methods for processing the image array data are presented below. All three utilize a thresholding method for locating the ship. Essentially, thresholding means acceptance of only pixels values of the array representing brightness that are above a defined threshold and setting to zero all values below this threshold. Ideally, all ship pixel values are required to be above the threshold and all background pixels values below. Ship pixel values below the background level may be lost. Technically, to remove all the background, the threshold must be set to the maximum background value. Loss of ship radiance values below this value is possible.

Care must be taken to compare appropriate background and ship values. Figures 4.1a and 4.2a show typical high signal-to-noise ratio images for vertical and horizontal polarizations, respectively. Figures 4.1b and 4.2b depict corresponding radiance profiles. The dark curves represent the average ship radiance profile. This is calculated by summing the ship radiance along each row of the image array and dividing by the number of ship pixels in that row. The gray curves depict the background radiance profile. This is calculated below the horizon by averaging all pixels that are not ship pixels. Above the horizon the average is calculated using only pixels along the edge of the image to avoid the Narcissus. Figures 4.3a and 4.4a show similar images for low signal-to-noise ratio images. Representative background profiles of the image in Figure 4.1a are depicted in Figure 4.5a and 4.6a. The upper curve in Figure 4.5a shows the sea radiance profile near the bottom of the image. The three lower curves show the sky radiance profiles. The topmost of the three curves represents the lowest elevation. The lower curves represent sequentially increasing elevation. Thus, the sky radiance decreases with elevation. Figure 4.6a shows a vertical slice through the image background. Analysis of this figure and Figure 4.5a reveals that the background varies significantly in the vertical and less in the horizontal ignoring effects from the Narcissus spot. The background is approximately constant in value below the horizon, but rises sharply above the horizon and then tapers off at higher elevations. Therefore, to accurately define the contrast between the ship and background, the ship values below the horizon should be compared with background values below the horizon. Likewise, ship values above the horizon should be compared with background values above the horizon. In addition, the pixels used to

calculate the background average values should be as close to the ship as possible to represent accurately the contrast between the ship and the background in the immediate vicinity.

Thresholding works well for targets with a high signal-to-noise ratio. However, choosing an appropriate threshold value is not clearly defined and somewhat subjective. Figure 4.7a shows the image from Figure 4.1a and 4.2a above using a threshold value equal to the background average value times 1.2. As the threshold value is increased to (1.3) x (background average) in Figure 4.7b and (1.5) x (background value) in Figure 4.7c more of the ship is deleted along the edges. From Figure 4.7a it is clear that choosing a threshold value is not difficult for high signal-to-noise ratio targets. Figure 4.8 shows the low signal-to-noise ratio image of Figures 4.3a and 4.4a with background multiplying factors of 1.01, 1.03, and 1.05, respectively. In this series of images some background exists in the remaining image along with the ship. In this particular case, the background can be separated from calculation of ship radiance by confining the calculations to a region near the ship. However, in many images, some background remains too close to the ship to avoid and also introduces a varying source of error. As the background factor is increased sequentially, thus increasing the threshold values, more of the background from the previous image is removed. However, increasing amounts of the ship image are removed, also. Appropriate thresholding is a balance between removing a sufficient quantity of background while retaining a representative amount of the target ship. This balance becomes increasingly difficult with lower signal-to-noise ratio targets. Often, a large part of the ship is not visible over the surrounding background and cannot be located in the image. These concepts are further described and applied in the following image processing programs.

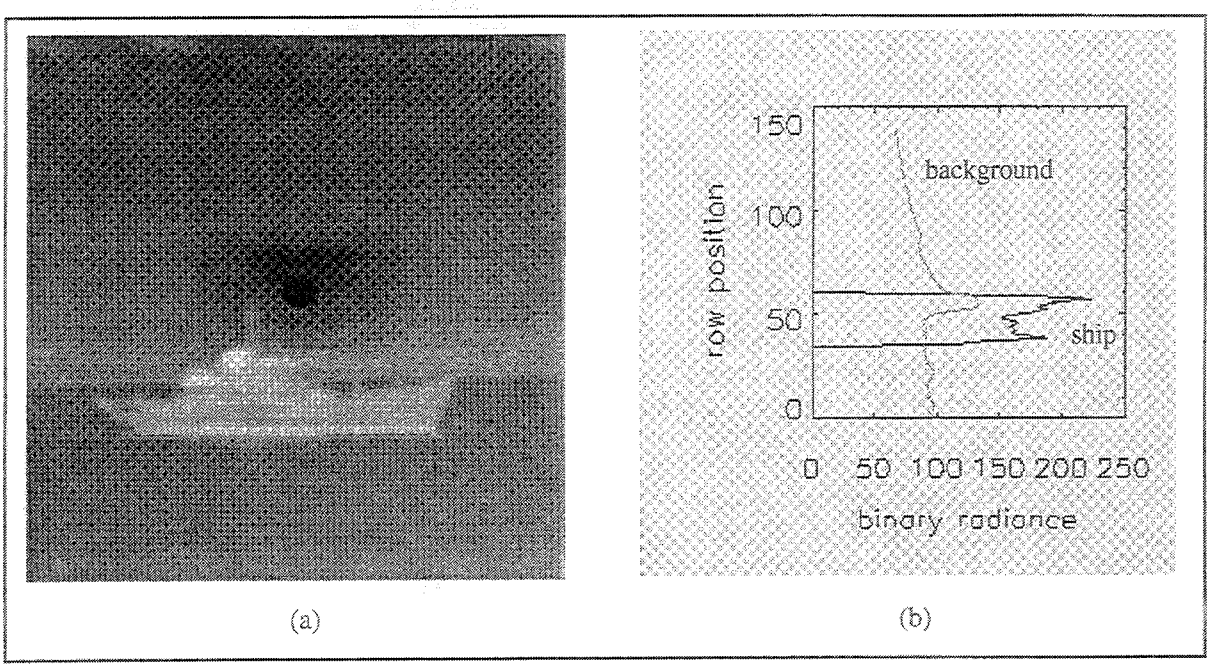

Figure 4.1 Vertical Polarization for high signal-to-noise ratio image (a) IDL generated image taken at 1313 Oct 19, 1993, (b) Average ship and average background apparent radiance profiles. Ship radiance is denoted by the black curve and background radiance by the gray curve.

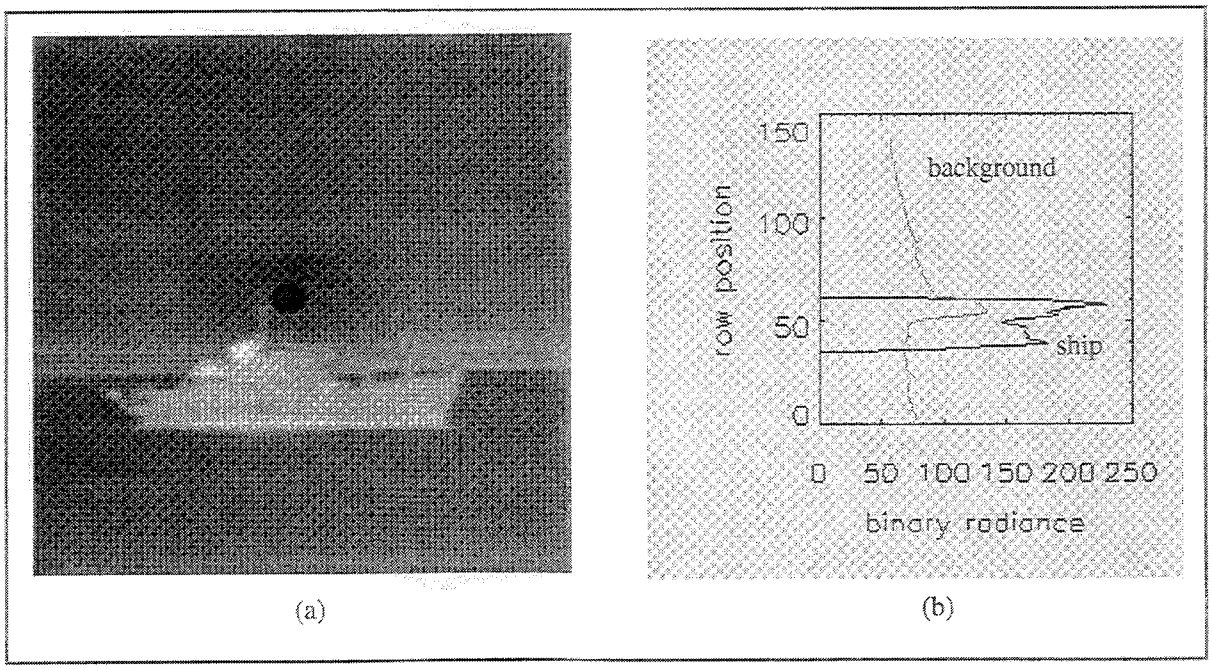

Figure 4.2 Horizontal Polarization for high signal-to-noise ratio image (a) IDL generated image taken at 1313 Oct 19, 1993, (b) Average ship and average background apparent radiance profiles. Ship radiance is denoted by the black curve and background radiance by the gray curve.

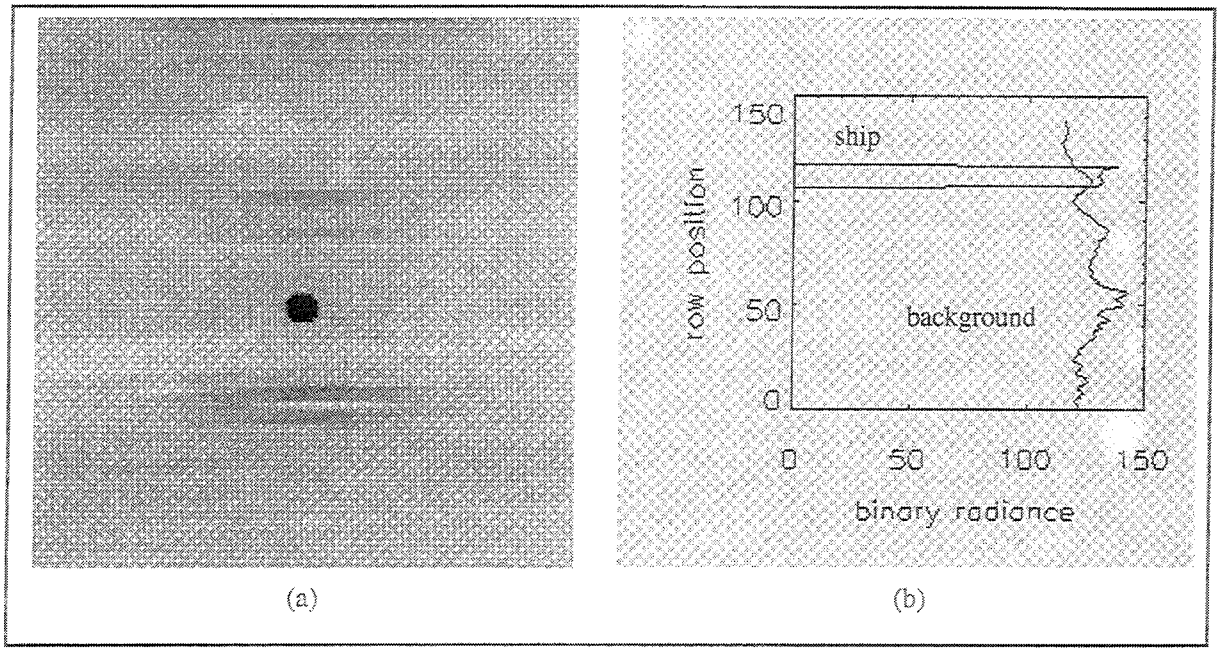

Figure 4.3 Vertical Polarization for low signal-to-noise ratio image (a) IDL generated image taken at 0915 Oct 28, 1993, (b) Average ship and average background apparent radiance profiles. Ship radiance is denoted by the black curve and background by the gray curve.

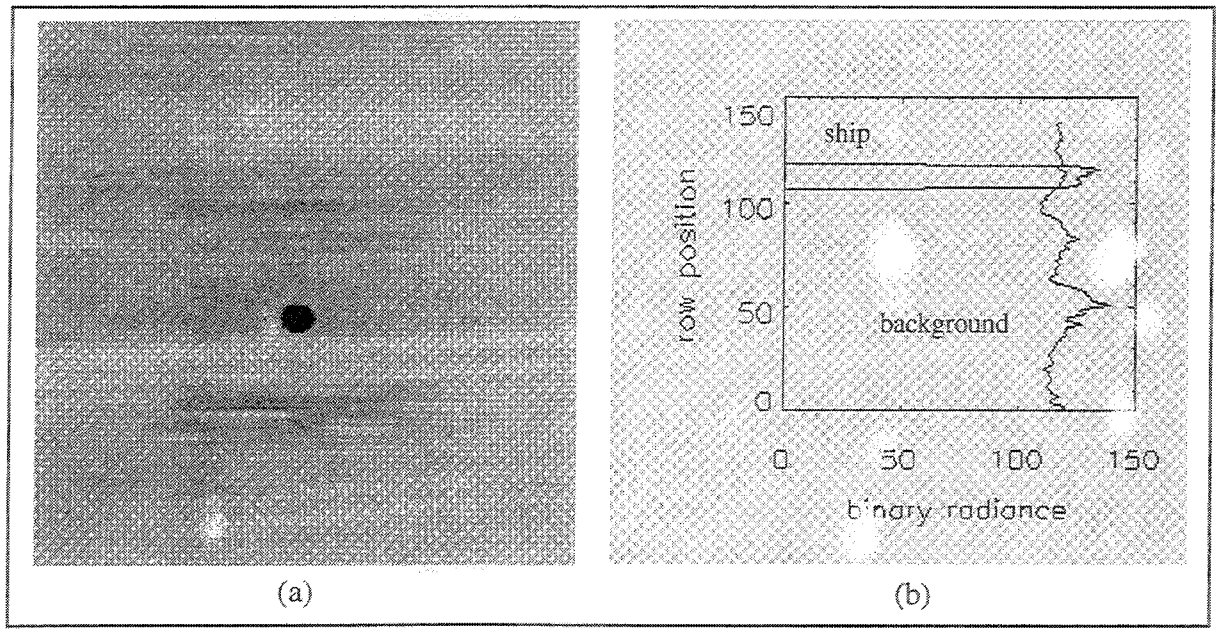

Figure 4.4 Horizontal Polarization for low signal-to-noise ratio image (a) IDL generated image taken 0915 Oct 28, 1993, (b) Average ship and average background apparent radiance profiles. Ship radiance is denoted by the black curve and background radiance by the gray curve.

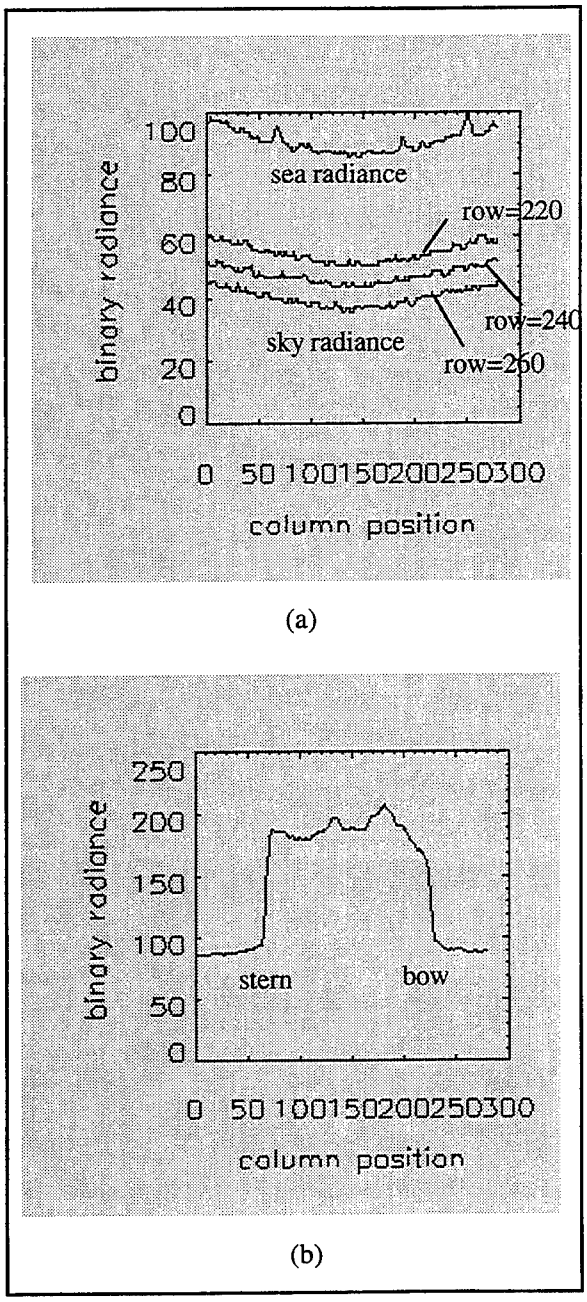

Figure 4.5 Horizontal profiles for high signal-to-noise ratio image (a) Upper curve shows sea background, lower three curves show sky background, with highest of the three representing the lowest elevation(b) Profile through ship. Wings represent sea background.

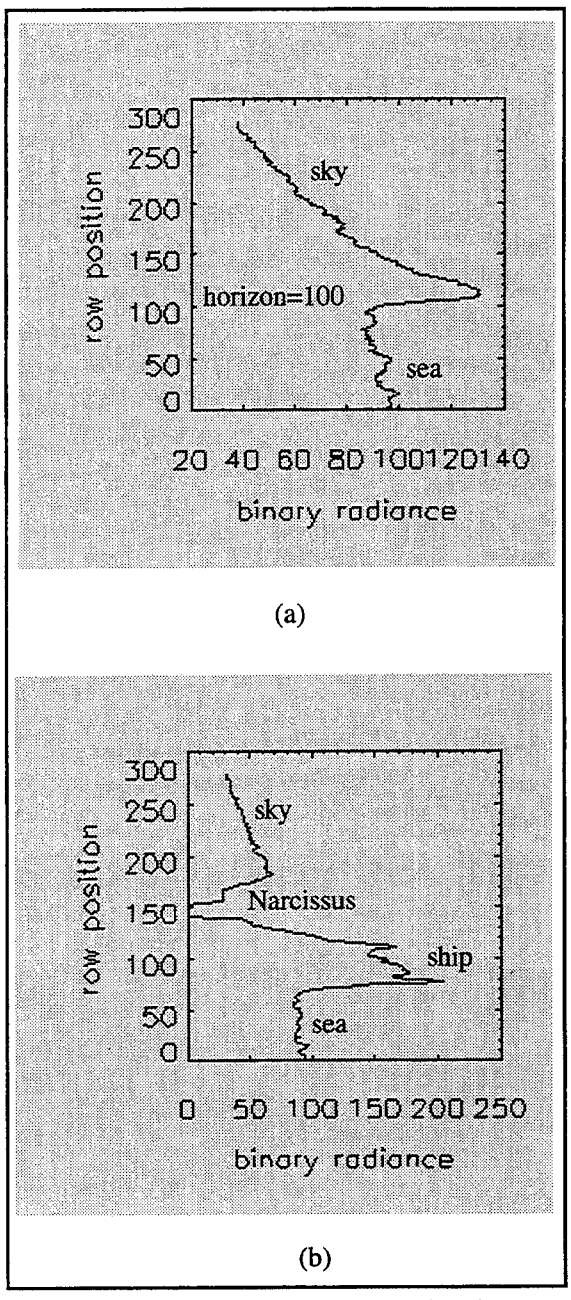

Figure 4.6 Vertical profiles for high signal-to-noise ratio image with horizon at position 100 (a) Background, (b) Profile through ship. Note cold spot from Narcissus where radiance drops to zero. Ship located at large spike centered on position 100.

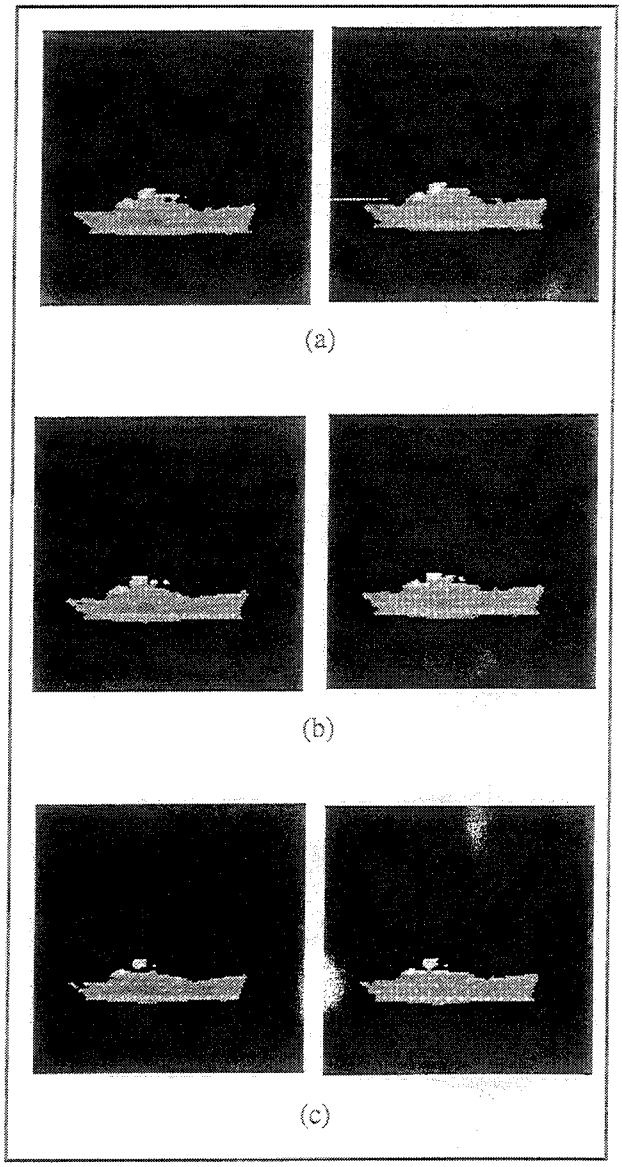

Figure 4.7 Thresholding high S/N ratio image. Left image is vertical polarization and right image is horizontal polarization (a) Background factor = 1.2 (b) Background factor = 1.3 (c) Background factor = 1.5.

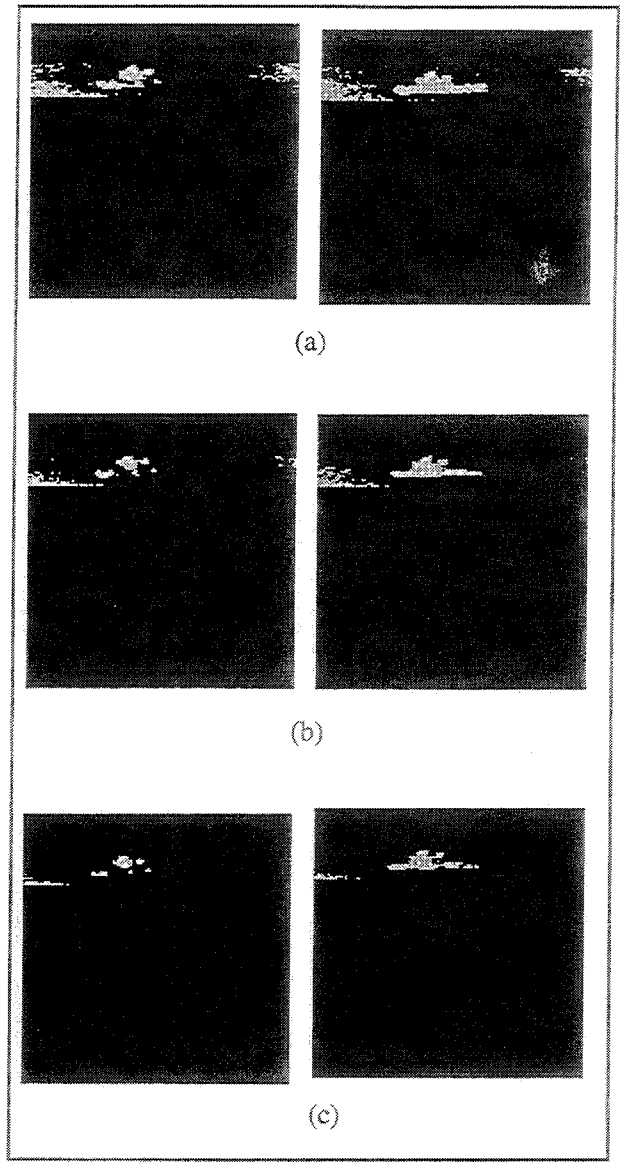

Figure 4.8 Thresholding low S/N ratio image. Left image is vertical polarization and right image is horizontal polarization (a) Background factor = 1.01 (b) Background factor = 1.03 (c) background factor = 1.05.

5. Image Processing Programs

This section presents three processing programs developed to calculate the contrast improvement factor associated with the visual improvement in contrast apparent in the MAPTIP images. Although contrast improvement in horizontal polarization over vertical polarization is visually apparent in the image pairs, the pursuit of these programs was to quantify the contrast improvement of horizontal and/or vertical polarization over unpolarized images. These methods are limited to the apparent radiance received and recorded as image files. The calculations do not consider visual modulation transfer functions associated with the detection or identification of an image as a ship, helicopter, airplane, etc. The computations account for the relative differences in apparent radiance between target images and background.

Crucial to these calculations is the concept of generating an unpolarized image from two images of opposite polarization. Stokes showed that light intensities of perpendicular polarizations can be added to obtain an unpolarized image or that the intensities of a polarized and unpolarized image can be added to obtain a partially polarized image (Collett, 1993). The AGA 780 response is proportional to the intensity of radiation received (AGA Operating Manual, 1980). Therefore, the addition of a vertically polarized image with the same image in horizontal polarization produces an unpolarized representation of the image. However, the CATS program stores the images scaled relative to 0-255 with zero being the lowest radiance received and 255 the highest radiance received. Also, IDL displays images as byte array values on the same scale. Therefore, to produce the unpolarized image with IDL, the two polarized images are averaged as

$$\langle N \rangle_{up} = \frac{\langle N \rangle_v + \langle N \rangle_h}{2} \qquad 4.2$$

Image registration is another important element in the process. Since the images are not taken simultaneously, the ship has moved between images. Vertically this is usually not more than a couple of scan rows, but even that may be significant. However, depending upon ship speed and range, the movement horizontally may be

substantial. This prevents the straight addition of the individual arrays. The ships within the arrays must be registered on to each other in order to average their values.

a. Contiguous Area Method

The contiguous area method was produced by W.J. Lentz at the Naval Postgraduate School. This program automatically finds the hottest spot in the image and works through a contiguous set of pixels to the edges of the ship where the temperature drops. The spot may be chosen if the hottest spot is background clutter. Pixel values above a set background threshold value are chosen and all others set to zero. The background threshold value may be varied. Each horizontal line in the image is ascribed a background temperature based on a smoothed average along the edges of the image. The values are used to find variations in temperature along the horizontal lines that could represent the ship. A small temperature difference might miss much of the ship. For this reason the search is iterative over the entire image using an edge threshold. Once the ship is detected, another threshold is taken in a box around the ship. This corrects for effects such as the Narcissus spot superimposed on the image. The output is a file that gives the contrast of the ship to background in a local box that extends to the limits of the ship.(Lentz, 1994)

The thresholding idea was first used to discern the ship from the background in a joint experiment with NOSC. In that experiment, the AGA 780 was used without polarizing filters, and it was relatively easy to find the ship. In the MAPTIP experiment, the signal-to-noise ratio was much worse both because of the polarizers that reduced the signal but also because the targets were generally much further away. The earlier program either could not find the ship or would include too much background with the ship. In addition, the sink-hole effect in the center of the AGA pictures caused by the Narcissus effect produced additional distortions that caused problems. The essential idea to correct these problems is the contiguous point finding program in IDL called search2D used in the subroutine shipfind.pro. It starts from the designated hot spot and eliminates noncontiguous points from the picture. Thus what remains is a continuous matrix of pixels values that are above threshold. All pixels not connected to the hot spot are set to zero. Then a box is defined at the x and y limits of the ship. Then the threshold which had been at the edge of the picture is redefined for the vertical edges of the box in which the ship is contained. The

process is repeated producing a cleaner ship with a lower allowable temperature difference for background.(Lentz, 1994)

Since ship pictures are taken in pairs, the program takes the next image and compares it to the previous image and combines the ship images to produce an unpolarized ship image. The ship may have moved slightly from picture to picture, so the program adjusts for the motion of the box. One polarization or the other will have an improved contrast over the background resulting in a larger ship image with more pixels. In some cases, for example, the ship will consist only of a smokestack with one polarization and in the other the entire ship will be clearly defined. In order to properly compare the contrasts, the ship with the larger number of pixels is used to redefine the ship outline in the poorer picture. The box and ship sizes are the same for both pictures giving a better calculation of the polarization improvement. The ship contrast is formed between all the points on the ship and all the points in the box containing the ship that are not the ship. This is done for both polarizations and for the sum of both polarizations. (Lentz, 1994)

The significant advantage of this program is its autonomy. Many image pairs can be processed in a minimum amount of time. However, this program does not compare the entire ship as observed. Since only contiguous areas are used, only the contiguous area containing the hot spot of each ship image is used to calculate contrast.

b. Outline Method

The "outline method" is an attempt to overcome the difficulty of finding a low signal to noise ratio ship image and is provided in Appendix A as the program outlin15.pro. The high signal-to-noise ratio ship image of Figure 4.1 was used to generate a block outline of the beam aspect of the ship. The outline was referenced to an IDL generated box function. This allowed for processing ship targets at various ranges since at longer ranges the ship takes up less area in the field of view. When the box is placed around the ship touching only the stack, bow, stern, and waterline, the outline is scaled to fit the ship. If only part of the ship is visible, then judgment is required to align the box properly.

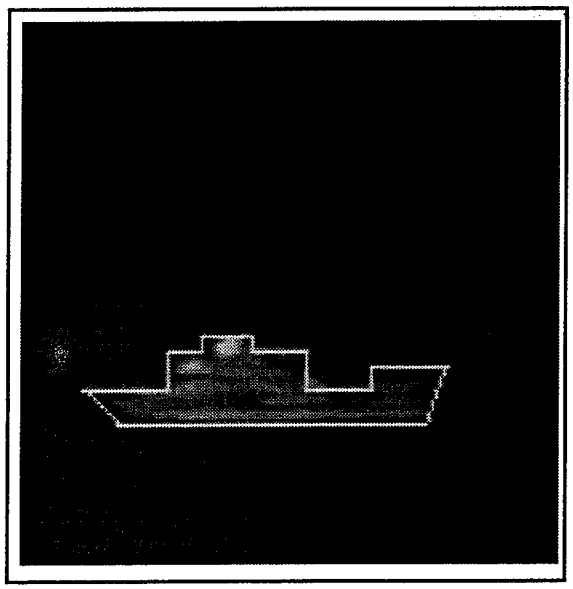

Figure 4.9 IDL ship image with outline in place.

Once the box is placed around the ship, average background values are calculated row by row using five pixels to either side of the box. The outline is drawn referenced to the box as shown in Figure 4.9 All processing was performed on raw data image files. Figure 9 is an expanded file of dimensions 280 x 280. This expansion process consists of doubling the size of each side of the image array. The new pixel positions are filled by linearly interpolating between the original pixels. Note the "steps" created during the expansion along the bow and stern outlines. All pixels outside of the box are then set to zero. The average background value of each row multiplied by an input factor to account for pixels above the average is used to set to zero any remaining pixels within the outline below the threshold. Originally, the background average values were calculated using the five pixels on either side of the outline. Ship edge effects and even a slight error in placement of the IDL box lead to significant errors in background average values when part of the ship registers as one or more of the 10 background pixels, i.e. part of the ship falls outside of the identified boundary. Therefore, five pixels on either side of the box were used to generate average background values for each row.

At this point all that remains in the array is the visible portion of the ship. Then the program steps through each row calculating the average ship value of that row using the remaining pixels in that row. This produces a profile of the average ship values which can be displayed graphically as in Figure 4.1b and 4.2b. A second image and profiles are produced for the perpendicular polarization. The profiles of contrast and contrast improvement may also be represented similarly. Then using these values average contrast and average contrast improvement for above and below the horizon may be determined.

However, coupling of the ship areas is required. Calculating average ship values of the individual polarizations without coupling the areas is comparable to comparing images of two different targets. However, this method erroneously accounted for this coupling. First, the "outline method" assumes that the ship images are registered exactly due to the outline placement. Therefore, each row of one image is compared to its respective row in the orthogonal polarization. A 140 x 140 image window on the computer monitor is 38mm x 38mm. This requires accurate placement of the box around the ship to within 0.27mm. The assumption of proper registration is

invalid. Second, coupling was achieved by comparing the number of ship pixels in a given row to the number of ship pixels in the same row of orthogonal polarization. The row with the most pixels and thus the larger area must represent the minimum actual ship area along that elevation. Then the sum of pixels along both rows was divided by the larger number of pixels to obtain the effective average ship radiance at that row. This erroneously reduces the apparent average radiance of the row with the lower number of pixels.

Several problems exist with the "outline method" in addition to the coupling described above. It is difficult to place the box properly around low signal-to-noise ratio ship images. Improper placement and sizing results in the outline pattern not including all of the ship on one side and including excess background on the opposite side. The major drawback with the "outline method" is that it is restricted to beam aspect only. The image array may be inverted without loss of information in order to utilize the outline on either the port or starboard aspect. However, more detailed programming is required to allow for other than beam aspects although this method is probably too cumbersome to provide accurate outlining in other than beam aspects.

c. Box Method

The "box method" is the most simple of the three methods presented. In fact it was the first one attempted, but later dropped to permit experimentation with the previous methods. This method simply places a box around the ship and determines the average background value about the ship row by row using the five pixels to either side of the box. All pixels outside of the box are set to zero. Then a threshold is obtained using the average background value and an additional amount to account for background values above the average. As before the values below this threshold within the box are set to zero. However, this method contains a significant change in the fundamental interpretation of the calculation of average ship value.

The "outline method" calculated the number of pixels per row that were ship pixels for both vertical and horizontal polarizations. The larger number of ship pixels along with the sum of ship values per row were used to calculate average ship value for vertical and horizontal polarizations. The two polarizations were then averaged to produce an unpolarized image. This method was flawed because it

improperly couples together the two images with respect to ship area. The image with the smaller number of pixels is considered to have an area greater than the actual area. Thus pixel values of zero are included in calculating its average radiance. Since the ship pixel values must be at least that of the background, assigning them a value of zero is incorrect. This error reduces the calculated average radiance. The "box method" corrects for this flaw.

6. Box Method Generation of Unpolarized Image

In the "box method" the respective ship areas in the vertical and horizontal polarizations are coupled. The ship areas are represented by the number of ship pixels in the image. Ship area is subdivided further with respect to ship area above and below the horizon. The image with the larger area or greater number of pixels above or below the horizon defines the ship area for that region. In the other image of smaller area, the "missing" pixels are given a value equal to the background value. The sum of all pixels in their respective regions is divided by the total number of ship pixels in that region. Now both ship images contain the same area of ship surface. This couples the ship areas by referencing the average ship values to the same ship area. The motivation for this is that while part of the ship in one image cannot be seen over the background it actually is being seen with the value of the background. Now the average ship value of each polarization is being referenced to the same size or area of ship although this area is not necessarily the true ship projected area. Even the image with the larger area may not represent the total projected area if part of its radiance is the same as the background average. Without this coupling provided, the smaller ship image average value is calculated erroneously lower than the actual value leading to erroneously low contrast and contrast improvement values. In certain instances, the "outline method" produced negative contrast values which was impossible since the detectable ship is of higher radiance than the background. The negative contrast values indicated the existence of and led to the identification of the area coupling flaw.

Some image information is lost with the "box method." Since the average ship values above and below the horizon are calculated as the sum of all ship radiance values divided by the total number of pixels, the row by row profile information is lost. If the two ship images could be accurately registered, then a row by row comparison would be possible. However, since the relative radiance values of the ship images with respect to polarization do not differ beyond what could be attributed to noise, the profile information from these images would provide no new meaningful information.

7. Ship Signature Polarization

In an attempt to analyze the polarization differences between horizontal and vertical polarizations, two methods were used. The first is a three dimensional surface plot or surface representation. The second is a cross-sectional view of the image array or profile representation.

a. Surface Representation

A three dimensional surface plot of an image array is shown in Figure 4.10. The top image is of the vertical polarization of a ship image and the bottom is of horizontal polarization. Figure 4.11 shows the same plot rotated about the vertical axis. The effect of the Narcissus can be seen better from this angle. The Narcissus can be seen as the depression or hole in the middle of the plot. Additional damage by Narcissus depression can be seen emanating away from the primary "hole" in the form of a trough. This cold spot reduces the effective dynamic range of the array values by forcing the target radiance values to be compressed at the upper end of the dynamic range.

Comparison of the two surface plots shows that it is difficult to discern ship radiance value differences. What differences are present cannot be justified as anything other than noise. Also, it is difficult to determine polarization affects on the background. Lastly, this data provides no numerical information, although it does provide some visual insight. Some images such as the Lynx helicopter in Figure 4.12 exhibit flat surfaces in these plots as shown in Figure 4.13. These flat surfaces represent pixels values that exceed 255. Their actual apparent values are undetermined.

b. Profile Representation

An alternate representation is shown in Figure 4.5b and 4.6b. These show horizontal and vertical slices through the ship. All the slices of either vertical or horizontal profiles can be averaged to obtain a representative profile of the ship. The Narcissus spot and the nature of the background lead to averaging the background pixel value of each row instead of each column to produce a representative vertical profile. Vertical profiles complement the process of comparing ship row values with their respective background row values. Comparison of vertical profiles of horizontal and vertical polarizations again shows little polarization of radiation from the ship. However, vertical profiles show the effect polarization filters have on the below-horizon background radiation received. This is demonstrated in Figures 4.14 and 4.15. These graphs show superpositions of the average horizontal and vertical background radiance values and ship values. The unpolarized radiance would be the average of the two and positioned midway between the lines shown. The background radiation received below the horizon is significantly reduced with the horizontal polarization filter. A small difference in radiation received exists above the horizon. Thus, the sea background radiation is predominantly vertical polarized. No discernable difference exists along the ships in Figures 4.14b and 4.15b and thus the ship radiance is essentially unpolarized.

c. Average Value Calculation

The average value of ship radiance for a given polarization may be calculated with two methods. The first method calculates the ship average values for both above and below the horizon. The "box method" program reduces the current image array to only ship pixels and all other pixels are set to zero. The horizon is marked with the mouse cursor. The average ship value above the horizon is calculated simply by summing the pixels above the marked horizon and dividing by the number of ship pixels above the horizon. The average ship value below the horizon is calculated similarly.

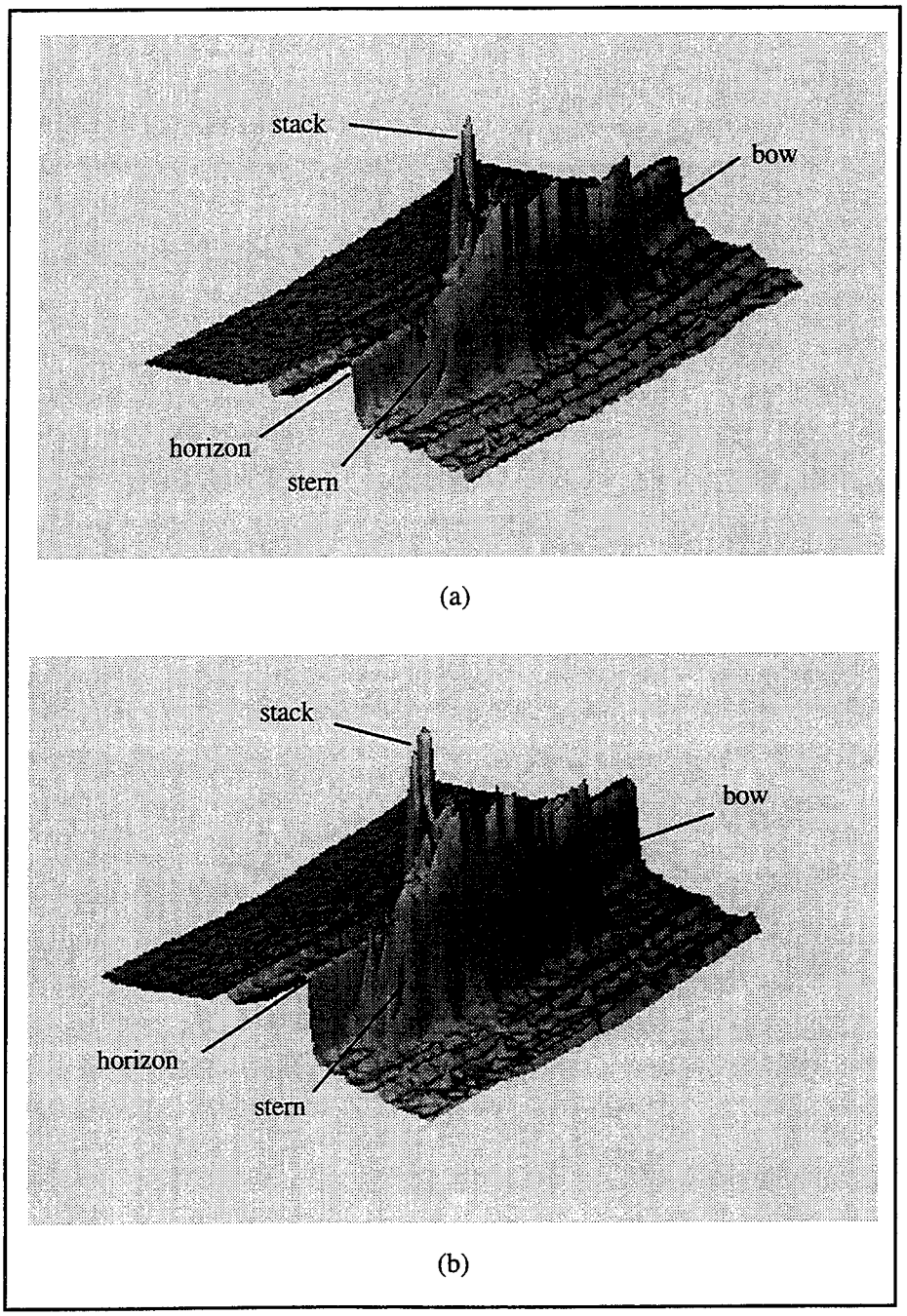

Figure 4.10 Surface plot of image in Figure 4.1a. Flatter base region represents background radiance value. Elevated portions show ship radiance values (a) Vertical polarization (b) Horizontal polarization.

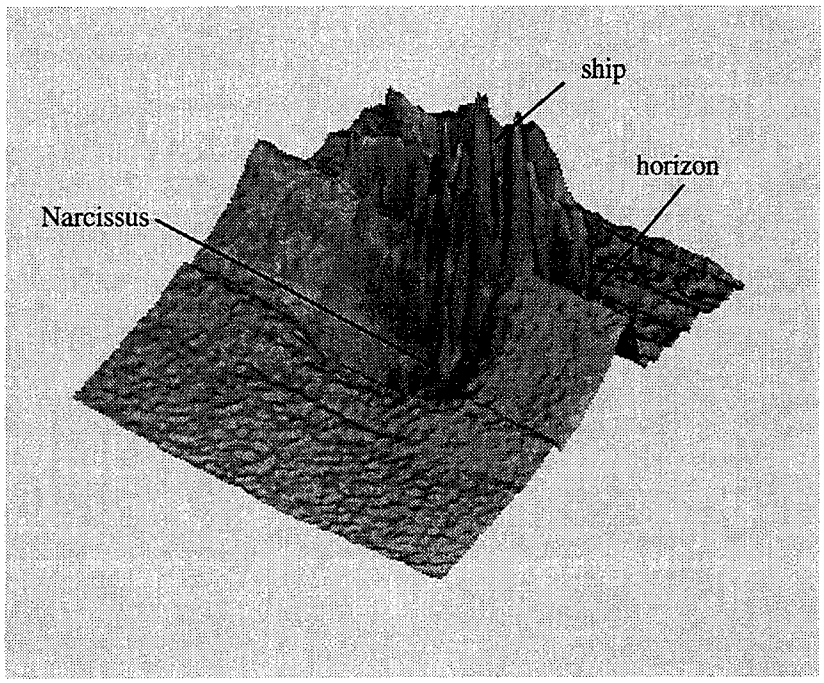

(a)

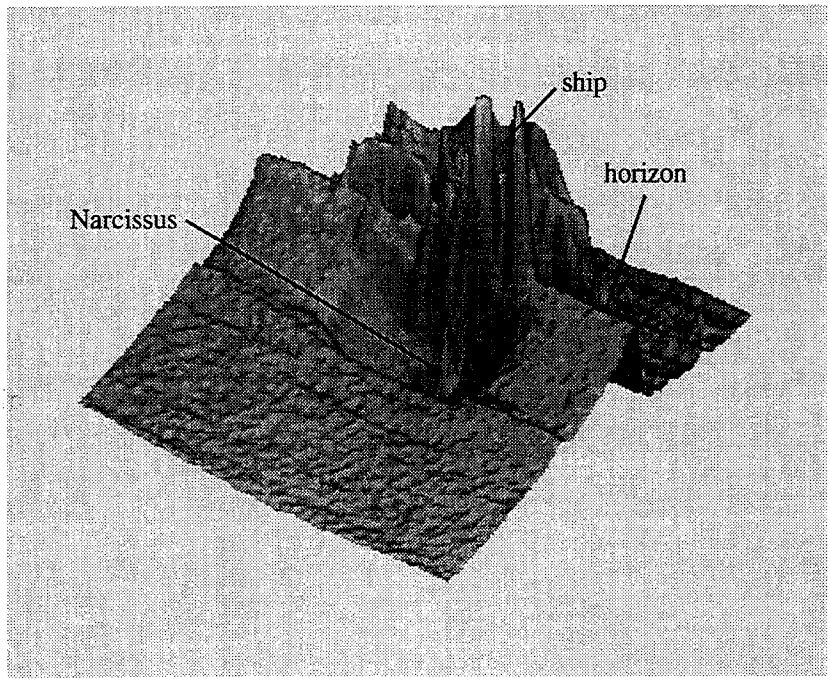

(b)

Figure 4.11 Surface plot of Figure 4.10 rotated (a) Vertical polarization (b) Horizontal polarization.

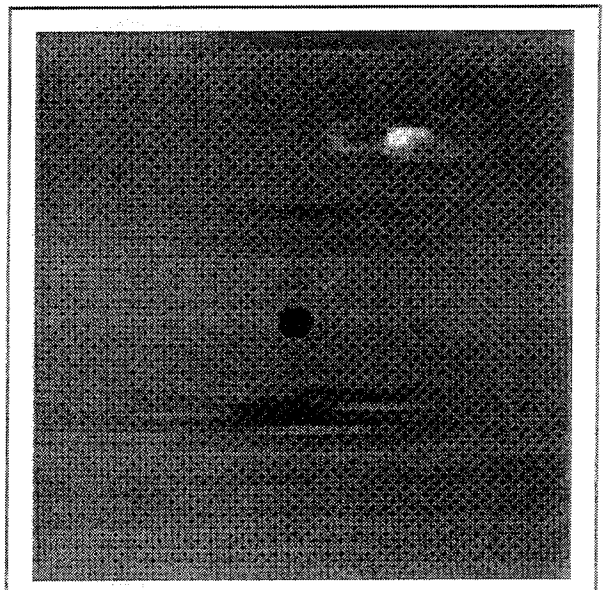

(a)

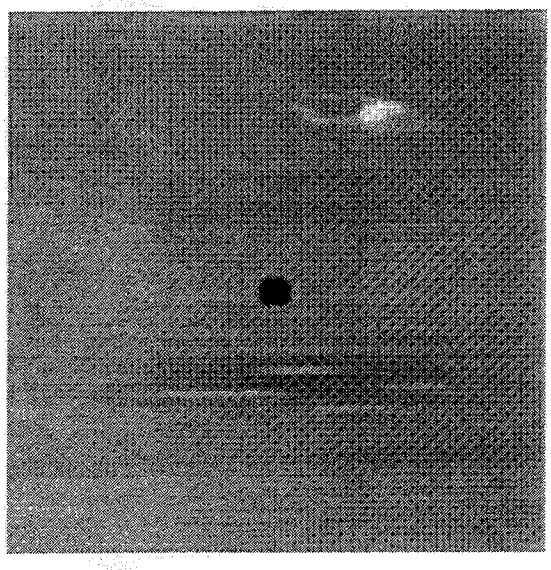

(a)

Figure 4.12 IDL generated image of Lynx helicopter
(a) Vertical polarization (b) Horizontal polarization.

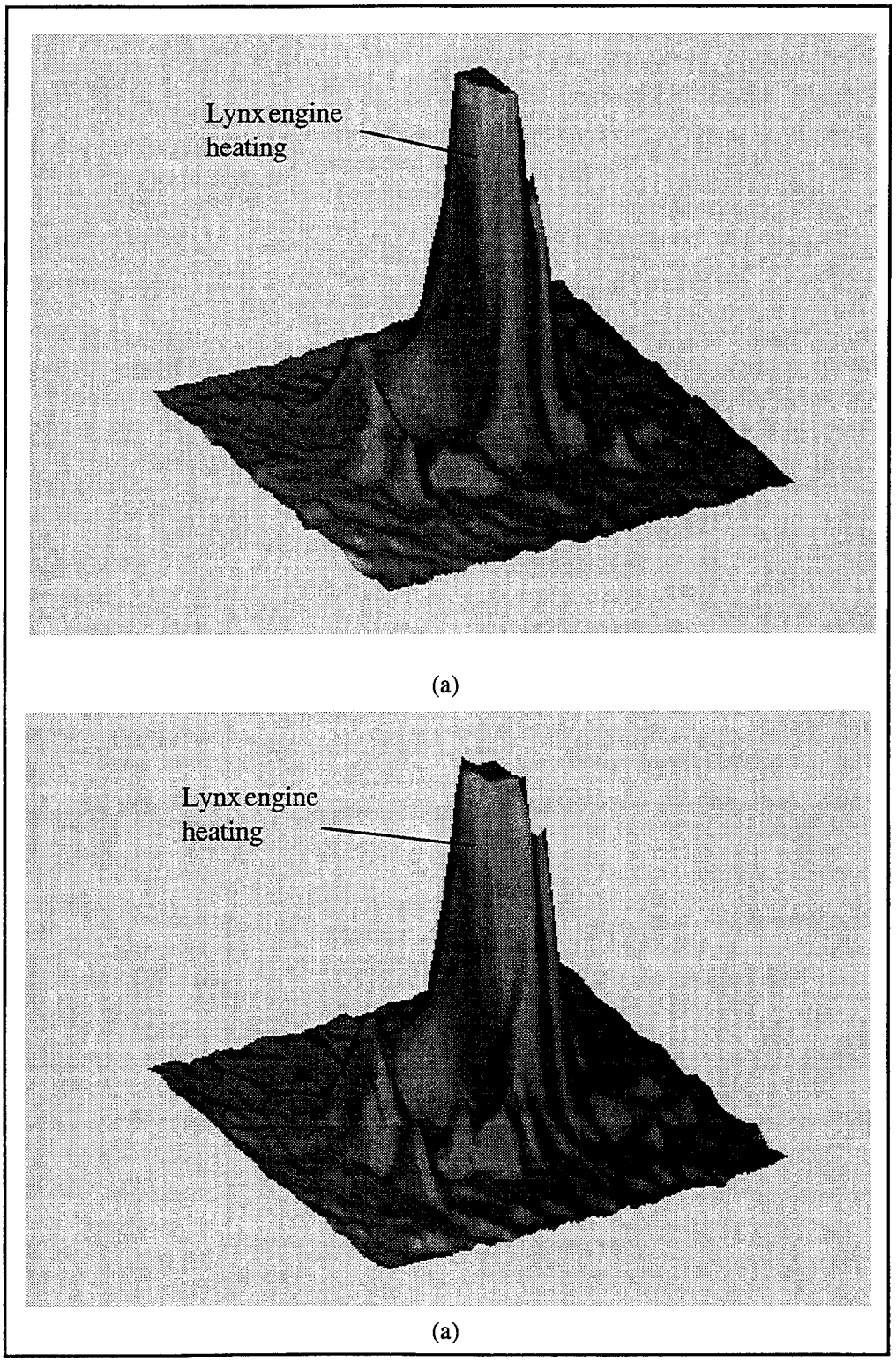

Figure 4.13 Surface plot of helicopter in Figure 4.12. Large spike shows the engine heating. Smaller peaks are from local hot spots on the helicopter (a) Vertical polarization (b) Horizontal polarization.

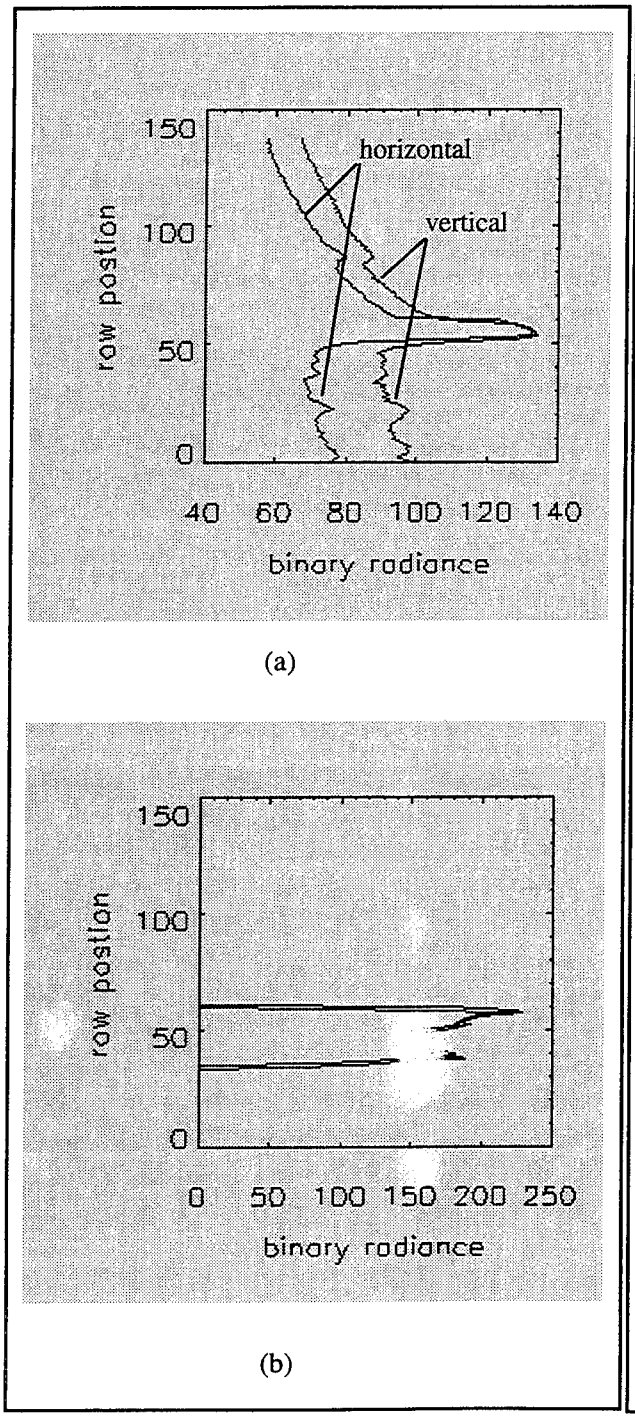

Figure 4.14 Characteristic apparent radiance profile comparisons for high S/N ratio image (a) Background comparison (b) Ship comparison.

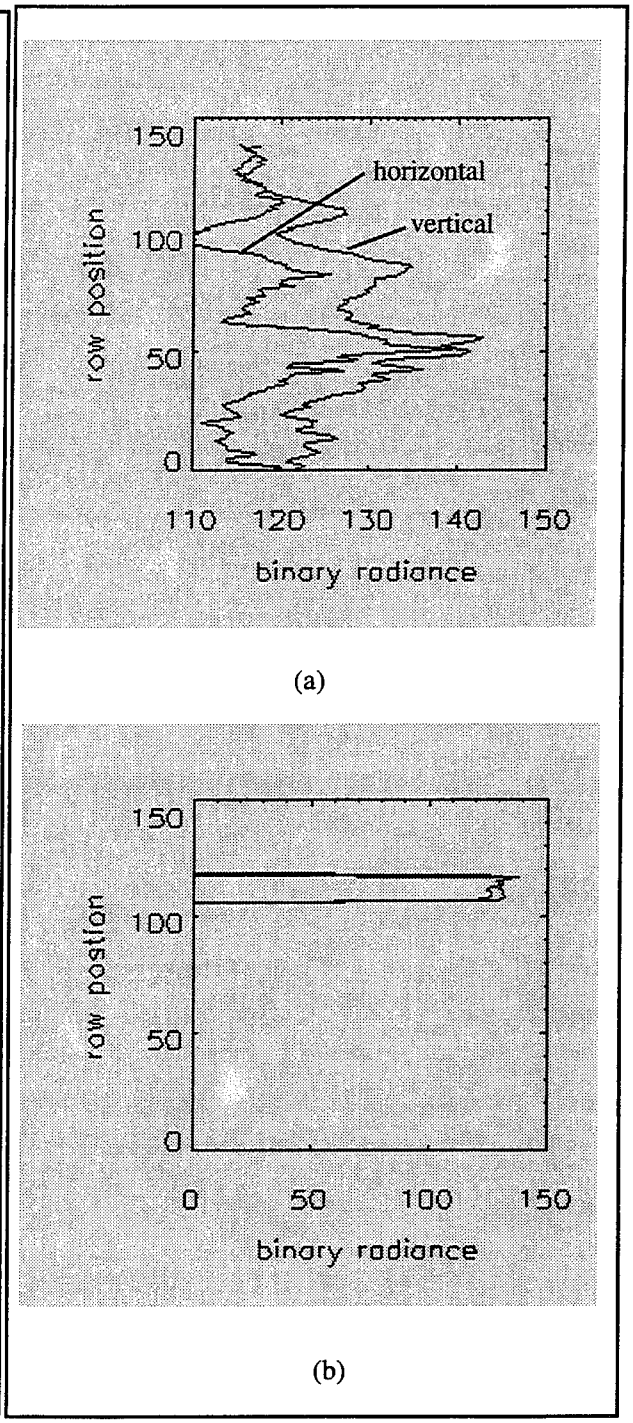

Figure 4.15 Characteristic apparent radiance profile comparisons for low S/N ratio image (a) Background comparison (b) Ship comparison.

Alternatively, the average value of ship radiance for a given polarization is calculated for each row. This average is calculated simply by summing each row between the top and bottom of the box and dividing by the number of ship pixels in a row. These averages then constitute the image representative vertical ship profile.

8. Background Polarization

Background polarization effects were analyzed using image profiles. Significant vertical polarization was observed below the horizon. Less vertical polarization was observed above the horizon.

a. Average Value Calculation

The average value of background radiation for a given polarization is calculated for each row. The procedure varies with the location of the target with respect to the Narcissus spot. For images where the target is above the Narcissus spot, the background above the ship (i.e. above the box) is calculated simply by summing each row and dividing by the number of pixels in a row (i.e. 140). Below the ship the first and last 20 pixels in each row are summed and divided by 40 to determine the average background value below the ship. Along the ship the five pixels to either side of the box are averaged to find the average background value along the ship. These averages then constitute the image representative vertical background profile.

b. Characteristic Profile

Previously, Figure 4.5 and 4.6 showed both horizontal and vertical profiles of an image. The horizontal profiles depict a background that is essentially constant at a given elevation disregarding the affect of the Narcissus. The vertical profiles depict a widely varying background with respect to elevation. A target is discernable from the background in the immediate vicinity if there exists an appreciable contrast between the ship radiance and the background radiance. The key is "immediate vicinity." Contrast must be based upon appropriately related ship and background values. It is not appropriate to compare ship radiance values below the horizon with background above the horizon. Therefore, the ship radiance values along a given row must be compared with background radiance values along that same row. Thus, all the pixels in each row are averaged to generate a characteristic profile.

The characteristic profiles of Figures 4.14a and 4.15a show a significant reduction in background radiance below the horizon while no significant difference exists in the radiation from the target ship. It is this reduction in background radiation that polarization filters can take advantage of and increase target to background contrast. By aligning the filters to block the predominantly vertically polarized background radiation the contrast will be enhanced.

9. Ship to Background Contrast

Once the ship and background average values have been determined, the contrast values may be calculated. Contrast is defined as a difference in radiance value between the target and surrounding background. This difference may be positive or negative depending on whether the target is of greater or lesser radiance than the background. Equation 4.3 below provides the mathematical definition of contrast. Ideally, contrast results from any one or a few adjacent pixels being of greater or lesser value than the surrounding background pixels. This introduces the concept of clutter. Clouds may reflect radiation into the detector with a value comparable to the ship radiance. The ship targets contain more than one individual pixel as is necessary to achieve classification or identification. So there exists a question as to what is detection that is not addressed by this thesis. As stated before, this thesis does not include modulation transfer functions for determining detection.

10. Contrast Improvement

The quantities of interest are the improvement in vertical or horizontal polarization contrast over the unpolarized contrast. Provided there is a significant improvement in one of the polarizations, then such a polarizer may prove useful in an actual target detection or tracking system. It is reasonable that a variable plane of polarization filter might be included in system design.

a. Definition of Contrast Improvement

Target to background contrast can be defined as the normalized

$$C=\frac{N_{tgt}-N_{bkgd}}{N_{bkgd}} \qquad 4.3$$

radiance difference between target and background where N_{tgt} and N_{bkgd} are apparent

radiance values, respectively. Therefore, the contrast for vertical, horizontal, and unpolarized target images is

$$C_v = \frac{(N_v)_{tgt} - (N_v)_{bkgd}}{(N_v)_{bkgd}} \quad 4.4$$

$$C_h = \frac{(N_h)_{tgt} - (N_h)_{bkgd}}{(N_h)_{bkgd}} \quad 4.5$$

$$C_{up} = \frac{(N_{up})_{tgt} - (N_{up})_{bkgd}}{(N_{up})_{bkgd}} \quad 4.6$$

Then the contrast improvement for vertical and horizontal polarizations is defined as

$$(C_{imp})_v = \frac{C_v}{C_{up}} \quad 4.7$$

$$(C_{imp})_h = \frac{C_h}{C_{up}} \quad 4.8$$

b. Background Dependency

As stated before, contrast calculations are dependent upon the background utilized in the calculations. If the background average is determined using the entire range of values from the lowest radiance at high elevations to the highest radiance just above the horizon, then this average may be significantly higher or lower than the average background value in the vicinity of the target. Care must be taken to associate the appropriate background with the target. This is most effectively done by comparing the below horizon background with the ship component below the horizon and the above horizon background with the ship component above the horizon. A more accurate method would be to do a row by row comparison. This is easily done with one image of vertical or horizontal polarization. However, for meaningful analysis the images must be summed. This leads to the problem of registration covered earlier.

c. Ship Area Reference Dependency

The contrast calculations depend on the area coupling discussed previously. Originally, row by row analysis was performed. This entailed summing the ship pixels along each row. The same size box was used in each polarization and assumed to register the ship image properly. The same row of each image was compared by using the larger number of ship pixels in each row from the respective vertical and horizontal images. This often leads to negative contrast values, since the calculated N_{tgt} may be erroneously low. This problem was resolved by first acknowledging the error in ship registration. Then instead of a row by row analysis the ship radiance was calculated as an average either above or below the horizon. Also, the difference in ship pixels was compensated for by assigning the background average to the "missing" pixels.

D. RESULTS OF ANALYSIS

Contrast improvement calculations were generated by the "contiguous area" and "box" methods. Visual review of the MAPTIP image data reveals a greater ship to background contrast in the horizontally polarized images than in the vertically polarized images. Of interest is the degree of contrast improvement achieved with polarizers over that without polarization filters. Unpolarized image data is not available for these images and must be artificially constructed. Both the contiguous area and box methods generate unpolarized images and calculate the contrast improvement obtained with vertical and horizontal filters as described above. The results of these calculations are provided in Appendix B.

Both methods show contrast improvement in the horizontal polarization. Sometimes even vertical polarization filtering shows a contrast improvement over unpolarized images. Horizontal polarization consistently provides a greater contrast improvement over vertical polarization except within a strong sunglint channel..

Tables 4.1 through 4.5 show results from selected images throughout different times of the day. Table 4.1 images were recorded in the early morning, Table 4.2 in mid-morning, Table 4.3 in mid-day, Table 4.4 in mid-afternoon, and Table 4.5 in the evening. Each table is in two parts. Part (a) lists the average radiance values for target and background both above and below the horizon as calculated from the "box method." Part (b) lists contrast and contrast improvement values. The last three

columns depict polarized target-to-background contrast (C), unpolarized target-to-background contrast (C_{up}), and contrast improvement (C_{imp}) as calculated from the "contiguous area method."

These values of contrast improvement require qualification. The results of both methods are not strictly comparable. Errors are inherent in both methods due to misidentification of the horizon or ignoring horizon effects. The contiguous area method calculates a ship contrast irrespective of the horizon. This is not a significant miscalculation in most low signal-to-noise ratio images. In these cases, the horizon is seldom visible and the apparent radiance just above and below the horizon is similar. This can be seen from the example low signal-to-noise ratio image of Figure 4.4. The results of calculations for this image are tabulated in Table 4.2 as file OC28L025 and OC28L026. The "box method" contrast and contrast improvement below the horizon is nearly the same as the overall contrast and contrast improvement calculated from the "contiguous area method." However, in images where the horizon difference is large, this error increases substantially. Image files OC19L105 and OC19L106 of Table 4.3 show the results for the example high signal-to-noise ratio image of Figure 4.1. Since in such images the sky radiance just above the horizon is much larger than below the horizon, then the overall ship to background contrast is falsely reduced because the average background is erroneously increased by averaging above and below background values. This results in the negative contrast values of several image pairs in the "contiguous area" method data as seen in Table 4.2b for file OC25L084. The "box method" avoids this error. However, accurate identification of the horizon is difficult. This also leads to an error in calculation of the above and below horizon background values.

Table 4.6 compares the "box method" contrast improvement (C_2) for horizontal polarization below the horizon and "contiguous area method" for contrast improvement (C_3) for horizontal polarization to two previous efforts to calculate contrast. The contrast in C_1 was calculated without correctly coupling the ship areas. In this method the ship image of smaller area was assumed to have the same area as the larger ship image. The total pixel radiance value was divided by this larger area which means the missing pixels were set to zero. This reduces the average ship radiance and contrast for that polarization. This reduced ship radiance also reduces the unpolarized ship

radiance and contrast which is calculated from both polarized radiance values. Therefore, opposite polarization contrast improvement will be increased when its contrast is divided by the reduced unpolarized contrast. If the vertically polarized image is of less area, then the horizontal contrast improvement will be inflated as shown in Table 4.6 as compared to C_2 which sets the missing pixels values of the smaller image equal to the background radiance. The last column shows ship-to-background contrast calculated from mean radiance data shown by Chan (Chan, 1993). This mean radiance data consists of the average ship or background radiance within a box placed either within the ship target or a box containing background only.

The "contiguous area" method is semi-autonomous. Once a threshold value is input, the only operator action necessary occurs when the program experiences a conflict in location of the ship hot spot. This spot is identified by the operator and the program continues. In several instances, the "contiguous area" method includes a large and significant portion of background in its calculation of ship average radiance value. The "box method" also avoids this by allowing the operator to set the size of the box to a tight fit around the ship.

Also, the "contiguous area" method occasionally does not include all of the ship in calculating average radiance. This happens when portions of the ship in both horizontal and vertical polarizations are in separate blocks of pixels. For, example some images will have the ship stack appear separated from a larger area of ship hull. The program will only use one of these areas in the calculation. For strict contrast, the stack area which is of a greater apparent temperature should be chosen. This leads again to the concept of detection. If the stack is to be chosen only because of higher apparent temperature, then in all images only the highest ship pixel value should be compared to the surrounding pixels. For the stack, the surrounding pixels are other ship pixels. The concept of pixel to pixel contrast works if the target is one pixel in area. The "contiguous area" method compares the ship "hot chunk" to background whereas the "box" method compares the entire infrared visible ship to background. The former applies more to pixel detection and the latter applies more to target detection.

Apparent in the "box" method data is the greater contrast improvement in below the horizon compared to that above the horizon in horizontal polarization. This

results from the sea background emission which is predominantly vertically polarized (Cooper, Crittenden, Milne, Walker, Moss, and Gregoris, 1992). The sky background immediately above the horizon is predominantly unpolarized where there exists a significant horizon contrast as depicted in Figure 14a. This figure shows no measurable change in apparent radiance in either polarization. This can only occur if the radiance is unpolarized.

Definitions of the results in Tables 4.1 through 4.5 are given below. The following values were calculated by the "box method."

$(N)_{abv}$ = apparent radiance above the horizon for given polarization

$(N)_{bel}$ = apparent radiance below the horizon for given polarization

$(N_{up})_{abv}$ = apparent radiance above the horizon for unpolarized image

$(N_{up})_{bel}$ = apparent radiance below the horizon for unpolarized image

C_{abv} = contrast above the horizon for given polarization

C_{bel} = contrast below the horizon for given polarization

$(C_{up})_{abv}$ = contrast above the horizon for unpolarized image

$(C_{up})_{bel}$ = contrast below the horizon for unpolarized image

$(C_{imp})_{abv}$ = contrast improvement above the horizon for given polarization

$(C_{imp})_{bel}$ = contrast improvement below the horizon for given polarization

The following values were calculated by the "contiguous area method."

C = contrast for given polarization without regard for horizon

C_{up} = contrast for unpolarized image without regard for horizon

C_{imp} = contrast improvement without regard for horizon

		target	target	bkgd	bkgd	target	target	bkgd	bkgd
TIME	FILE	$(N)_{abv}$	$(N)_{bel}$	$(N)_{abv}$	$(N)_{bel}$	$(N_{up})_{abv}$	$(N_{up})_{bel}$	$(N_{up})_{abv}$	$(N_{up})_{bel}$
04:02:08	OC25L015V	235.7	222.6	196.5	191.1	234.0	223.3	189.9	181.0
	OC25L016H	232.2	224.0	183.2	170.9				
04:07:15	OC25L025V	119.5	122.5	105.0	101.5	125.8	124.4	104.6	98.6
	OC25L026H	132.1	126.3	104.2	95.6				
04:12:03	OC25L036V	157.1	150.8	143.0	141.4	156.5	151.6	139.8	136.4
	OC25L037H	155.8	152.4	136.5	131.3				
04:17:47	OC25L044V	166.6	158.9	99.3	95.9	166.5	153.1	110.0	102.0
	OC25L045H	166.4	147.3	120.7	108.1				
04:20:15	OC25L055V	150.9	141.3	127.5	125.2	151.0	142.7	124.8	121.5
	OC25L056H	151.1	144.1	122.1	117.8				

Table 4.1a Radiance values for selected vertical/horizontal image pairs and unpolarized image with respect to target or background source and horizon. Images taken during the early morning. "V" and "H" denote vertical and horizontal polarizations, respectively.

TIME	FILE	C_{abv}	C_{bel}	$(C_{up})_{abv}$	$(C_{up})_{bel}$	$(C_{imp})_{abv}$	$(C_{imp})_{abv}$	C	C_{up}	C_{imp}
04:02:08	OC25L015V	0.20	0.16	0.23	0.23	0.86	0.70	0.0	0.07	0.0
	OC25L016H	0.27	0.31			1.15	1.33	0.14		1.96
04:07:15	OC25L025V	0.14	0.21	0.20	0.26	0.68	0.79	0.06	0.07	0.79
	OC25L026H	0.27	0.32			1.32	1.22	0.09		1.20
04:12:03	OC25L036V	0.10	0.07	0.12	0.11	0.83	0.59	0.03	0.05	0.61
	OC25L037H	0.14	0.16			1.18	1.44	0.08		1.4
04:17:47	OC25L044V	0.68	0.66	0.51	0.50	1.32	1.31	0.30	0.36	0.81
	OC25L045H	0.38	0.36			0.74	0.72	0.43		1.19
04:20:15	OC25L055V	0.18	0.13	0.21	0.18	0.87	0.74	0.14	0.11	1.27
	OC25L056H	0.24	0.22			1.13	1.28	0.08		0.74

Table 4.1b. The first six columns show contrast and contrast improvement values for selected image pairs with respect to horizon for horizontal polarization as calculated by "box method." Last three columns show overall contrast and overall contrast improvement as calculated by "contiguous area method." Images taken during the early morning. "V" and "H" denote vertical and horizontal polarizations, respectively.

		target	target	bkgd	bkgd	target	target	bkgd	bkgd
TIME	FILE	$(N)_{abv}$	$(N)_{bel}$	$(N)_{abv}$	$(N)_{bel}$	$(N_{up})_{abv}$	$(N_{up})_{bel}$	$(N_{up})_{abv}$	$(N_{up})_{bel}$
09:04:45	OC25L071V	154.4	131.7	96.7	99.6	148.4	137.8	93.5	94.4
	OC25L072H	142.3	143.9	90.2	89.3				
09:06:27	OC25L075V	107.5	81.6	45.5	49.7	93.9	83.7	42.8	44.0
	OC25L076H	80.2	85.8	40.1	38.4				
09:09:05	OC25L079V	105.1	94.3	55.0	58.5	113.0	100.9	55.2	55.9
	OC25L080H	120.8	107.4	55.5	53.3				
09:13:34	OC25L084V	162.9	146.9	114.3	118.0	153.9	150.0	106.8	107.8
	OC25L085H	145.0	153.1	99.3	97.6				
09:23:28	OC28L025V	131.1	127.1	117.0	120.4	129.6	127.0	116.2	118.0
	OC28L026H	128.1	126.9	115.4	115.7				

Table 4.2a Radiance values for selected vertical/horizontal image pairs and unpolarized image with respect to target or background source and horizon. Images taken during the mid-morning. "V" and "H" denote vertical and horizontal polarizations, respectively.

TIME	FILE	C_{abv}	C_{bel}	$(C_{up})_{abv}$	$(C_{up})_{bel}$	$(C_{imp})_{abv}$	$(C_{imp})_{abv}$	C	C_{up}	C_{imp}
09:04:45	OC25L071V	0.60	0.32	0.59	0.46	1.02	0.70	0.28	0.29	0.97
	OC25L072H	0.58	0.61			0.98	1.33	0.30		1.03
09:06:27	OC25L075V	1.36	0.64	1.19	0.90	1.14	0.71	0.44	0.50	0.87
	OC25L076H	1.00	1.24			0.84	1.37	0.57		1.13
09:09:05	OC25L079V	0.91	0.61	1.04	0.81	0.87	0.76	0.47	0.48	0.97
	OC25L080H	1.18	1.02			1.13	1.26	0.49		1.02
09:13:34	OC25L084V	0.42	0.24	0.44	0.39	0.96	0.62	-0.03	0.11	-0.23
	OC25L085H	0.46	0.57			1.04	1.45	0.25		2.26
09:23:28	OC28L025V	0.12	0.06	0.12	0.08	1.05	0.74	0.06	0.09	0.74
	OC28L026H	0.11	0.10			0.95	1.27	0.11		1.27

Table 4.2b. The first six columns show contrast and contrast improvement values for selected image pairs with respect to horizon for horizontal polarization as calculated by "box method." Last three columns show overall contrast and overall contrast improvement as calculated by "contiguous area method." Images taken during the mid-morning. "V" and "H" denote vertical and horizontal polarizations, respectively.

		target	target	bkgd	bkgd	target	target	bkgd	bkgd
TIME	FILE	$(N)_{abv}$	$(N)_{bel}$	$(N)_{abv}$	$(N)_{bel}$	$(N_{up})_{abv}$	$(N_{up})_{bel}$	$(N_{up})_{abv}$	$(N_{up})_{bel}$
13:13:35	OC19L103V	192.9	195.6	105.3	71.8	204.7	193.8	95.3	52.9
	OC19L104H	216.5	191.9	85.4	34.0				
13:13:50	OC19L105V	183.2	160.1	111.7	94.3	175.7	160.3	105.0	83.2
	OC19L106H	175.6	167.4	98.8	74.4				
13:14:05	OC19L107V	152.5	141.8	115.2	106.4	152.9	141.7	110.8	100.0
	OC19L108H	153.3	141.5	106.4	93.7				
13:14:19	OC19L109V	127.4	128.1	116.6	113.8	130.3	127.6	115.3	111.3
	OC19L110H	133.1	127.1	114.0	108.8				
13:14:39	OC19L111V	124.4	123.1	117.5	115.8	125.0	122.9	116.7	114.5
	OC19L112H	125.7	122.6	115.9	113.3				

Table 4.3a Radiance values for selected vertical/horizontal image pairs and unpolarized image with respect to target or background source and horizon. Images taken during the mid-morning. "V" and "H" denote vertical and horizontal polarizations, respectively.

TIME	FILE	C_{abv}	C_{bel}	$(C_{up})_{abv}$	$(C_{up})_{bel}$	$(C_{imp})_{abv}$	$(C_{imp})_{bel}$	C	C_{up}	C_{imp}
13:13:35	OC19L103V	0.83	1.72	1.15	2.66	0.73	0.65	0.80	0.94	0.85
	OC19L104H	1.53	4.64			1.34	1.74	1.10		1.17
13:13:50	OC19L105V	0.53	0.71	0.67	0.93	0.79	0.77	0.44	0.51	0.85
	OC19L106H	0.78	1.25			1.1	1.33	0.59		1.16
13:14:05	OC19L107V	0.32	0.33	0.38	0.42	0.85	0.80	0.22	0.24	0.91
	OC19L108H	0.44	0.51			1.16	1.23	0.26		1.10
13:14:19	OC19L109V	0.09	0.13	0.13	0.15	0.71	0.86	0.08	0.09	0.88
	OC19L110H	0.17	0.17			1.29	1.15	0.11		1.12
13:14:39	OC19L111V	0.06	0.06	0.07	0.07	0.82	0.82	0.04	0.04	0.97
	OC19L112H	0.08	0.08			1.18	1.13	0.04		1.03

Table 4.3b. The first six columns show contrast and contrast improvement values for selected image pairs with respect to horizon for horizontal polarization as calculated by "box method." Last three columns show overall contrast and overall contrast improvement as calculated by "contiguous area method." Images taken during the mid-morning. "V" and "H" denote vertical and horizontal polarizations, respectively.

		target	target	bkgd	bkgd	target	target	bkgd	bkgd
TIME	FILE	$(N)_{abv}$	$(N)_{bel}$	$(N)_{abv}$	$(N)_{bel}$	$(N_{up})_{abv}$	$(N_{up})_{bel}$	$(N_{up})_{abv}$	$(N_{up})_{bel}$
15:18:02	OC23L013V	151.9	146.4	107.2	105.6	154.6	138.2	98.2	89.5
	OC23L014H	157.2	130.1	89.1	73.4				
15:20:23	OC23L015V	175.6	156.1	69.9	75.2	192.1	164.2	65.8	57.5
	OC23L016H	208.6	172.3	61.7	39.8				
15:20:51	OC23L017V	156.3	137.0	103.2	102.9	161.2	144.1	95.9	91.3
	OC23L018H	166.0	151.3	88.6	79.8				

Table 4.4a Radiance values for selected vertical/horizontal image pairs and unpolarized image with respect to target or background source and horizon. Images taken during the mid-morning. "V" and "H" denote vertical and horizontal polarizations, respectively.

TIME	FILE	C_{abv}	C_{bel}	$(C_{up})_{abv}$	$(C_{up})_{bel}$	$(C_{imp})_{abv}$	$(C_{imp})_{abv}$	C	C_{up}	C_{imp}
15:18:02	OC23L013V	0.42	0.39	0.36	0.47	0.73	0.71	0.14	0.17	0.81
	OC23L014H	0.76	0.77			1.33	1.42	0.21		1.20
15:20:23	OC23L015V	1.51	1.08	1.92	1.86	0.79	0.58	0.34	0.43	0.79
	OC23L016H	2.38	3.33			1.24	1.79	0.53		1.22
15:20:51	OC23L017V	0.51	0.33	0.68	0.58	0.76	0.57	0.20	0.26	0.78
	OC23L018H	0.87	0.90			1.28	1.55	0.32		1.22

Table 4.4b. The first six columns show contrast and contrast improvement values for selected image pairs with respect to horizon for horizontal polarization as calculated by "box method." Last three columns show overall contrast and overall contrast improvement as calculated by "contiguous area method." Images taken during the mid-morning. "V" and "H" denote vertical and horizontal polarizations, respectively.

		target	target	bkgd	bkgd	target	target	bkgd	bkgd
TIME	FILE	$(N)_{abv}$	$(N)_{bel}$	$(N)_{abv}$	$(N)_{bel}$	$(N_{up})_{abv}$	$(N_{up})_{bel}$	$(N_{up})_{abv}$	$(N_{up})_{bel}$
20:58:50	OC22L235V	205.1	210.0	190.8	185.4	213.1	213.3	181.7	171.8
	OC22L236H	221.1	216.7	172.7	158.2				
21:01:26	OC22L237V	225.5	216.7	204.9	200.3	222.8	217.6	187.0	176.8
	OC22L238H	220.0	218.5	169.2	153.4				
21:02:07	OC22L239V	226.3	222.3	211.7	206.9	226.1	223.0	198.7	187.9
	OC22L240H	225.9	223.7	185.7	168.8				
21:03:24	OC22L243V	199.0	196.7	162.8	158.5	184.2	181.9	121.0	99.6
	OC22L244H	169.5	166.9	79.2	40.7				
21:03:43	OC22L245V	159.5	144.9	126.4	123.1	158.4	145.6	114.1	103.4
	OC22L246H	157.4	146.3	101.9	83.6				

Table 4.5a Radiance values for selected vertical/horizontal image pairs and unpolarized image with respect to target or background source and horizon. Images taken during the mid-morning. "V" and "H" denote vertical and horizontal polarizations, respectively.

TIME	FILE	C_{abv}	C_{bel}	$(C_{up})_{abv}$	$(C_{up})_{bel}$	$(C_{imp})_{abv}$	$(C_{imp})_{bel}$	C	C_{up}	C_{imp}
20:58:50	OC22L235V	0.08	0.13	0.17	0.24	0.44	0.55	0.04	0.06	0.66
	OC22L236H	0.28	0.37			1.62	1.53	0.08		1.37
21:01:26	OC22L237V	0.10	0.08	0.19	0.23	0.53	0.35	0.05	0.08	0.61
	OC22L238H	0.30	0.43			1.57	1.84	0.11		1.43
21:02:07	OC22L239V	0.07	0.07	0.14	0.19	0.50	0.40	0.05	0.07	0.68
	OC22L240H	0.22	0.33			1.57	1.74	0.09		1.33
21:03:24	OC22L243V	0.22	0.24	0.52	0.83	0.43	0.29	0.04	0.19	0.22
	OC22L244H	1.14	3.10			2.18	3.75	0.38		2.03
21:03:43	OC22L245V	0.26	0.18	0.39	0.41	0.67	0.43	0.10	0.13	0.77
	OC22L246H	0.54	0.75			1.40	1.83	0.17		1.24

Table 4.5b. The first six columns show contrast and contrast improvement values for selected image pairs with respect to horizon for horizontal polarization as calculated by "box method." Last three columns show overall contrast and overall contrast improvement as calculated by "contiguous area method." Images taken during the mid-morning. "V" and "H" denote vertical and horizontal polarizations, respectively.

Image Pair	File Name	Pol.	C_1	C_2	C_3	C_4
1	OC19L087/88	V/H	7.7	1.33	1.00	1.15
2	OC19L103/04	V/H	2.8	1.74	1.17	1.14
3	OC19L105/06	V/H	1.33	1.33	1.16	1.14
4	OC19L107/08	V/H	1.24	1.23	1.10	1.13
5	OC19L109/10	V/H	1.22	1.15	1.12	1.14
6	OC19L111/12	V/H	1.21	1.13	0.97	1.11
7	OC19L122/23	V/H	1.24	1.14	1.07	1.12
8	OC19L124/25	V/H	1.24	1.14	1.06	1.10

Table 4.6 Contrast improvement comparison. C_1 calculated without setting "missing" pixels in smaller image to background value, C_2 calculated "box method", C_3 calculated using "contiguous area method," C_4 calculated using mean radiance data obtained by Chan. C_1 and C_2 represent contrast improvements below the horizon for horizontally polarized images. C_3 and C_4 are contrast improvements for horizontal polarizations.

V. CONCLUSIONS AND RECOMMENDATIONS

The below horizon contrast improvement values confirm that a significant improvement in detection ability is possible with horizontal filtering. The below horizon values are significant because in most operational environments a sea background will dominate target scenes. For an aircraft flying as low as 500 feet, the distance to the horizon is 25 nautical miles given by

$$D=1.14\sqrt{(h)} \qquad 5.1$$

where D = distance to horizon in nautical miles

h = height of observer in feet

(Tobin, 1974). Then the distance to a 150 ft high surface vessel that is completely below the horizon is 22.5 nautical miles as shown below.

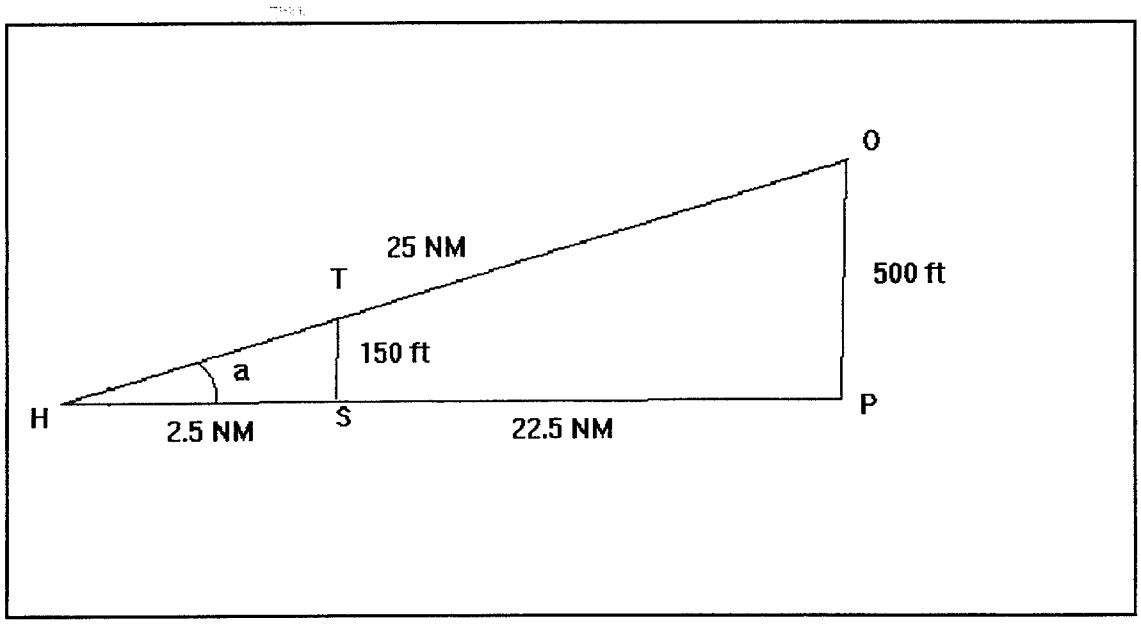

Figure 5.1 Observer to horizon geometry.

The surface is approximated to be flat in the diagram. The target ship height is denoted by TS, the observer height is denoted by OP, and the horizon by H. FLIR acquisition ranges are often displayed as a function of target-to-background temperature difference. For a typical 400 ft long destroyer from a beam aspect, unclassified acquisition ranges show a maximum acquisition range of less than 20

nautical miles (Cooper class notes, 1994). Thus a significant operational improvement is possible with infrared detection and imaging systems using horizontal polarizing filters because the filters would reduce sea component of background radiance.

These calculations are for detection only. The "box" method more closely approximates recognition improvement by using the entire ship radiance in the average radiance calculation. Further consideration needs to be applied to the resolution requirements necessary to recognize a detected target. Target detection in the presence of clutter is felt by some to require some resolution capability - e.g. FLIR resolution requirements are established at 1.5 line pairs for detection (Rosell and Harvey, 1979). Given a system resolution capability requirement, the improvements in detection and recognition of horizontal filtering over no filtering should be explored. As an example, some image pairs show a sizeable increase in total ship area detected with horizontal polarization (see Figure 4.9). A system's resolution requirements would be less with the increased area of ship radiance received in excess of background radiance received.

It is difficult to develop a technique for evaluating the contrast which would be observed and be applicable to detection/recognition criterion. As a minimum the method chosen must be consistent with visual results. The "box method" is believed to be such a method. Validation of that conclusion is needed. Contrast improvement refers only to apparent contrast. This must be dependent on the range at which the target is viewed. Range dependence of the contrast should be included and validated.

Image registration remains a problem. The inability to properly sum two images precludes correct generation of an unpolarized image. A related problem is the time difference between image pairs. The atmosphere is dynamic and thus the radiance received is time dependent. The atmospheric changes between images are unknown and may or may not be significant.

One possible solution to both problems is in progress. This involves a lens adapter system to be mounted on the AGA 780. This system serves two purposes. First, the design is such that the Narcissus spot will be removed. Second, the system splits the incoming beam of radiation. Each beam then passes through either a horizontal or vertical polarizing filter. The resulting image will contain both polarizations each 140 x 70. Since these images were taken simultaneously, then they

will be registered perfectly. Then they may be summed to produce an unpolarized image. Once this system is constructed and mounted on the AGA 780 it must be calibrated and tested to verify or disprove the assertion that an unpolarized image may be produced with the AGA 780 by summing a vertical and horizontal image. (Skowroneck, 1994)

Environmental data acquired from the MAPTIP experiment could be used for further analysis of the MAPTIP images. Calculations in this thesis were based on apparent radiance. This is the radiance actually received at the AGA 780. This is not the radiance emitted from the target. Contrast and contrast enhancement are relative - based on relative radiances. This does not pose a problem as would absolute radiances. With the environmental data from MAPTIP, an atmospheric transmission model such as modified LOWTRAN6 may be used to determine the actual radiance of the ship and background. This information is necessary for proper modelling of electro-optic system requirements.

APPENDIX A.

A. OUTLINE METHOD PROGRAM

```
;outlin14 constructs outline of ship referenced to box placed around ship          ;
box must touch top, bow tip, stern tip, waterline

!order=0
print,'flirs makes movie of flirs'
close,1
;close in case of crash
intfn=0
shpnmbr=1
ct=0
loadct,ct
;window,0,xsize=280,ysize=280,xpos=0,ypos=0
on_ioerror,problem
path1='                    '
file1='                    '
print,'file size must be 20446 with header'
read,'input path to *.img files',path1
if path1 ne '' then path=path1
print,'path= ',path
read,'input type of files eg *.img or names to search for',file1

if file1 eq '' then file1='*.img
files=findfile(path+'\'+file1,count=num)
for i=0,num-1 do print,files(i),i
loop: print,n_elements(files)-1,' last number'
read,'input i for number to plot or -1 to stop',i
if i lt 0 then goto, problem
istart=i
read,'input stop number',istop
for i=istart, istop do begin
f=files(i)
openr,1,f
print,'opening ',f,i
head=bytarr(846)
y=bytarr(140,70)
y1=bytarr(140,70)
yy=bytarr(140,140)
readu,1,head
readu,1,y
readu,1,y1
close,1
index=indgen(70)
yy(*,index*2)=y1(*,index)
```

```
yy(*,index*2+1)=y(*,index)
if(max(yy) eq 255) then begin
        y1=yy( where(yy gt 254))
        nover=n_elements(y1)
endif else begin
        nover=0
endelse
yy=yy(*,139-indgen(140))

;*************************************
;save ship images
;*************************************
ship1=bytarr(140,140)
ship2=bytarr(140,140)
if shpnmbr eq 1 then begin
  ship1=yy
  ship11=yy
  shpnmbr=2
  title1='vert'
  window,1,xpos=0,ypos=0,xsize=140,ysize=140,title=title1
  tvscl,ship1
endif else begin
  ship2=yy
  title2='hor'
  window,2,xpos=0,ypos=160,xsize=140,ysize=140,title=title2
  tvscl,ship2
  shpnmbr=1
endelse

endfor

;*****************************************
;invert outline for port beam aspect
;*****************************************
 read,'invert outline for port beam aspect? yes=1 no=0',aspect
 if aspect eq 1 then begin
   ship11=ship11(139-indgen(140),*)
   ship2=ship2(139-indgen(140),*)
   wset,1
   tvscl,ship11
   wset,2
   tvscl,ship2
 endif

;**********invert signal**********
y1=1
y=1
;*********reset variables**********
```

```
yy=congrid(yy,140*2,140*2,Interp=1)
;!order=1
loadct,0
;wset,0
print,'Scaled plot of data in 0'
;tvscl,yy
range=double(head,770)
level=double(head,762)
dlevel=double(head,618)
emiss=double(head,626)
ct=double(head,650)
r=double(head,570)
b=double(head,578)
f=double(head,586)
amt=double(head,674)
at=double(head,666)
p1=emiss*ct
p2=(1-emiss)/emiss
p3=1.0-ct
iamb=r/(exp(b/amt)-f)
iatm=r/(exp(b/at)-f)
y=range*(float(yy)-128.)/256.0+level+dlevel
y=y/p1-p2*iamb-p3/p1*iatm
t=b/alog(abs((r/y+f)))-273.15
; get rid of old variables
;delvar,y,y1,yy,head

shpave1=fltarr(140)
shpave1(*)=0.0
shpave2=fltarr(140)
shpave2(*)=0.0
shptot1=fltarr(140)
shptot1(*)=0.0
shptot2=fltarr(140)
shptot2(*)=0.0
;index1=fltarr(140)
;index1(*)=0
;index2=fltarr(140)
;index2(*)=0
shppix1=fltarr(140)
shppix1(*)=0.0
shppix2=fltarr(140)
shppix2(*)=0.0
outline=fltarr(140,140)
outline(*,*)=0.0
outline1=fltarr(140,140)
outline1(*,*)=0.0
outline2=fltarr(140,140)
```

```
outline2(*,*)=0.0

redo:read,'enter BF value',dd
BF=dd
image=1
nextimg:
wset,image
zz=boxfun(x0,y0,nx,ny,init=intfn,/message)
intfn=1
box=tvrd(x0,y0,nx,ny)
bkgdave=fltarr(140)
bkgdave(*)=0.0
delta1=0
delta2=1
;*************************************************************
;box or outline
;*************************************************************

;*************************************************************
;assign image array to outline array and mark horizon
;*************************************************************
if image eq 1 then begin
  outline=ship11
  boat=ship11
  print,'click on horizon or bottom to exit'
  replot1: cursor,xv,yv,3,/device
  if yv lt 5 then goto,exit1
    xv1=xv
    yv1=yv
    print,'horizon=',yv1
    print,'click on point or bottom to exit'
    goto,replot1
    exit1:print,'exiting'
endif
if image eq 2 then begin
  outline=ship2
  boat=ship2
  print,'click on horizon or bottom to exit'
  replot2: cursor,xv,yv,3,/device
  if yv lt 5 then goto,exit2
    xv2=xv
    yv2=yv
    print,'horizon=',yv2
    print,'click on point or bottom to exit'
    goto,replot2
    exit2:print,'exiting'
endif
;*************************************************************
```

```
;calculate background average values
;************************************************************
if y0+ny/2.0 lt 69 then begin
 ;box below narcissus
 ;background average below box
 for n=0,y0-1 do begin
  bkgdave(n)=total(outline(0:139,n))/140.0
 endfor
 ;background average around box
 for n=y0,y0+ny-1 do begin
  bkgdave(n)=(total(outline(x0-5:x0-1,n))+total(outline(x0+nx:x0+nx+4)))/10.0

 endfor
 ;background average above box
 for n=y0+ny,139 do begin
  bkgdave(n)=(total(outline(0:19,n))+total(outline(120:139,n)))/40.0
 endfor
endif else begin
 ;box above narcissus
 ;background average below box
 for n=0,y0-1 do begin
  bkgdave(n)=(total(outline(0:19,n))+total(outline(120:139,n)))/40.0
 endfor
 ;background average around box
 for n=y0,y0+ny-1 do begin
  bkgdave(n)=(total(outline(x0-5:x0-1,n))+total(outline(x0+nx:x0+nx+4)))/10.0

 endfor
;background average above box
 for n=y0+ny,139 do begin
  bkgdave(n)=(total(outline(0:139,n)))/140.0
 endfor
endelse

;*****************************************************************
;generate outline and ship average values
;*****************************************************************
 outline(*,0:y0-1)=0.0
;waterline
 temp1=x0+(9.0/94.0)*nx
 temp2=x0+(89.0/94.0)*nx
 for m=temp1,temp2 do begin
  if outline(m,y0) le BF*bkgdave(y0) then outline(m,y0)=0.0
 endfor
 boat(temp1:temp2,y0)=255
 outline(0:temp1-1,y0)=0.0
 outline(temp2+1:139,y0)=0.0
;angled portions of bow and stern
```

```
for n=y0+1,y0+(9.0/23.0)*ny do begin
  temp1=x0+(9.0/94.0)*nx-delta1
  temp2=x0+(89.0/94.0)*nx+delta2/3.0
  for m=temp1,temp2 do begin
   if outline(m,n) le BF*bkgdave(n) then outline(m,n)=0.0
  endfor
  boat(x0+(9.0/94.0)*nx-delta1,n)=255
  boat(x0+(89.0/94.0)*nx+delta2/3.0,n)=255
  outline(0:x0+(9.0/94.0)*nx-delta1-1,n)=0.0
  outline(x0+(89.0/94.0)*nx+delta2/3.0+1:139,n)=0.0
  delta1=delta1+1
  delta2=delta2+1
endfor
;top of angled portion of bow
for n=y0+(9.0/23.0)*ny+1,y0+(15.0/23.0)*ny do begin
  temp1=x0+(75.0/94.0)*nx
  temp2=x0+(89.0/94.0)*nx+delta2/3.0
  temp3=x0+(22.0/94.0)*nx
  temp4=x0+(58.0/94.0)*nx
  for m=temp1,temp2 do begin
   if outline(m,n) le BF*bkgdave(n) then outline(m,n)=0.0
  endfor
  for m=temp3,temp4 do begin
   if outline(m,n) le BF*bkgdave(n) then outline(m,n)=0.0
  endfor
  boat(x0+(89.0/94.0)*nx+delta2/3.0,n)=255
  boat(temp3,n)=255
  boat(temp4,n)=255
  boat(temp1,n)=255
  outline(x0+(89.0/94.0)*nx+delta2/3.0+1:139,n)=0.0
  outline(x0+(58.0/94.0)*nx+1:x0+(75.0/94.0)*nx-1,n)=0.0
  outline(0:x0+(22.0/94.0)*nx-1,n)=0.0
  delta2=delta2+1
endfor
  boat(x0+(75.0/94.0)*nx:x0+(89.0/94.0)*nx+delta2/3.0,y0+(15.0/23.0)*ny)=255
;fantail and foredeck
 temp5=y0+(9.0/23.0)*ny
 boat(x0:x0+(22.0/94.0)*nx,temp5)=255
 boat(temp4:temp1,temp5)=255
;back of superstructure
  temp1=x0+(22.0/94.0)*nx
  temp2=x0+(58.0/94.0)*nx
  temp4=y0+(15.0/23.0)*ny+1
  temp5=y0+(19.0/23.0)*ny
  temp6=y0+(9.0/23.0)*ny
  for n=temp4,temp5 do begin
   for m=temp1,temp2 do begin
    if outline(m,n) le duck*bkgdave(n) then outline(m,n)=0.0
```

```
   endfor
endfor
  boat(temp1,temp4:temp5)=255
  outline(0:x0+(22.0/94.0)*nx-1,temp4:139)=0.0
  outline(x0+(58.0/94.0)*nx+1:139,temp4:139)=0.0
;top of superstructure rear of stack
 temp1=x0+(22.0/94.0)*nx
 temp2=x0+(58.0/94.0)*nx
 temp3=y0+(19.0/23.0)*ny
 boat(temp1:x0+(31.0/94.0)*nx,temp3)=255
;rear of stack
 temp1=x0+(31.0/94.0)*nx
 temp2=x0+(44.0/94.0)*nx
 temp3=y0+(19.0/23.0)*ny+1
 temp4=y0+ny-1
 for n=temp3,temp4 do begin
  for m=temp1,temp2 do begin
   if outline(m,n) le duck*bkgdave(n) then outline(m,n)=0.0
 endfor
endfor
 boat(temp1,temp3:temp4)=255
 outline(0:temp1-1,temp3+1:139)=0.0
 outline(temp2+1:139,temp3+1:139)=0.0
;top of stack
 boat(temp1:temp2,temp4)=255
 outline(*,temp4+1:139)=0.0
;front of stack:  stack average already calculated
 temp1=x0+(44.0/94.0)*nx
 temp3=y0+(19.0/23.0)*ny+1
 temp4=y0+ny-1
 boat(temp1,temp3:temp4)=255
;top of superstructure front of stack: already calculated
 boat(x0+(44.0/94.0)*nx:x0+(58.0/94.0)*nx,y0+(19.0/23.0)*ny)=255
;front of superstructure: superstructure already calculated
 boat(x0+(58.0/94.0)*nx,y0+(9.0/23.0)*ny:y0+(19.0/23.0)*ny)=255



;*****************************************************
;reposition outline if needed
;*****************************************************
window,20,xsize=140,ysize=140,xpos=150,ypos=0
tvscl,boat
read,'reposition outline? yes=1 no=0',repos
if repos eq 1 then goto,redo
;*****************************************************

;*****************************************************
```

```
;calculate results and display
;*************************************************
if image eq 1 then begin
  ;save image and average arrays
    bkgdave1=bkgdave
    outline1=outline
    image1=boat
  ;increment and go to next image
    image=image+1
    goto,nextimg
endif
if image eq 2 then begin
  ;save image and average arrays
   outline2=outline
   for n=y0,y0+ny do begin
     shptot1(n)=total(outline1(*,n))
     shptot2(n)=total(outline2(*,n))
     index1=where(outline1(*,n),count)
     shppix1(n)=count
     index2=where(outline2(*,n),count)
     shppix2(n)=count
     if shppix2(n) ne 0.0 then begin
       shpave1(n)=shptot1(n)/shppix2(n)   ;use horizontal ship area to find average
       shpave2(n)=shptot2(n)/shppix2(n)
     endif else begin
       shpave1(n)=0.0
       shpave2(n)=0.0
     endelse
   endfor
    bkgdave2=bkgdave
    image2=boat
 ;calculate average ship and bkgd values above and below horizon
    max1=max(where(shpave1 gt bkgdave1))
    min1=min(where(shpave1 gt bkgdave1))
    shpbel1=total(shpave1(min1:yv1))/(yv1-min1+1)
    shpabv1=total(shpave1(yv1+1:max1))/(max1-(yv1+1)+1)
    bkgbel1=total(bkgdave1(min1:yv1))/(yv1-min1)
    bkgabv1=total(bkgdave1(yv1+1:max1))/(max1-(yv1+1)+1)
 ;display image with outline
    title3=title1
    window,3,xsize=140,ysize=140,xpos=150,ypos=0,title=title3
    tvscl,image1
 ;generate and display outlined image with excess background
    outline1=outline(x0-10:x0+nx+20-1,y0-10:y0+ny+20-1)
    shpimg1=boat(x0-10:x0+nx+20-1,y0-10:y0+ny+20-1)
    title5=title1
    window,5,xsize=nx+20,ysize=ny+20,xpos=300,ypos=0,title=title5
    tvscl,shpimg1
```

```
;display ship and background average profiles
  title7='ship1'
  window,7,xsize=280,ysize=280,xpos=450,ypos=0,title=title7
  plot,shpave1
  oplot,bkgdave1
;calculate and display contrast profile
  cntrst1=(shpave1-bkgdave1)/bkgdave1
  title9='cntrst1'
  window,9,xsize=280,ysize=280,xpos=0,ypos=300,title=title9
  plot,cntrst1(min1:max1)
;calculate contrast above and below horizon for first image
  cnt1bel=(shpbel1-bkgbel1)/bkgbel1
  cnt1abv=(shpabv1-bkgabv1)/bkgabv1
;calculate average ship and bkgd values above and below horizon
  min2=min(where(shpave2 gt bkgdave2))
  max2=max(where(shpave2 gt bkgdave2))
  shpbel2=total(shpave2(min2:yv2))/(yv2-min2+1)
  shpabv2=total(shpave2(yv2+1:max2))/(max2-(yv2+1)+1)
  bkgbel2=total(bkgdave2(min2:yv2))/(yv2-min2+1)
  bkgabv2=total(bkgdave2(yv2+1:max2))/(max2-(yv2+1)+1)
;display image with outline
  title4=title2
  window,4,xsize=140,ysize=140,xpos=150,ypos=160,title=title4
  tvscl,image2
;generate and display outlined image with excess background
  title6=title2
  outline2=outline(x0-10:x0+nx+20-1,y0-10:y0+ny+20-1)
  shpimg2=boat(x0-10:x0+nx+20-1,y0-10:y0+ny+20-1)
  window,6,xsize=nx+20,ysize=ny+20,xpos=300,ypos=160,title=title6
  tvscl,outline2
;generate and display unpolarized outlined image with excess background
  shpimgup=shpimg1/2.0+shpimg2/2.0
  outlinup=outline1/2.0+outline2/2.0
  title0='unp'
  window,0,xsize=nx+20,ysize=ny+20,xpos=300,ypos=80,title=title0
  tvscl,shpimgup
;display ship and background average profiles
  title8='ship2'
  window,8,xsize=280,ysize=280,xpos=730,ypos=0,title=title8
  plot,shpave2
  oplot,bkgdave2
;calculate and display horizontal contrast profile
  cntrst2=(shpave2-bkgdave2)/bkgdave2
  title10='cntrst2'
  window,10,xsize=280,ysize=280,xpos=0,ypos=300,title=title10
  plot,cntrst2(min2:max2)
;calculate and display unpolarized contrast profile
   shpaveup=shpave1/2.0+shpave2/2.0
```

```
      bkgaveup=bkgdave1/2.0+bkgdave2/2.0
      cntrstup=(shpaveup-bkgaveup)/bkgaveup
      title12='cntrstup'
      window,12,xsize=280,ysize=280,xpos=0,ypos=0,title=title12
      plot,cntrstup(y0:y0+ny-1)
   ;calculate contrast above and below horizon for second image
     cnt2bel=(shpbel2-bkgbel2)/bkgbel2
     cnt2abv=(shpabv2-bkgabv2)/bkgabv2
   ;calculate contrast above and below horizon for unpolarized image
     shpupbel=shpbel1/2.0+shpbel2/2.0
     shpupabv=shpabv1/2.0+shpabv2/2.0
     bkgupbel=bkgbel1/2.0+bkgbel2/2.0
     bkgupabv=bkgabv1/2.0+bkgabv2/2.0
     cntupbel=(shpupbel-bkgupbel)/bkgupbel
     cntupabv=(shpupabv-bkgupabv)/bkgupabv
   ;calculate contrast improvement above and below horizon for v and h
     impbel1=cnt1bel/cntupbel
     impabv1=cnt1abv/cntupabv
     impbel2=cnt2bel/cntupbel
     impabv2=cnt2abv/cntupabv
   ;print contrast values above and below horizon
     print,'contrast above horizon'
     print,'    vert        hor        unp'
     print,cnt1abv,cnt2abv,cntupabv
     print,''
     print,'contrast below horizon
     print,'    vert        hor        unp'
     print,cnt1bel,cnt2bel,cntupbel
     print,''
     print,'contrast improvement above/below horizon'
     print,'vertical:    ',impabv1,impbel1
     print,'horizontal:',impabv2,impbel2
endif

;endfor
goto, loop
problem: close,1
print,'I had a problem and so I quit'
end
```

B. CONTIGUOUS AREA METHOD PROGRAM

```
;flirashp finds the ship in a picture completely automatic
;cursor is asked for if at picture boundary
;stores output in chosen file name
;uses shipfind
;modular version uses readflir and shipfind
iscale=2                    ;scale displayed pictures by 2x

close,1             ;close in case of crash
on_ioerror,problem      ;if error, quit program

path1='                 '
file1='                 '
read,'input path to *.img files',path1
if path1 ne '' then path=path1
print,'path= ',path
read,'input type of files eg *.img or names to search for',file1

if file1 eq '' then file1='*.img
files=findfile(path+'\'+file1,count=num)
for i=0,num-1 do print,files(i),i
;**********loop point to start program over after successful processing****

loop: print,n_elements(files)-1,' last number'
read,'input i for number to plot or -1 to stop',i
istart=i
if i lt 0 then goto, problem
read,'input stop number',istop
if(fix((istop-istart+1)/2)*2 ne fix(istop-istart+1)) then begin
  print,istart,istop,' must use even number of points'
  goto, loop
endif
read,'input first guess difference t level, eg 5 to include all of ship',tdif
tdifsave=tdif                   ;save tdif so that changes will not affect batch

;**********************loop point*****************************
contrast=dblarr((istop-istart+1)/2,5)
for ii=istart, istop,2 do begin
  for i=ii,ii+1 do begin
  tdif=tdifsave                 ;restore the tdif if changed in loop
  f=files(i)
  file=f
  readflir,f,yy,t,bar,tt,head       ;modular input returns binary, temparature

;*********************display data in windows for visual inspection**********
;
!order=0
```

```
ct=0
loadct,ct
if(ii eq i) then window,0,xsize=280,ysize=280,xpos=0,ypos=0,title='0 binary data' $
else  window,5,xsize=280,ysize=280,xpos=280,ypos=0,title='5 binary unscaled data'

print,'UNScaled plot of binary data in 0'
;tvscl,congrid(yy,140*iscale,140*iscale,Interp=1)
tv,congrid(yy,140*iscale,140*iscale,Interp=1)

wait,1
loadct,16
window,1,xsize=280,ysize=330,xpos=600,ypos=0,title='1 temperature'

tvscl,rebin(tt,140*iscale,165*iscale)

;*************temperature point option bypassed*******************************

goto,skip
print,'Click in scale bar to exit'
print,'click in picture for point temperature'
replot: cursor,xv,yv,3,/device
if yv lt 50 then goto,skip
print,t(xv,330-yv),mint,maxt
goto, replot
skip:
;****************************************hold ship*************************


;************************take two bars at right and left of picture and

;************************use the lower average value, then smooth it

thres0=(t(137,*)+t(138,*)+t(139,*))/3.0
thres=(t(0,*)+t(1,*)+t(2,*))/3.0
thres=thres > thres0                    ;changed to larger of backgrounds

  minthres=min(thres)
  maxthres=max(thres)
  avthres=total(thres)/n_elements(thres)
thres=smooth(thres,3)
thres=rebin(thres,140,140)                ;make the vertical line xy array
thres0=thres                            ;save in thres1 for debug 140x140 array


;ship=(t gt thres+tdif)*t                ;ship is greater than threshold

;shipb=(t gt thres+tdif)*yy              ;get binary version for display
```

```
ship=(t gt thres)*t                    ;ship is greater than threshold

shipb=(t gt thres)*yy                  ;get binary version for display
;new version uses threshold tdif later

if(total(ship) eq 0) then stop         ;zero values mean error◂



;***make linear array for averages
shipt=ship(where(ship gt 0))     ;Pick only nonzero values for average

                         ;shipt is linear array now
avship=total(shipt)/n_elements(shipt)
  maxship=max(shipt)
  minship=min(shipt)
;print,minship,maxship,avship,' ship min,max,average temperature'

;rint,minthres,maxthres,avthres, '  min max average background'



;Find the MAXIMUM temperature
point************************************************
  maxt=max(ship,it)              ;find the max in the ship thresholded

  ix=it mod 140
  iy=it/140

window,4,xsize=280,ysize=280,xpos=600,title='#4 binary ship'
tvscl,rebin(shipb,140*iscale,140*iscale)       ;make ship twice as big for display

tvcrs,ix*iscale,iy*iscale,/device              ;put the cursor on the peak location

;print,'right button, use auto position, left, new cursor position'
!err=4
if(i ne istart) then begin
  print,ix,iy,nx,ny,x0,y0,format='(6(i3,2x),A19)',' ix,iy,nx,ny,x0,y0'

  if(ix lt 10 or iy lt 10) then cursor,x0,y0,/device                    ;AUTOMATIC LINE
OUT
  if(nx/ny gt 5 or ny lt 10 or nx lt 10) then cursor,x0,y0,/device
;AUTOMATIC LINE OUT ;left button 1, middle 2 right 4
endif
if(!err eq 1) then begin
  iy=y0/iscale
  ix=x0/iscale
  x0=ix
```

```
   y0=iy

endif else begin
   x0=ix
   y0=iy
endelse
;**********************ship loop find point************************************

;following necessary for reship loop, otherwise ship will not change with threshold

reship:
;****************Find
Ship************************************************************

   x0=ix
   y0=iy

shipfind,shipb,ship,x0,y0,nx,ny,iscale    ;use find on the binary version to avoid neg t

;WARNING SHIPFIND SETS ALL VALUES IN SHIP AND SHIPB ZERO NOT ON
THE SHIP
tvscl,rebin(shipb,140*iscale,140*iscale)  ;show the contiguous thresholded=0 ship

;box:xy=boxfun(x0,y0,nx,ny,/init,/message);option to readjust the box
boxdraw,x0,y0,nx,ny                    ;show where the box is
x0=x0/iscale                          ;rescale from picture to data size
y0=y0/iscale
nx=nx/iscale
ny=ny/iscale

;print,x0,y0,nx,ny

thres=(t(x0+nx,*))                      ;right side of box
thres1=t(x0,*)                         ;left side of box
thres=thres > thres1                   ;changed to greater than for background

thres=smooth(thres,2)
thres=rebin(thres,140,140)                  ;make an array 140x140
thres1=fltarr(140,140)
thres1(*,*)=0.0
thres1(x0:x0+nx,y0:y0+ny)=thres(x0:x0+nx,y0:y0+ny)  ;extract part of array
;Now use the threshold to clean up the ship and check for loop
;the ship and shipb cannot be any larger than tdif=0, so whittle
ship=(t gt thres1+tdif)*ship                ;ship is greater than threshold

shipb=(t gt thres1+tdif)*shipb
 ;get binary version for display
x0=ix
```

```
y0=iy
shipfind,shipb,ship,x0,y0,nx,ny,1        ;use find on the binary version to avoid neg t


window,2,xsize=280,ysize=280,xpos=300,title='#2 local threshold'
tvscl,rebin(shipb,140*iscale,140*iscale)          ;redisplay

;above is entire 140x140 picture thresholded

box=t(x0:x0+nx,y0:y0+ny)              ;temperature in box
raw=yy(x0:x0+nx,y0:y0+ny)              ;raw signal in box
      ship1=ship(x0:x0+nx,y0:y0+ny)   ;ship temperature in box
      raw1=shipb(x0:x0+nx,y0:y0+ny)   ;ship binary in box
      ship1b= box*(ship1 eq 0)        ;ship temperature BACKGROUND in box

      raw1b= raw*(raw1 eq 0)          ;ship binary BACKGROUND in box
;ship1 and raw1 are box sized subset of ship and shipb

window,3,xsize=nx*iscale*2,ysize=ny*iscale*2,xpos=0,ypos=0

tvscl,congrid(ship1,(nx+1)*iscale*2,(ny+1)*iscale*2)
tdif1=0.0
;read,'input new tdif or 0 to stop ',tdif1     ;AUTOMATIC LINE OUT
if(tdif1 gt 0) then begin
     tdif=tdif1
;remake the ship variables using the NEW box threshold
      ship=(t gt thres+tdif)*t                    ;ship is greater than threshold

      shipb=(t gt thres+tdif)*yy                  ;get binary version for display

     goto,reship                ;loop up to reship************************************

endif
;*********************RESHIP LOOP
POINT************************************************
;*********************************save
stuff*****************************************
if(i eq ii) then begin
          tdifsave=tdif
          x0save=x0                ;box position
          y0save=y0
          nxsave=nx
          nysave=ny
          ixsave=ix                ;peak position
          iysave=iy                ;peak position
endif

if(i eq ii) then begin
```

```
   ship1sv=ship1
   raw1sv=raw1
   ship1bsv=ship1b
   raw1bsv=raw1b
   tsave=t
   yysave=yy
   shipsv=ship          ;save the temperature thresholded full picture
   shipbsv=shipb        ;save the binary thresholded
endif else begin

   ;if the first box is bigger, renormalize to it
   ;otherwiser renormalize all data to the second box
   ;The following are necessary for correct contrast using binary
   ;raw1,raw1b,raw1sv,raw1bsv - only two of these are destroyed
   ;only one set of the two needs to be recomputed based on the new box
   ;size which is larger
print, nxsave,nysave,nx,ny,'  nxsave,y,nx,ny'
    if(nxsave*nysave gt nx*ny) then begin
       print,'using old ship size'
       ;use save box and make raw1 and raw1b match old ship shipsv
       x0=x0save
       y0=y0save
       nx=nxsave
       ny=nysave

       raw1=yy*(shipbsv gt 0)          ;mask saved correct ship on current data
       raw1b=yy*(shipbsv eq 0)         ;mask for background = not ship
       raw1=raw1(x0:x0+nx,y0:y0+ny)       ;select the current (saved ) box
       raw1b=raw1b(x0:x0+nx,y0:y0+ny)


   endif else begin
       print,'using new ship size'
       raw1sv= yysave*(shipb gt 0)       ;mask current ship on old data 140x140
       raw1bsv=yysave*(shipb eq 0)
       ;current not ship binary times old data
       raw1sv=raw1sv(x0:x0+nx,y0:y0+ny)    ;now select the current box
       raw1bsv=raw1bsv(x0:x0+nx,y0:y0+ny)  ;background
       ;it would also be nice later to update the ship1 (temperature) stuff
   endelse
endelse

;*************************************************************
;

   endfor
;*****************************************************************************
;
****
```

```
;*********************************display*****************************************
****
;*************************************************************************************
****
loadct,0
;;in order
;ship 1 average value
;ship 1 background average value
;ship 2 average value
;ship 2 background average value
;ship unpolarized
;ship background unpolarized
;ship unpolarized average value
;ship background unpolarized average value
;contrast ship1
;contrast shipsv (ship0)
;contrast unpolarized
;contrast ship1/contrast unpolarized
;contrast shipsv/contrast unpolarized

 ship1av=total(ship1)/total((ship1 gt 0))
 ship1bav = total(ship1b)/total((ship1b gt 0))
 shipsav=total(ship1sv)/total( (ship1sv gt 0))
 shipsbav = total(ship1bsv)/total( (ship1bsv gt 0))
 shipup=(ship1+ship1sv)/2.0
 shipbup=(ship1b+ship1bsv)/2.0
 shipupav=total(shipup)*2.0/total((ship1 gt 0)+(ship1sv gt 0))
 shipubav=total(shipbup)*2.0/total((ship1b gt 0)+(ship1sv gt 0))

;above are taken for temperature, below for raw dataq

 ship1av=total(raw1)/total((raw1 gt 0))
 ship1bav = total(raw1b)/total((raw1b gt 0))
 shipsav=total(raw1sv)/total( (raw1sv gt 0))
 shipsbav = total(raw1bsv)/total( (raw1bsv gt 0))
;WARNING, adding binary will exceed 255 and give error
;one must first float the numbers; using temperature above is ok
 shipup=(float(raw1)+float(raw1sv))/2.0
 shipbup=(float(raw1b)+float(raw1bsv))/2.0
 shipupav=total(shipup)*2.0/total((raw1 gt 0)+(raw1sv gt 0))
 shipubav=total(shipbup)*2.0/total((raw1b gt 0)+(raw1bsv gt 0))

 ;total shipup gt 0 does not work because of registration

 cship1=(ship1av-ship1bav)/ship1bav
 cshipsv=(shipsav-shipsbav)/shipsbav
 cshipu =(shipupav-shipubav)/shipubav
 cc1u=cship1/cshipu
```

```
 ccsu=cshipsv/cshipu
;raw1 = ship picture in binary 0-255 (in box)
;raw1sv= same picture 0
;raw1b = binary background in box
;raw1bsv = binary saved background
;yy = full picture (same as t for temperature
;yysave= picture 0 binary
;t=temperature picture
;tsave=old picture temperature
;*************************************************************************

Print,'Contrast and enhancement,first file =',file,tdif,tdifsave
if(istop-istart gt 0) then begin
print,files(ii+1),files(ii),'    unpolarized ,first/unpolarized,second/unpolarized'

print,cship1,cshipsv,cshipu,cc1u,ccsu
contrast((ii-istart)/2,0:4)=[cship1,cshipsv,cshipu,cc1u,ccsu]
;save the values

endif else begin
;print,'     first contrast ',file
;print,cship1
endelse


;display difference image for both polarizations
  window,2,xsize=nx*4,ysize=ny*4,xpos=0,ypos=0,title=files(istop)

  tvscl,rebin(raw1,(nx+1)*4,(ny+1)*4)
  window,3,xsize=nx*4,ysize=ny*4,xpos=0,ypos=140,title=files(istart)

  tvscl,congrid(raw1sv,(nx+1)*4,(ny+1)*4)
;**********************************skip plots in automatic
mode**************************
goto, noplot
;plot ship average value compared to background average value and make .tif file

;horizontal polarization
  title1='horizontal'+' polarization'
  window,4,xsize=350,ysize=300,xpos=300,ypos=0,title=title1     ;files(istop)

  wset,4
;call to external function avrow averages rows
plot,avrow(ship1sv),indgen(140),background=255,color=0

  oplot,avrow(ship1bsv),indgen(140),color=150
;  oplot,bkgdave(*),indgen(140),color=150
  plot1=tvrd()
```

```
  plot1=plot1(*,299-indgen(300))
  tiff_write,title1+'.tif',plot1

;plot comparison of ship average values with respect to polarization and make .tif file

  title2='polarization'+' comparison'
  window,5,xsize=350,ysize=300,xpos=300,ypos=330,title=title2  ;'vertical/horizontal'

  wset,5
  plot,avrow(ship1),indgen(140),background=255,color=0

  oplot,avrow(ship1sv),indgen(140),color=150
  plot2=tvrd()
  plot2=plot2(*,299-indgen(300))
  tiff_write,title2+'.tif',plot2

;plot first ship average value compared to background average value and make .tif file

;vertical polarization
  title3='vertical'+' polarization'
  window,6,xsize=350,ysize=300,xpos=660,ypos=0,title=title3      ;files(istart)

  wset,6
  plot,avrow(ship1),indgen(140),background=255,color=0

  oplot,avrow(ship1b),indgen(140),color=150
  plot3=tvrd()
  plot3=plot3(*,299-indgen(300))
  tiff_write,title3+'.tif',plot3

;plot comparison of backgrounds with respect to polarization and make .tif file

  title4='background'+' comparison'
  window,7,xsize=350,ysize=300,xpos=660,ypos=330,title=title4

  wset,7
  plot,avrow(ship1bsv),indgen(140),background=255,color=0

  oplot,avrow(ship1b),indgen(140),color=150
  plot4=tvrd()
  plot4=plot4(*,299-indgen(300))
  tiff_write,title4+'.tif',plot4
;**********************end of temperature
windows************************************

;plot ship average value compared to background average value and make .tif file

;horizontal polarization
```

```
  title1='hzpol'
  window,10,xsize=350,ysize=300,xpos=300,ypos=0,title=title1     ;files(istop)

;call to external function avrow averages rows
plot,avrow(raw1sv),indgen(140),background=255,color=0,title='horizontal'+' polarization'

  oplot,avrow(raw1bsv),indgen(140),color=150
;  oplot,bkgdave(*),indgen(140),color=150
  plot1=tvrd()
  plot1=plot1(*,299-indgen(300))
  tiff_write,title1+'.tif',plot1

;plot comparison of ship average values with respect to polarization and make .tif file

  title2='comp'
  window,12,xsize=350,ysize=300,xpos=300,ypos=330,title=title2
;'vertical/horizontal'
  plot,avrow(raw1),indgen(140),background=255,color=0,title='polarization'+'
comparison'

  oplot,avrow(raw1sv),indgen(140),color=150
  plot2=tvrd()
  plot2=plot2(*,299-indgen(300))
  tiff_write,title2+'.tif',plot2

;plot first ship average value compared to background average value and make .tif file

;vertical polarization
  title3='vpol'
  window,13,xsize=350,ysize=300,xpos=660,ypos=0,title=title3     ;files(istart)

  plot,avrow(raw1),indgen(140),background=255,color=0,title='vertical'+' polarization'

  oplot,avrow(raw1b),indgen(140),color=150
  plot3=tvrd()
  plot3=plot3(*,299-indgen(300))
  tiff_write,title3+'.tif',plot3

;plot comparison of backgrounds with respect to polarization and make .tif file

  title4='bkgnds'
  window,14,xsize=350,ysize=300,xpos=660,ypos=330,title=title4

  plot,avrow(raw1bsv),indgen(140),background=255,color=0,title='background'+'
comparison'
  oplot,avrow(raw1b),indgen(140),color=150
  plot4=tvrd()
  plot4=plot4(*,299-ir  en(300))
```

```
  tiff_write,title4+'.tif',plot4

noplot:
endfor

;saveflr8.pro prints results
;saveflr8.pro prints results
fileout='                    '
close,2
read,'input output filename',fileout
openw,2,fileout
printf,2,systime(),'  date of analysis'
printf,2,'Temperature difference = ',tdif
printf,2,istop-istart+1,'number of files'
j=istart
for i=0,(n_elements(contrast(*,0))-1) do begin;printf,2,files(2*i),files(2*i+1)
printf,2,files(j+1),files(j),format='(2(A30))'
j=j+2
printf,2,'first,second,unpolarized ,first/unpolarized,second/unpolarized'
printf,2,contrast(i,*),format="(5(f9.6,5x))"
print,i,contrast(i,*),format="(i3,1x5(f9.6,5x))"
endfor

close,2
print,'finished'

goto, loop
problem: close,1
print,'I had a problem and so I quit'
end
```

C. BOX METHOD PROGRAM

```
;lasthope.pro

!order=0
print,'flirs makes movie of flirs'                                    close,1

;close in case of crash                                              intfn=0
                                                          shpnmbr=1
ct=0                                                                 loadct,ct

;window,0,xsize=280,ysize=280,xpos=0,ypos=0
on_ioerror,problem                                                   path1='
                    '                                          file1='
  '                                                    print,'file size must be 20446
with header'                                        read,'input path to *.img files',path1
                                      if path1 ne '' then path=path1
                          print,'path= ',path
```

```
            read,'input type of files eg *.img or names to search for',file1
  if file1 eq '' then file1='*.img
files=findfile(path+'\'+file1,count=num)                                    for
i=0,num-1 do print,files(i),i

;*********************************************************
;print time of analysis and number of files analyzed
;*********************************************************
printf,7,'        ',systime()
printf,7,'        ',strmid(files(5),17,5),'.txt'
;*********************************************************

loop: print,n_elements(files)-1,' last number'
read,'input i for number to plot or -1 to stop',i                           if i lt 0
then goto, problem                                                      istart=i
                                                                read,'input stop
number',istop                                                      for i=istart, istop do begin
                                                        f=files(i)

;*********************************************************
;open output file
;*********************************************************
openr,1,f
print,'opening ',f,i
head=bytarr(846)
y=bytarr(140,70)
y1=bytarr(140,70)
yy=bytarr(140,140)
readu,1,head                                                                readu,1,y
                                                                    readu,1,y1
                                                            close,1
                                                    index=indgen(70)
                                            yy(*,index*2)=y1(*,index)
                                    yy(*,index*2+1)=y(*,index)
        if(max(yy) eq 255) then begin
   y1=yy( where(yy gt 254))
nover=n_elements(y1)                                                        endif else begin
                                                                    nover=0
                                                    endelse
                                            yy=yy(*,139-indgen(140))


;*************************************
;save ship images
;*************************************
ship1=bytarr(140,140)
ship2=bytarr(140,140)
if shpnmbr eq 1 then begin
```

```
  ship1=yy
  ship11=yy
  shpnmbr=2
  shpname1=files(i)
  title1='vert'
  window,1,xpos=0,ypos=0,xsize=140,ysize=140,title=title1
tvscl,ship1
endif else begin
  ship2=yy
  shpname2=files(i)
  title2='hor'
  window,2,xpos=0,ypos=160,xsize=140,ysize=140,title=title2
tvscl,ship2
  shpnmbr=1
endelse
endfor

;**********invert signal**********                                    y1=1
                                                              y=1

;*********reset variables**********
yy=congrid(yy,140*2,140*2,Interp=1)                                   ;!order=1

loadct,0
;wset,0
print,'Scaled plot of data in 0'                                      ;tvscl,yy
range=double(head,770)
level=double(head,762)
dlevel=double(head,618)
emiss=double(head,626)
ct=double(head,650)
r=double(head,570)
b=double(head,578)
f=double(head,586)
amt=double(head,674)
at=double(head,666)
p1=emiss*ct
p2=(1-emiss)/emiss
p3=1.0-ct
iamb=r/(exp(b/amt)-f)
iatm=r/(exp(b/at)-f)
y=range*(float(yy)-128.)/256.0+level+dlevel
y=y/p1-p2*iamb-p3/p1*iatm
t=b/alog(abs((r/y+f)))-273.15
idate=head(482:487)
itime=head(488:495)
; get rid of old variables
;delvar,y,y1,yy,head
```

```
shpup=fltarr(140)
shpup(*)=0.0
shp1=fltarr(140)
shp1(*)=0.0
shp2=fltarr(140)
shp2(*)=0.0
bkgdup=fltarr(140)
bkgdup(*)=0.0
bkgd1=fltarr(140)
bkgd1(*)=0.0
bkgd2=fltarr(140)
bkgd2(*)=0.0
shpave=fltarr(140)
shpave(*)=0.0
;shpave1=fltarr(140)
;shpave1(*)=0.0
;shpave2=fltarr(140)
;shpave2(*)=0.0
;shptot1=fltarr(140)
;shptot1(*)=0.0
;shptot2=fltarr(140)
;shptot2(*)=0.0
shppix1=fltarr(140)
shppix1(*)=0.0
shppix2=fltarr(140)
shppix2(*)=0.0
outline=fltarr(140,140)
outline(*,*)=0.0
outline1=fltarr(140,140)
outline1(*,*)=0.0
outline2=fltarr(140,140)
outline2(*,*)=0.0

image=1
nextimg:
wset,image
zz=boxfun(x0,y0,nx,ny,init=intfn,/message)
intfn=1
box=tvrd(x0,y0,nx,ny)
bkgdave=fltarr(140)
bkgdave(*)=0.0
shppix=fltarr(140)
shppix(*)=0.0

;************************************************************

;assign image array to outline array and mark horizon
```

```
;************************************************************

if image eq 1 then begin
  outline=ship11
  print,'click on horizon or bottom to exit'
  replot1: cursor,xv,yv,3,/device
  if yv lt 5 then goto,exit1
    xv1=xv
    yv1=yv
    yvy=yv
    print,'horizon=',yv1
    print,'click on point or bottom to exit'
    goto,replot1
    exit1:print,'exiting'
endif
if image eq 2 then begin
  outline=ship2
  print,'click on horizon or bottom to exit'
  replot2: cursor,xv,yv,3,/device
  if yv lt 5 then goto,exit2
    xv2=xv
    yv2=yv
    yvy=yv
    print,'horizon=',yv2
    print,'click on point or bottom to exit'
    goto,replot2
    exit2:print,'exiting'
endif
;************************************************************

;calculate background average values
;************************************************************

if y0+ny/2.0 lt 69 then begin
 ;box below narcissus
 ;background average below box
 for n=0,y0-1 do begin
  bkgdave(n)=total(outline(0:139,n))/140.0
 endfor
 ;background average around box
 for n=y0,y0+ny-1 do begin
  bkgdave(n)=(total(outline(x0-5:x0-1,n))+total(outline(x0+nx:x0+nx+4)))/10.0    endfor

 ;background average above box
 for n=y0+ny,139 do begin
  bkgdave(n)=(total(outline(0:19,n))+total(outline(120:139,n)))/40.0                endfor

endif else begin
```

```
 ;box above narcissus
 ;background average below box
 for n=0,y0-1 do begin
  bkgdave(n)=(total(outline(0:19,n))+total(outline(120:139,n)))/40.0                endfor

 ;background average around box
 for n=y0,y0+ny-1 do begin
  bkgdave(n)=(total(outline(x0-5:x0-1,n))+total(outline(x0+nx:x0+nx+4)))/10.0    endfor

;background average above box
 for n=y0+ny,139 do begin
  bkgdave(n)=(total(outline(0:139,n)))/140.0
 endfor
endelse

;*****************************************************
read,'enter background factor',dd
duck=dd
if image eq 1 then begin
  factor1=duck
endif else begin
  factor2=duck
endelse

again:
shppix(*)=0
outline(0:139,0:y0-1)=0.0
outline(0:139,y0+ny:139)=0.0
outline(0:x0-1,0:139)=0.0
outline(x0+nx:139,0:139)=0.0
for n=y0,y0+ny-1 do begin
  for m=x0,x0+nx-1 do begin
    if outline(m,n) le duck*bkgdave(n) then outline(m,n)=0.0
    if outline(m,n) gt 0.0 then shppix(n)=shppix(n)+1
  endfor
  if shppix(n) eq 0 then shpave(n)=0.0
  if shppix(n) ne 0 then shpave(n)=total(outline(*,n))/shppix(n)
endfor
numbel=total(shppix(y0:yvy))
numabv=total(shppix(yvy+1:y0+ny-1))

shpabv=total(outline(x0:x0+nx-1,yvy+1:y0+ny-1))
shpbel=total(outline(x0:x0+nx-1,y0:yvy))
bkgdabv=total(bkgdave(yvy+1:y0+ny-1))/((y0+ny-1)-(yvy+1)+1)
bkgdbel=total(bkgdave(y0:yvy))/(yvy-y0+1)

window,3,xsize=140,ysize=140,xpos=420,ypos=0
tvscl,outline
```

```
read,'enter new background factor or zero to continue',qq
duck=qq
if duck gt 0.0 then begin
  if image eq 1 then begin
    outline=ship11
    factor1=duck
    goto,again
  endif else begin
    outline=ship2
    factor2=duck
    goto,again
  endelse
endif
if image eq 1 then begin
  outline1=outline
  shp1(*)=shpave(*)
  bkgd1(*)=bkgdave(*)
  shpabv1=shpabv
  shpbel1=shpbel
  bkgdabv1=bkgdabv
  bkgdbel1=bkgdbel
  numabv1=numabv
  numbel1=numbel
  image=image+1
  window,4,xsize=140,ysize=140,xpos=280,ypos=0
  outline(*,yv1)=255
  tvscl,outline
  window,5,xsize=140,ysize=140,xpos=140,ypos=0
  tv,ship11
  goto,nextimg
endif
if image eq 2 then begin
  outline2=outline
  shp2(*)=shpave(*)
  bkgd2(*)=bkgdave(*)
  bkgdup(*)=bkgd1(*)/2.0+bkgd2(*)/2.0
  shpup(*)=shp1(*)/2.0+shp2(*)/2.0

  shpabv2=shpabv
  shpbel2=shpbel
  bkgdabv2=bkgdabv
  bkgdbel2=bkgdbel

  shpabv1a=shpabv1/numabv1
  shpbel1a=shpbel1/numbel1

  numabv2=numabv
  numbel2=numbel
```

```
  if numabv2 ge numabv1 then begin
    shpabv1=(shpabv1+bkgdabv1*(numabv2-numabv1))/numabv2
    shpabv2=shpabv2/numabv2
  endif else begin
    shpabv1=shpabv1/numabv1
    shpabv2=(shpabv2+bkgdabv2*(numabv1-numabv2))/numabv1
  endelse
  if numbel2 ge numbel1 then begin
    shpbel1=(shpbel1+bkgdbel1*(numbel2-numbel1))/numbel2
    shpbel2=shpbel2/numbel2
  endif else begin
    shpbel1=shpbel1/numbel1
    shpbel2=(shpbel2+bkgdbel2*(numbel1-numbel2))/numbel1
  endelse

  cntabv1=(shpabv1-bkgdabv1)/bkgdabv1
  cntbel1=(shpbel1-bkgdbel1)/bkgdbel1
  cntabv2=(shpabv2-bkgdabv2)/bkgdabv2
  cntbel2=(shpbel2-bkgdbel2)/bkgdbel2

  shpabvu=shpabv1/2.0+shpabv2/2.0
  shpbelu=shpbel1/2.0+shpbel2/2.0
  bkgdabvu=bkgdabv1/2.0+bkgdabv2/2.0
  bkgdbelu=bkgdbel1/2.0+bkgdbel2/2.0
  cntabvup=(shpabvu-bkgdabvu)/bkgdabvu
  cntbelup=(shpbelu-bkgdbelu)/bkgdbelu

  impabvh=cntabv2/cntabvup
  impbelh=cntbel2/cntbelup
  impabvv=cntabv1/cntabvup
  impbelv=cntbel1/cntbelup


  window,6,xsize=140,ysize=140,xpos=280,ypos=160
  outline(*,yv2)=255
  tvscl,outline
  window,7,xsize=140,ysize=140,xpos=140,ypos=160
  tv,ship2
endif


print,'     shpbel1a     shpabv1a
print,shpbel1a,shpabv1a
print,'     shpbel1     shpbel2     shpbelu'
print,shpbel1,shpbel2,shpbelu
print,'     bkgdbel1     bkgdbel2     bkgdbelu'
print,bkgdbel1,bkgdbel2,bkgdbelu
```

```
print,''
print,'     cntabv1      cntabv2      cntabvup'
print,cntabv1,cntabv2,cntabvup
print,'     cntbel1      cntbel2      cntbelup'
print,cntbel1,cntbel2,cntbelup
print,'     numabv1      numabv2'
print,numabv1,numabv2
print,'     numbel1      numbel2'
print,numbel1,numbel2
print,'     impabvv      impabvh'
print,impabvv,impabvh
print,'     impbelv      impbelh'
print,impbelv,impbelh
print,'bkgd factor v/h',factor1,factor2
print,'horizon v/h',yv1,yv2

ship=string('ship')
bkgd=string('bkgd')
cntabv=string('cntabv')
cntbel=string('cntbel')
numabv=string('numabv')
numbel=string('numbel')
impabv=string('impabv')
impbel=string('impbel')
BF=string('BF')
hrzn=string('hrzn')

printf,7,'          ',shpname1,'\',strmid(shpname2,17,12)
printf,7,'vert','hor','unpol',itime(0),itime(2),itime(4),format='(20x,a4,5x,a3,6x,a5,2x,i2,1h:,
i2,1h:,i2)'
printf,7,'shipabv',shpabv1,shpabv2,shpabvu,format='(10x,a7,1x,f6.2,3x,f6.2,3x,f6.2)'
printf,7,'bkgdabv',bkgdabv1,bkgdabv2,bkgdabvu,format='(10x,a7,1x,f6.2,3x,f6.2,3x,f6.2)'

printf,7,'shipbel',shpbel1,shpbel2,shpbelu,format='(10x,a7,1x,f6.2,3x,f6.2,3x,f6.2)'
printf,7,'bkgdbel',bkgdbel1,bkgdbel2,bkgdbelu,format='(10x,a7,1x,f6.2,3x,f6.2,3x,f6.2)'
printf,7,'cntabv',cntabv1,cntabv2,cntabvup,format='(10x,a6,2x,f6.2,3x,f6.2,3x,f6.2)'
printf,7,'cntbel',cntbel1,cntbel2,cntbelup,format='(10x,a6,2x,f6.2,3x,f6.2,3x,f6.2)'
printf,7,'numabv',numabv1,numabv2,format='(10x,a6,2x,f6.2,3x,f6.2)'
printf,7,'numbel',numbel1,numbel2,format='(10x,a6,2x,f6.2,3x,f6.2)'
printf,7,'impabv',impabvv,impabvh,format='(10x,a6,2x,f6.2,3x,f6.2)'
printf,7,'impbel',impbelv,impbelh,format='(10x,a6,2x,f6.2,3x,f6.2)'
printf,7,'BF',factor1,factor2,format='(10x,a2,6x,f6.2,3x,f6.2)'
printf,7,'hrzn',yv1,yv2,format='(10x,a4,4x,f6.2,3x,f6.2)'
printf,7,''

intfn=0
shpnmbr=1
```

```
goto, loop                                          problem:
close,1                                        print,'I had a
problem and so I quit'
end
```

LIST OF REFERENCES

Basener, R.F., and G.C. McCoyd, "Polarization of Infrared Light Emitted by the Sea, " Grumman Research Department Memorandum RM-360, 1976.

Bramson, M.A., *Infrared Radiation A Handbook for Application*, Plenum Press, New York, 1968.

Chan, P., "Experimental Investigation of Infrared Polarization Effects in Target and Background Discrimination," Master's Thesis, Naval Postgraduate School, December, 1993.

Collett E., *Polarized Light Fundamentals and Applications*, Marcel Dekker, Inc., New York, 1993.

Cooper, A.W., Crittenden, E.C., Milne, E.A., Walker, P.L., Gregoris, D., and Moss, E. "Mid and Far Infrared Measurements of Sun Glint from the Sea Surface," *SPIE Proceedings,* Vol. 1749, 1992.

Cooper, A.W., Lentz, W.J., Walker, P.L., Chan, P.M., "Infrared Polarization Measurements of Ship Signatures and Background Contrast," *SPIE Proceedings,* Vol. 2223, April 1994.

Cooper, Crittenden class notes for PH4253, Sources, Signals and Systems, Naval Postgraduate School.

Coulson, K.L., *Polarization and Intensity of Light in the Atmosphere*, A. Deepak Publishing, Hampton, Virginia, 1988.

Gregoris, D.J., Yu, S., Cooper, A.W. and Milne, E.A., "Dual-band Infrared Polarization Measurements of Sun Glint from the Sea Surface," *SPIE Proceedings on Characterization, Propagation, and Simulation of Sources and Backgrounds II,* Vol. 1166, 1989.

Grum, F. and Becherer, R.J., *Optical Radiation Measurements*, Academic Press, New York, 1979.

Hackforth, H.L., *Infrared Radiation*, McGraw-Hill, New York, 1960.

Hudson, R.D., *Infrared System Engineering*, John Wiley & Sons, Inc., New York, 1969.

Jamieson, J.A., McFee, R.H., Plass, G.N., Grube, R.H., and Richards, R.G., *Infrared Physics and Engineering*, McGraw-Hill, New York, 1963.

Jensen, D.R. and de Leeuw, G., "Work Plan for the Marine Aerosol Properties and Thermal Imager Performance Trial (MAPTIP)." Naval Command, Control and Ocean Surveillance Center RDT&E Division, September, 1993.

Lentz, W.J., personal communication, 1994.

Lloyd, J.M., *Thermal Imaging Systems,* Plenum Press, New York, 1975.

Rosell, F., and Harvey, G., Editors, *The Fundamentals of Thermal Imaging Systems*, Electro-optical Technology Program Office, Naval Research Laboratory, Washington, D.C., 1979.

Sandus, O., "A Review of Emission Polarization," *Applied Optics,* Vol. 4, No. 12, December, 1965.

Skowronek, P.J.,*Infrared Polarization Imaging Characteristics*, Master's Thesis, Naval Postgraduate School, September, 1994.

Sidran, M., "Broadband Reflectance and Emissivity of Specular and Rough Water Surfaces," *Applied Optics,* Vol. 20, No. 18, 15 September, 1981.

Smith, F.G., Ed., Accetta, J.S. and Shumaker, D.L., Executive Editors, *The Infrared and Electro-Optical Systems Handbook Volume II, Atmospheric Propagation of Radiation*, Environmental Research Institute of Michigan, Ann Arbor and SPIE Optical Engineering Press, Bellingham, Washington, 1993.

Tobin, W.E., *The Mariners Pocket Companion*, Naval Institute Press, Annapolis, 1974.

Wolfe, W.L. and Zissis, G.J., Editors, *The Infrared Handbook*, Environmental Research Institute of Michigan, Ann Arbor, 1978.

AGA Thermovision 780 Operating Manual, AGA Infrared Systems AB, Publication No. 556 492, ed. II, 1980.

INITIAL DISTRIBUTION LIST

1. Defense Technical Information Center — 2
   Cameron Station
   Alexandria, VA 22304-6145

2. Library, Code 52 — 2
   Naval Postgraduate School
   Monterey, CA 93943-5101

3. Department Chairman, Code PH — 2
   Department of Physics
   Naval Postgraduate School
   Monterey, CA 93943-5117

4. Professor A. W. Cooper, Code PH/Cr — 3
   Department of Physics
   Naval Postgraduate School
   Monterey, CA 93943-5117

5. Professor Scott Davis, Code PH/Dv — 1
   Department of Physics
   Naval Postgraduate School
   Monterey, CA 93943-5117

6. W. J. Lentz, Code PH/Lz — 1
   Department of Physics
   Naval Postgraduate School
   Monterey, CA 93943-5117

7. NCCOSC-RDT&E Division — 1
   Naval Research and Development (NRaD)
   Code 54
   271 Catalina Boulevard
   San Diego, CA 92152-5000
   Attn: Dr. J. H. Richter

8. NCCOSC-RDT&E Division — 1
   Naval Research and Development (NRaD)
   Code 543
   271 Catalina Boulevard
   San Diego, CA 92152-5000
   Attn: Dr. D. R. Jensen

9. The Johns Hopkins University 1
Applied Physics Laboratory
Johns Hopkins Road
Laurel, MD 20707
Attn: D. V. Webster, Surface Combat Systems (FP1)

10. LT David G. Moretz 1
Department Head Class 137
Surface Warfare Officers School Command
446 Cushing Road
Newport, RI 02841-1209